UNIVERSIDAD NACIONAL AUTÓNOMA DE MÉXICO
DOCTORADO EN CIENCIAS BIOMÉDICAS
INSTITUTO DE INVESTIGACIONES BIOMÉDICAS

*"INTERACCIONES DE E6*I Y E6*II DEL VPH-16 CON ISOFORMAS DE p53 Y LA INDUCCIÓN DE LA APOPTOSIS EN LÍNEAS CELULARES DERIVADAS DE CÁNCER"*

T E S I S

QUE PARA OPTAR POR EL GRADO DE

DOCTORA EN CIENCIAS

P R E S E N T A

M. en C. VERÓNICA ANTONIO VÉJAR

DIRECTOR DE TESIS

DR. ALEJANDRO MANUEL GARCÍA CARRANCÁ
INSTITUTO DE INVESTIGACIONES BIOMÉDICAS

COMITÉ TUTOR

DR. KARLEN GAZARIAN GAZARIAN
INSTITUTO DE INVESTIGACIONES BIOMÉDICAS

DR. VICENTE MADRID MARINA
FACULTAD DE MEDICINA

Ciudad de México, noviembre del 2023.

El presente trabajo de tesis doctoral se realizó en el Laboratorio de Virus y Cáncer de la Unidad de Investigación Biomédica en Cáncer del Instituto de Investigaciones Biomédicas-UNAM, con sede en el Instituto Nacional de Cancerología-SSA en la Ciudad de México.

Bajo la dirección del:

Dr. Alejandro Manuel García Carrancá

Instituto de Investigaciones Biomédicas-UNAM

Y la asesoría de:

Dr. Karlen Gazarian Gazarian

Instituto de Investigaciones Biomédicas, UNAM

Dr. Vicente Madrid Marina

Facultad de Medicina, UNAM

Esta investigación se desarrolló con el financiamiento del Consejo Nacional de Ciencia y Tecnología, CONACYT, becas Núm. 0253804 bajo la dirección del Dr. Alejandro García Carrancá y Núm. 179894 bajo la asesoría de la Dra. Elizabeth Ortíz Sánchez y por el programa de financiamiento intramuros del Instituto Nacional de Cancerología al Dr. Alejandro García Carrancá y el Dr. Greco Hernández.

Durante el período en el que la C. Verónica Antonio Véjar fue estudiante de doctorado en el Programa de Doctorado en Ciencias Biomédicas de la Universidad Nacional Autónoma de México, recibió la beca con número de CVU/becario: 265243/269673 del CONACyT.

AGRADECIMIENTOS

A mi tutor, **Dr. Alejandro M. García-Carrancá** por confiar en mí y recibirme tan cálidamente en su grupo de trabajo. Valoro sobremanera todo su apoyo y múltiples palabras de aliento que siempre tuvo para mí durante mi formación doctoral.

A los miembros de mi comité tutor, **Dr. Karlen Gazarian Gazarian** y **Dr. Vicente Madrid Marina**, por la importante asesoría brindada durante el desarrollo de este proyecto.

A los miembros del Jurado, **Dr. Juan Carlos Gómora Martínez, Dra. Rocío Brenda Anguiano Serrano, Dra. Érika Patricia Rendón Huerta y Dr. Emilio Rojas Del Castillo** por sus pertinentes observaciones y sugerencias para la mejora de la redacción de la tesis.

A la **Dra. Yolanda Irasema Chirino López**, Coordinadora del Programa de Doctorado en Ciencias Biomédicas del Instituto de Investigaciones Biomédicas, UNAM, por el acompañamiento que recibí de su parte durante el proceso de graduación y que me dio la oportunidad de conocer la gran persona que es.

A la **Dra. Elizabeth Ortíz Sánchez** y al **Dr. Greco Hernández** por su valiosa asesoría durante el desarrollo de los experimentos y revisión del manuscrito pero sobre todo por su amistad.

A la **M en C. Miriam C. Guido Jiménez** y la **Dra. Rocío S. Méndez Martínez** por su apoyo técnico en el desarrollo de esta investigación.

Al **Dr. Pedro Rosendo Chalma y Dr. Carlos César Patiño Morales** por su amistad sincera y apoyo invaluable en el desarrollo de los experimentos de este proyecto.

A mis compañeros y amigos del Laboratorio Virus y Cáncer con los que tuve la fortuna de coincidir y disfrutar innumerables experiencias: **Dr. Heriberto A. Valencia González**, **Dr. Gabriele Davide Bigoni Ordoñez**, **Biol. Verónica Martínez Báez**, **Dra. Graciela Ruiz Ramírez**, **QBP. Karen Griselda de la Cruz López**, **Dra. Yakelin Díaz Tejeda**, **M en C. Marco Meraz Muñoz y M en C. Eduardo Alvarado Ortiz.**

A **Raquel López Paniagua** por su apoyo técnico, atenciones, solidaridad, pero sobre todo por su amistad.

A todos gracias, gracias, gracias.

Verónica Antonio Véjar

DEDICATORIAS

Para mi amada hija Camila,
tu existencia y tu amor son mi fuerza…

Para mi familia, mi red de amor y apoyo incondicional siempre:

Ma. Teresa Véjar Islas, Leopoldo Antonio Gutiérrez, Fidel Antonio Padilla†, Ma. Del Rosario Antonio Véjar, Fidel Carlos Antonio Véjar†, Yadira Antonio Véjar, Alicia Antonio Véjar, Julio César Zeferino Estrada, Isis Mariana Antonio Véjar, Carla Ximena Olivares Antonio, Regina Zeferino Antonio, Valentino Zeferino Antonio e Isabella Antonio Véjar.

Para Héctor Hugo Salgado Delgado

Por la certeza que me das desde el primer día.

Verónica Antonio Véjar

ÍNDICE

ABREVIATURAS

CaCu	Cáncer cervicouterino
VPH	Virus del papiloma humano
VPH-AR	Virus del papiloma humano de alto riesgo
VPH-16	Virus del papiloma humano tipo 16
E6-AP	Proteína ubiquitina ligasa asociada a E6
Co-IP	Co-inmunoprecipitación
IC50	Concentración inhibitoria media

I. RESUMEN

Una característica importante de los cánceres asociados con los virus del papiloma humano de alto riesgo (VPH-AR) es la incapacidad de p53 para activar la apoptosis debido al efecto de la oncoproteína E6. Sin embargo, el efecto de las variantes de empalme de E6 del VPH-16 (E6*I y E6*II), su interacción con las isoformas de p53 (Δ40p53 and Δ133p53) y su influencia en la apoptosis no son totalmente claros. Aquí reportamos el efecto de la expresión ectópica de E6, E6*I y E6*II del VPH-16 sobre los niveles relativos de p53, Δ40p53 y Δ133p53 y su interacción con estas proteínas. Adicionalmente, evaluamos el efecto de la expresión ectópica de p53, Δ40p53 y Δ133p53 sobre la apoptosis en una línea de células de cáncer de pulmón nulas para p53 (H1299) co-transfectada con las isoformas de E6; y líneas celulares de cáncer cervicouterino (CaCu) con VPH-AR y $p53^{+/+}$ (SiHa y HeLa), transfectadas con las isoformas de p53 y tratadas con cisplatino, una droga convencional usada para tratar el CaCu. Nuestros resultados muestran que E6 y E6*II indujeron una disminución significativa en p53, pero solamente E6 disparó una disminución de Δ40p53 y que E6*II interactúa con p53 pero no con Δ40p53 ni Δ133p53. Por otro lado, E6*I no mostró ningún efecto o interacción con las isoformas de p53. Establecimos que la apoptosis fue elevada en células H1299 transfectadas con p53 (p=0.0001) y Δ40p53 (p=0.0001). Un efecto apoptótico débil fue observado cuando Δ133p53 fue expresada ectópicamente (p=0.0195). Observamos que tanto p53 (p=0.0006) como Δ40p53 (p=0.0014) indujeron apoptosis en las células SiHa tratadas con cisplatino, sin embargo, en las células HeLa tratadas con cisplatino, solamente p53 indujo apoptosis (p=0.0029). No observamos diferencias significativas en la apoptosis con la expresión ectópica de p53, Δ40p53 y Δ133p53 en células SiHa y HeLa. Nuestros hallazgos sugieren una posible aplicación terapéutica de la combinación de p53 o Δ40p53 con cisplatino para inducir el aumento de la apoptosis de células de cáncer que expresen las isoformas de E6 del VPH-16.

Palabras clave: cáncer cervicouterino, virus del papiloma humano, E6, p53, apoptosis.

II. ABSTRACT

An important characteristic of cancers associated with high-risk human papillomaviruses (HR-HPV) is the inability of p53 to activate apoptosis due to the effect of the oncoprotein E6. However, the effect of HPV-16 E6 splice variant isoforms (namely E6*I and E6*II), their interaction with the p53 isoforms (Δ40p53 and Δ133p53), and their influence on apoptosis is unclear. Here, we report the outcome of ectopic expression of HPV-16 E6, E6*I, and E6*II on the relative levels of p53, Δ40p53 and Δ133p53 and their interaction with these proteins. Additionally, we evaluated the effect of ectopic expression of p53, Δ40p53, and Δ133p53 on apoptosis in a p53 null pulmonary cell line (H1299) co-transfected with E6 isoforms; and $p53^{+/+}$ cell lines with HR-HPV (SiHa and HeLa), transfected with p53 isoforms and treated with cisplatin, a conventional drug used to treat cervical cancer. Our results show that E6 and E6*II induced a significant decrease in p53, but only E6 triggered a Δ40p53 decrease and that E6*II interacts with p53 but not with Δ40p53 and Δ133p53. On the other hand, E6*I did not show any effect or interaction with the p53 isoforms. We found that apoptosis was elevated in H1299 cells transfected with p53 (p=0,0001) and Δ40p53 (p=0,0001). A weak apoptotic effect was observed when Δ133p53 was ectopically expressed (p=0,0195). We observed that both p53 (p=0,0006) and Δ40p53 (p=0,0014) induced apoptosis in cisplatin-treated SiHa cells; however in cisplatin-treated HeLa cells, only p53 induced apoptosis (p=0,0029). No significant differences in apoptosis were observed upon ectopic expression of p53, Δ40p53, and Δ133p53 in SiHa and HeLa cells. Our findings suggest a possible therapeutic application for the combining of p53 or Δ40p53 with cisplatin to induce an increased apoptosis of cancer cells expressing E6 isoforms from HPV-16.

KEYWORDS: Cervical cancer; Human Papillomavirus; E6; p53; Apoptosis.

III. INTRODUCCIÓN

III.1 Datos generales del virus del papiloma humano (VPH).

Un estudio reciente basado en GLOBOCAN 2018 reporta que los tipos 16 y 18 del virus del papiloma humano de alto riesgo (VPH-AR) causan el 72% de todos los cánceres atribuibles al VPH, en su mayoría cáncer cervicouterino (CaCu), mientras que los tipos 31, 33, 45, 52 y 58 se detectan en un 17% de los casos [1]. Está bien establecido que la oncoproteína E6 del VPH-AR se une a p53 a través de la proteína ubiquitina ligasa asociada a E6 (E6-AP, por sus siglas en inglés), promoviendo su degradación a través de una vía dependiente de la ubiquitina-proteasoma que contribuye a la oncogenicidad de estos virus [2-7].

Por otro lado, está bien documentado que un pre-ARNm bicistrónico del VPH-16 codifica las oncoproteínas E6 y E7, sin embargo, además de generar el transcrito E6 maduro, dicho pre-ARNm genera transcritos empalmados alternativamente que codifican a E6*I, E6*II y E6^E7 [8-11]. Figura 1.

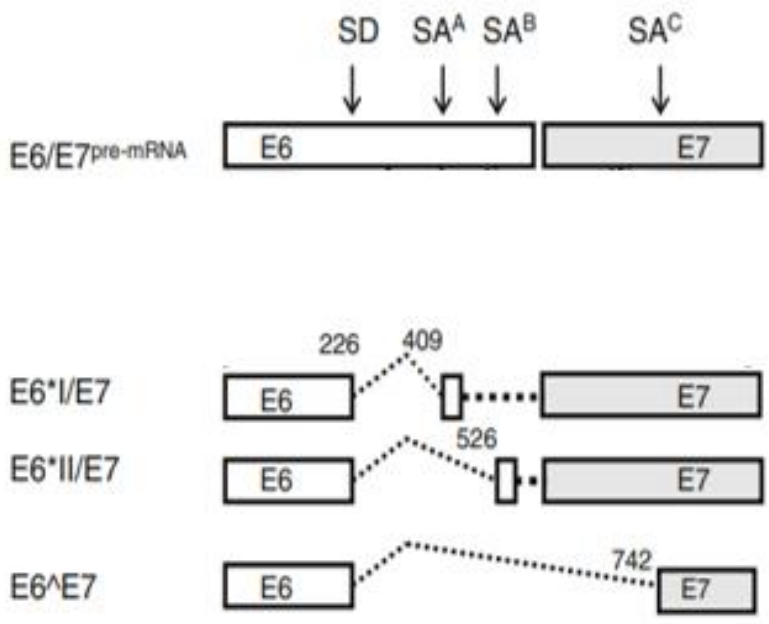

Figura 1. Organización genómica de los genes E6/E7 del VPH-16. El intrón 1 tiene un sitio donante de empalme (SD) en el nucleótido 226 y tres sitios aceptores en los nucleótidos 409 (SA^A), 526 (SA^B) y 742 (SA^C), respectivamente. La línea discontinua entre recuadros representa las secuencias empalmadas alternativamente. Los recuadros claros representan el ORF total o parcial de E6, mientras que los recuadros sombreados representan a E7. Modificada de Del Moral-Hernández, O., *et al*, 2010 [11].

Los productos proteicos generados a partir de los transcritos E6*I y E6*II del VPH-16 son bastante similares y sólo difieren en siete aminoácidos de un total de 50 y 55 aminoácidos, respectivamente [10]. Figura 2. Algunos estudios sugieren que las variantes de empalme de E6 del VPH-16 podrían desempeñar diferentes funciones celulares. Por ejemplo, a la E6*I se le han atribuido funciones parciales o similares a la E6, pero también se ha reportado que E6*I puede desempeñar un papel antagónico al inhibir las actividades oncogénicas de E6 [10-12]. El efecto de E6*II del VPH-16 en la carcinogénesis del cuello uterino no ha sido bien dilucidado.

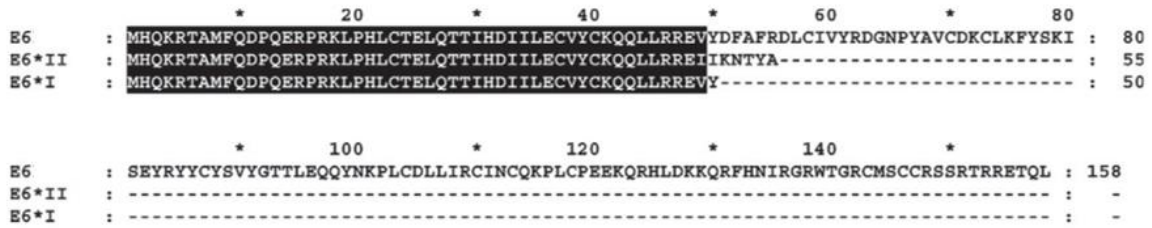

Figura 2. Alineamiento de las secuencias proteicas para E6, E6*I y E6*II. Los aminoácidos comunes para las tres proteínas están resaltados. Modificada de Filippova, M., *et al*. 2014. [10].

III.2 Isoformas de p53.

En los humanos, el gen TP53 puede expresar hasta nueve ARN mensajeros distintos que codifican 12 variantes proteicas funcionales diferentes y que han sido detectadas tanto en tejidos sanos como en tejidos de diferentes tipos de cáncer: p53 (también nombrada p53 de longitud completa, FLp53, p53 canónica y TAp53α), p53β (o p53i9), p53γ, Δ40p53α (o ΔNp53, p44 o p47), Δ40p53β, Δ40p53γ, Δ133p53α, Δ133p53β, Δ133p53γ, Δ160p53α, Δ160p53β, y Δ160p53γ) [13, 14, 15], cada una con dominios proteicos distintos, resultado del uso de promotores alternativos, del empalme alternativo y de sitios alternativos del inicio de la traducción [13, 16]. Figura 3.

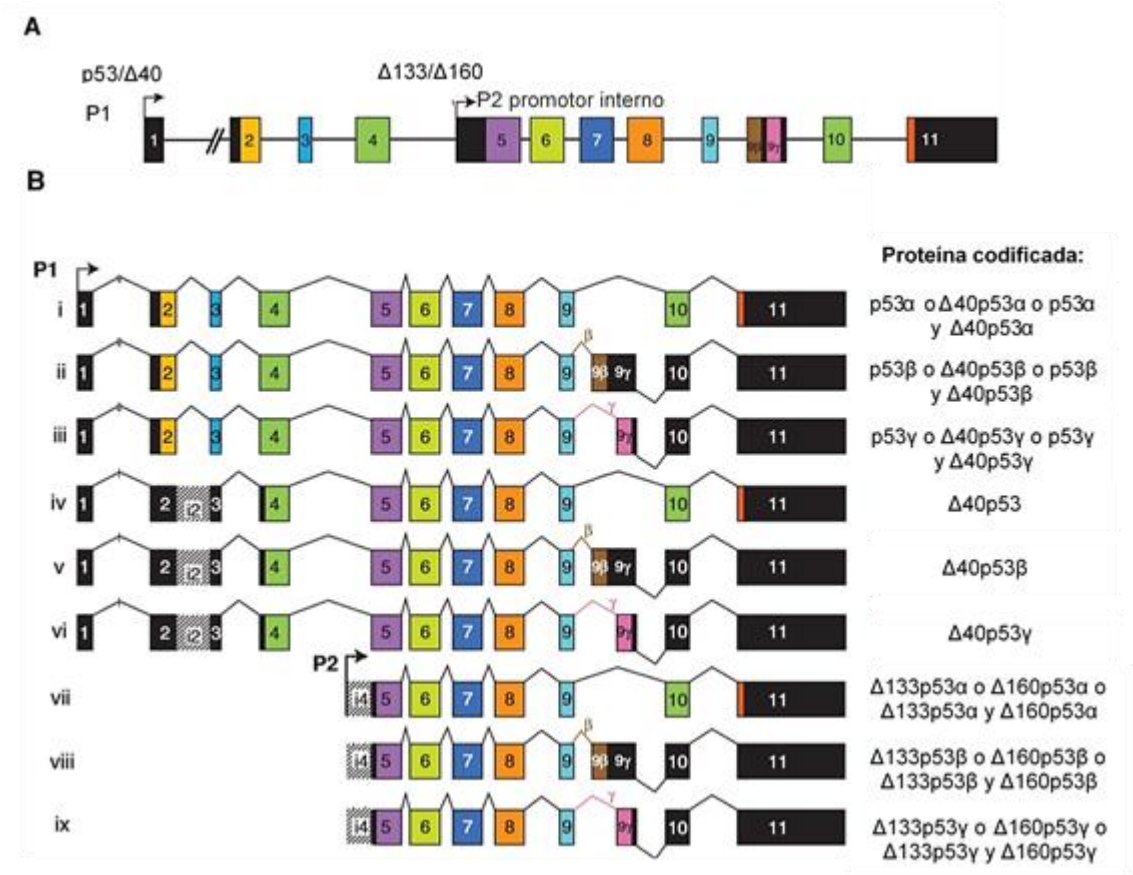

Figura 3. Gen TP53 y RNAm de p53. Las cajas negras representan secuencias no codificantes, mientras que las secuencias codificantes están coloreadas. **(A)** Estructura del gen TP53 humano. El gen TP53, que está compuesto por 11 exones y dos exones crípticos (9β y 9γ), codifica varias isoformas p53. **(B)** ARNm de p53. El gen TP53 codifica nueve ARNm diferentes atribuibles a los promotores alternativos (↱ P1 y P2) y al empalme (^). El promotor P1, localizado río arriba del exón-1, genera los ARNm empalmados con el intrón 2 (i, ii y iii) o los ARNm con retención del intrón 2 (iv, v y vi). Los ARNm con exclusión del intrón-2 pueden codificar las proteínas de longitud completa y/o Δ40, mientras que el ARNm que retiene el intrón-2 solo puede codificar las proteínas Δ40. El promotor P2 localizado en el intrón 4, genera tres ARNm (vii, viii y ix), que codifican las formas Δ133 y Δ160. Modificada de Joruiz, S.M. & Bourdon, J.C., 2016 [15].

Se ha demostrado que las isoformas codificadas por el gen TP53 desempeñan un papel fundamental en la regulación de la vía de p53, ya que cooperan y modulan su actividad para promover la supervivencia o la muerte celular, la respuesta al estrés celular, los mecanismos de reparación del daño del ADN, la detención del ciclo celular

y la senescencia celular [17-22]. Aunado a esto, la expresión de las isoformas de p53 es diferente en una amplia gama de tejidos humanos sanos [13].

Como se mencionó, las isoformas de p53 difieren de la p53 completa por la ausencia de dominios estructurales y funcionales que pueden alterar las propiedades bioquímicas esenciales para la función supresora de p53 y sólo una región del dominio de unión al ADN (DBD, por sus siglas en inglés) (específicamente los residuos 133-257) es común para la mayoría de las isoformas [23]. Además, todas las isoformas de p53 tienen versiones α, β y ɣ C-terminal [13].

III. 3 Isoformas ∆40p53.

Las isoformas ∆40p53 (∆40p53α, también nombrada Δ40p53, DNp53, p44 o p47; Δ40p53β y Δ40p53γ) se generan mediante el empalme alternativo del intrón 2 o por el inicio alternativo de la traducción. La retención de una parte del intrón 2 (i2) genera un codón de paro entre los exones 2 y 3 en el ácido ribonucleico mensajero p53i2 (ARNm) que conduce al inicio de la traducción en AUG40. Existe un sitio interno de entrada al ribosoma (IRES) que contribuye al inicio alternativo de la traducción en el codón AUG40 en lugar de AUG1 y por lo tanto, a la expresión de Δ40p53. [13, 24-27]. Las isoformas ∆40p53 carecen de los primeros 39 aminoácidos y por lo tanto, del dominio de transactivación principal de la p53 canónica (TADI), pero retienen el dominio secundario (TADII), no obstante, con solo el dominio TADII son capaces de inducir la expresión de genes [13, 24-27]. Figura 4. Específicamente Δ40p53 puede regular la actividad transcripcional de p53 porque puede unirse a los elementos de respuesta de p53 y neutralizar su actividad de transactivación, contrarrestando su

efecto supresor [24] Por otro lado, se ha reportado que Δ40p53 y p53 coexpresadas en líneas celulares pueden interactuar directamente formando un heterooligómero que protege a p53 de la degradación mediada por HDM2 ya que dicho complejo es más estable que el complejo constituido solo por p53 [28].

III.4 Isoformas ∆133p53.

Las isoformas ∆133p53 (Δ133p53α (o Δ133p53), Δ133p53β, Δ133p53γ) se producen a partir del promotor interno (P2) de TP53 localizado en el intrón 4, iniciando la traducción en el codón 133, por lo que carecen de 132 aminoácidos, es decir, carecen de los dominios de transactivación TADI y TADII y parte del DBD [13, 15]. Figura 4. Cualquier cambio en el DBD altera la especificidad y la afinidad al ADN debido a la ausencia del aminoácido Lys-120, que se sabe es crucial para la unión de p53α al ADN, por lo tanto, ∆133p53 podría ser menos eficiente en la unión al ADN, no obstante, esta isoforma retiene otros aminoácidos del DBD que están involucrados en la unión al ADN que son Ser-241, Arg-248, Arg-273, Ala-276, Cys-277 y Arg-280 [29]. Además, ∆133p53 es capaz de formar dímeros o tetrámeros con p53 u otras isoformas de p53. Por lo tanto, ∆133p53 se une a un conjunto diferente de genes y actúa de una

manera dependiente del contexto celular [30].

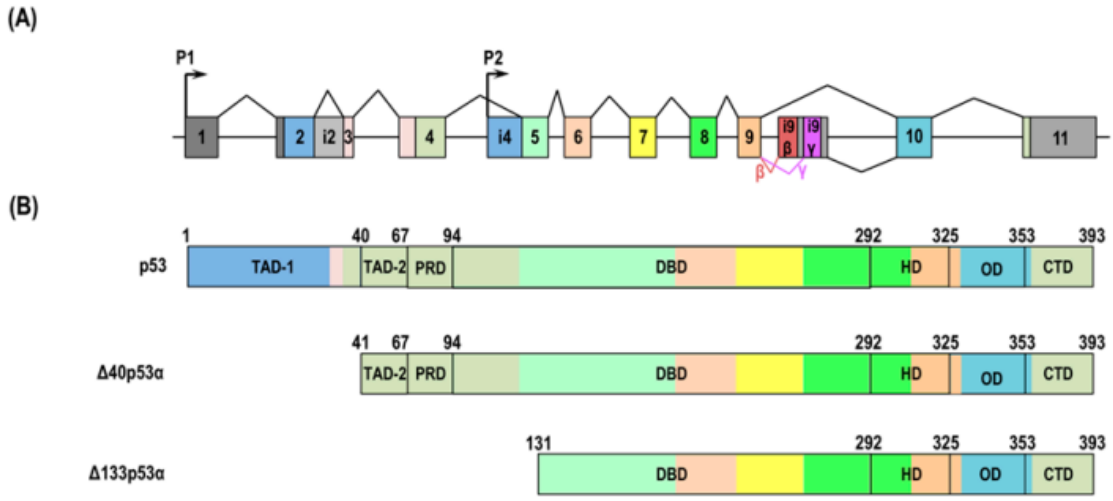

Figura 4. El gen humano TP53 y las isoformas Δ40p53 y Δ133p53. (A) Estructura del gen TP53 humano. Los recuadros indican los exones y las líneas los intrones. Los exones e intrones no están a escala. Los recuadros grises muestran las secuencias no codificantes. Los demás colores muestran las secuencias codificantes. El gen TP53 humano está compuesto por 11 exones y codifica varias isoformas de p53 utilizando promotores alternativos (P1 y P2) y sitios de empalme (líneas en zigzag). El gen también incluye dos exones únicos que forman parte del intrón 9 y codifican las isoformas β y γ. **(B)** Las isoformas humanas Δ40p53 y Δ133p53. Los colores del dominio de la proteína coinciden con los exones correspondientes. p53 tiene dos dominios de transactivación (TAD-1 aa 1-40 y TAD-2 aa 41-67), un dominio rico en prolina (PRD, aa 68-98), un dominio de unión al ADN (DBD, aa 94-292), un dominio de oligomerización (OD, aa326-353) y un dominio regulador carboxi-terminal (CTD, aa 353-393). Δ40p53 carece de TAD1 debido a la iniciación alternativa en el ATG40. Δ133p53α se transcribe a partir de P2 y carece de todo el N-terminal (TAD-1, TAD-2 y PRD) y parte del DBD. Modificada de Fujita, K., 2019 [31]

Lo anterior sugiere que las isoformas de p53 ejercen sus efectos ya sea a través de sus propiedades funcionales autónomas, diferentes de las de p53 y/o modulando la actividad de p53 [23]. Además, la expresión de las isoformas de p53 es específica de cada tejido y se han observado patrones de expresión anómalos en varias enfermedades malignas [13, 20].

La expresión de Δ40p53 y Δ133p53 se ha estudiado en diferentes tipos de cáncer como melanoma, cáncer colorrectal, cáncer de ovario, colangiocarcinoma, glioblastoma, cáncer de pulmón y el carcinoma de células escamosas de cabeza y cuello [19, 32-38], lo que sugiere un papel clave de la expresión alterada de estas isoformas en el desarrollo y la progresión del cáncer.

III. 5 El cisplatino en el tratamiento del cáncer.

El cisplatino, (SP-4-2)-diamminedichloridoplatinum(II) o CDDP es el fármaco quimioterapéutico más utilizado para el tratamiento de numerosos tumores sólidos en humanos, incluyendo el CaCu. Su mecanismo de acción se ha relacionado con su capacidad para entrecruzarse con las bases púricas del ADN, interfiriendo con la síntesis y la reparación del ADN y generando la activación de varias vías de transducción de señales que conllevan a la apoptosis de las células cancerosas. No obstante, un problema importante ha sido la resistencia tumoral al fármaco, además de los numerosos efectos secundarios no deseados en los pacientes. Las terapias combinadas de cisplatino con otros fármacos se han considerado para superar la farmacorresistencia y reducir la toxicidad. Por ello es importante el desarrollo de estrategias moleculares terapéuticas no sólo para superar la resistencia al fármaco, sino también para mejorar su eficacia contra el cáncer [39, 40-42].

IV. PLANTEAMIENTO DEL PROBLEMA

Debido a que no se ha analizado ampliamente el papel de las variantes de empalme E6*I y E6*II del VPH-16 en la carcinogénesis del cuello uterino, así como su interacción con las isoformas de p53, es importante determinar si la expresión ectópica de E6, E6*I y E6*II del VPH-16 tiene algún efecto sobre los niveles relativos de p53, Δ40p53 y Δ133p53, si la inhibición del proteasoma restablece los niveles de las isoformas de p53 y si existe interacción entre las proteínas virales y celulares mencionadas. Además, investigar el efecto de la expresión ectópica de p53, Δ40p53 y Δ133p53 sobre la apoptosis de líneas celulares derivadas de cáncer, como son las células H1299, las cuales son derivadas de un cáncer de pulmón de células no pequeñas y nulas para p53; así como de las líneas celulares SiHa y HeLa derivadas de CaCu, p53+/+ y positivas para el VPH-16 y el VPH-18, respectivamente y que fueron tratadas con cisplatino, un fármaco convencional utilizado comúnmente en la terapia del CaCu [39].

V. HIPÓTESIS

La expresión ectópica de E6, E6*I y E6*II del VPH-16 afecta de manera diferente los niveles relativos de p53, Δ40p53 y Δ133p53, consecuencia de la interacción distinta de dichas proteínas virales y celulares, mientras que la expresión ectópica de p53, Δ40p53 o Δ133p53 resulta en el incremento de la apoptosis de las células de cáncer tratadas con cisplatino.

VI. OBJETIVO GENERAL

Evaluar el efecto de E6, E6*I y E6*II del VPH-16 sobre los niveles relativos de p53, Δ40p53 y Δ133p53 y la interacción entre dichas proteínas virales y celulares, así como el efecto de p53, Δ40p53 y Δ133p53 en la apoptosis de las líneas celulares H1299, SiHa (positiva a VPH-16) y HeLa (positiva a VPH-18) tratadas con cisplatino.

VII. OBJETIVOS ESPECÍFICOS

1. Analizar los niveles relativos de p53, Δ40p53 y Δ133p53 en células H1299 co-transfectadas con E6 y las variantes de empalme E6*I y E6*II del VPH-16.
2. Analizar los niveles relativos de p53, Δ40p53 y Δ133p53 en células H1299 co-transfectadas con E6, E6*I y E6*II del VPH-16 en presencia y ausencia del inhibidor del proteasoma MG132.
3. Determinar si existe interacción de E6*I y E6*II del VPH-16 con p53, Δ40p53 y Δ133p53 en un modelo de células H1299.
4. Determinar el nivel de apoptosis de células H1299 transfectadas con p53, Δ40p53 o Δ133p53 y tratadas con cisplatino.
5. Determinar el nivel de apoptosis de células SiHa y HeLa transfectadas con p53, Δ40p53 y Δ133p53 y tratadas con cisplatino.

VIII. MATERIALES Y MÉTODOS

VIII.1 Condiciones de cultivo celular.

Para este estudio se utilizaron las líneas celulares humanas H1299 (ATCC® CRL-5803™) derivada de cáncer de pulmón de células no pequeñas [43] y nulas para p53 [44, 45], SiHa (ATCC® HTB-35™) derivada de un carcinoma cervical de células escamosas de grado II y positiva al VPH-16 [46-48] and p53 silvestre ($p53^{+/+}$) [49] y HeLa (ATCC® CRM-CCL-2) derivada de un adenocarcinoma del cuello uterino positiva al VPH-18 [46-48] y p53 silvestre ($p53^{+/+}$) [49] fueron obtenidas de la American Type Culture Collection (ATCC, Manassas, VA, EE.UU). Las células H1299 fueron cultivadas en RPMI (Thermo Fisher Scientific Inc., Waltham, MA, EE. UU.) y las células SiHa and HeLa fueron cultivadas en DMEM (Thermo Fisher Scientific). Todas las células fueron suplementadas con 10% de suero fetal bovino (Thermo Fisher Scientific) y 100 U/mL de penicilina/estreptomicina (Thermo Fisher Scientific) y fueron incubadas a 37 °C en una atmósfera húmeda con 5% CO_2.

VIII.2 Plásmidos.

El vector vacío pSV y los plásmidos de expresión de p53 (pSV-p53) y las isoformas de p53 (pSV-Δ40p53 y pSV-Δ133p53), en lo sucesivo referidos como plásmidos de expresión de las isoformas de p53, fueron amablemente donados por el Dr. Jean-Christophe Bourdon (Dundee Cancer Center, University of Dundee, DUN, UK) [13]. Los plásmidos de expresión de las proteínas de fusión E6-GFP del VPH-16 ($E6^{SD}$-GFP, E6-GFP, E6*I-GFP, E6*II-GFP), posteriormente referidos como plásmidos de expresión de las isoformas de E6 y el vector vacío pEGFP-N1 fueron amablemente

proporcionados por el Dr. Nicolás Villegas Sepúlveda (Departamento de Biomedicina Molecular, Centro de Investigación y de Estudios Avanzados-IPN (CINVESTAV-IPN), CDMX, Mx) [11, 50]. El plásmido pRL-CMV (*Renilla* luciferase reporter vector) (Promega Corporation, Madison, WI, EE. UU.) fue usado para la normalización de las transfecciones en los ensayos de Western blot.

VIII.3 Transfecciones y cotransfecciones.

Se sembraron 4 x 10^5 células H1299 por placa, en placas de 60 mm por triplicado, y se realizaron transfecciones transitorias y co-transfecciones utilizando el reactivo Lipofectamine® y el reactivo Plus™ (Thermo Fisher Scientific) de acuerdo con el protocolo del fabricante. Para las transfecciones transitorias, se utilizó 1 µg de los plásmidos de expresión de las isoformas de p53 o del vector vacío pSV, como control de transfección. Para las co-transfecciones, se utilizaron 2 o 4 µg de cada uno de los plásmidos de expresión de las isoformas E6 o el vector vacío pEGFP-N1 en combinación con 1 µg de los plásmidos de expresión de las isoformas p53 o el vector vacío pSV. Las células H1299 transfectadas y co-transfectadas se incubaron durante 24 h a 37 °C con un 5% de CO_2. Además, las células H1299 co-transfectadas se trataron con 20 µM de inhibidor del proteasoma MG-132 (Sigma-Aldrich, San Luis, MI, EE. UU.) y se incubaron durante 4 h a 37 °C con 5% de CO_2. Posteriormente, se realizó la extracción de proteínas de las células H1299 transfectadas y co-transfectadas.

Por otro lado, se sembraron 4 x 10^5 células SiHa y HeLa por placa, en placas de 60 mm por triplicado y se realizaron transfecciones transitorias utilizando el reactivo Lipofectamine® y el reactivo Plus™ (Thermo Fisher Scientific) según las

recomendaciones del fabricante. Para las transfecciones, se utilizó 1 µg de los plásmidos de expresión de las isoformas de p53 o del vector vacío pSV, como control de transfección. Las células se incubaron durante 4 h a 37 °C con un 5% de CO_2.

VIII.4 Actividad de la luciferasa de Renilla.

La actividad de la luciferasa de *Renilla* (RLuc) se utilizó como control interno de normalización para la SDS-PAGE de la siguiente manera: se sembraron 2 X 10^5 células H1299 en placas de seis pocillos con medio de cultivo completo y se co-transfectaron con 1 µg de plásmidos de expresión de las isoformas de p53, 2 µg de los plásmidos de expresión de las isoformas de E6 y 50 ng de pRL-CMV *Renilla.* Las co-transfecciones se realizaron con Lipofectamine™ 3000 (Thermo Fisher Scientific) según el protocolo del fabricante. Veinticuatro horas después de las transfecciones, las células H1299 se rasparon vigorosamente en 150 µL del tampón de lisis pasiva, PBL (Promega) con un gendarme de goma. Se transfirieron 100 µL de lisado a un tubo con solución cOmplete™ EDTA-free Protease Inhibitor Cocktail (Sigma-Aldrich) y se transfirieron 10 µL a otro tubo para medir la actividad RLuc utilizando el Dual-Luciferase® Reporter Assay System (Promega). Las actividades de RLuc se determinaron utilizando un Luminómetro GloMax® 20/20 (Promega). Los volúmenes de extracto que representan las actividades RLuc equivalentes a RLU (Unidades Relativas de Luz) se cargaron en geles para la SDS-PAGE. Todos los ensayos se realizaron por triplicado.

VIII.5 Anticuerpos.

Se utilizó el anticuerpo DO-1(sc-126), que reconoce los residuos 21 a 25 (epítopo TADI) de p53; Pab1801 (sc-98), que reconoce los residuos 46-55 (epítopo TADII) de p53 y Δ40p53; y HR231 (sc-65226), que reconoce los residuos 371-380 (epítopo en el BR) de Δ133p53. Para la detección de las diferentes versiones de las proteínas de fusión E6-GFP, se utilizó el anticuerpo anti-GFP (B-2) (sc-9996 HRP). Además, se utilizó el anticuerpo actina (I-19) (sc-1616), el anticuerpo GAPDH (L-18) (sc-48167) y los anticuerpos secundarios IgG-HRP antiratón de cabra (sc-2005) y IgG-HRP anticabra de burro (sc-2020). Todos los anticuerpos se adquirieron en Santa Cruz Biotechnology Inc., Dallas, TX, EE.UU.

VIII.6 Extracción de proteínas y ensayos de Western blot.

Las proteínas totales de los cultivos celulares al 70-80% de confluencia se obtuvieron utilizando una solución tampón de lisis que contenía 150 mM de NaCl, 50 mM de Tris-HCl [pH 8], 1% (v/v) de Tritón X-100, 5 mM de EDTA, 1X de PMSF y 1.2 mg/mL de cOmplete™ EDTA-free Protease Inhibitor Cocktail (Sigma-Aldrich) Los extractos de proteínas se pasaron repetidamente a través de una aguja de calibre 22 y se centrifugaron durante 10 min a 13.000 rpm a 4 °C, el sobrenadante se recuperó en un tubo previamente enfriado y se utilizó inmediatamente o se almacenó a -80 °C hasta su análisis. Los lisados de proteínas se cuantificaron mediante el kit de ensayo de proteínas BCA de Pierce (Thermo Fisher Scientific).

Para los ensayos de Western Blot, 30 µg de lisados celulares totales se resolvieron en geles de SDS-PAGE al 12%, seguido de la transferencia a membranas

de nitrocelulosa que posteriormente se bloquearon con leche al 5% y TBS 1X-Tween 20 durante 1 h. Los anticuerpos contra p53 (DO-1, 1:1000), Δ40p53 (PAb1801, 1:1000), Δ133p53 (HR231, 1:1000), GAPDH (L-18, 1:10000) y actina (I-19, 1:10000) se incubaron durante la noche a 4 °C. Después, las membranas se incubaron con anticuerpos secundarios anti-IgG de ratón-HRP (1:10000) o anti-IgG de cabra-HRP (1:5000) durante 2 h a temperatura ambiente. Para la detección de las diferentes versiones de las proteínas de fusión E6-GFP, las membranas se incubaron con el anticuerpo anti-GFP (B-2) conjugado con HRP (1:1000) durante 1 h a temperatura ambiente. La señal se detectó por quimioluminiscencia según las instrucciones del fabricante (Millipore Corporation, Burlington, MA, EE. UU.). Las imágenes se capturaron con un escáner de Western Blot de quimioluminiscencia C-DiGit (LI-COR Biotechnology, Lincoln, NE, EE. UU.) y se analizaron y procesaron en el software Image Studio™ Lite versión 5.2 (LI-COR Biotechnology). El análisis densitométrico para cuantificar los niveles relativos de expresión de las proteínas se realizó con el software ImageJ 1.50i (National Institutes of Health, EE. UU.).

VIII.7 Ensayos de co-inmunoprecipitación.

Los ensayos de co-inmunoprecipitación (Co-IP) se realizaron por triplicado. Se sembraron 4 x 10^5 células H1299 por placa en placas de 60 mm y se realizaron ensayos de cotransfección utilizando 1 µg de plásmidos de expresión de las isoformas de p53 en combinación con plásmidos de expresión de las isoformas de E6. Tras la cotransfección, las células se lavaron con PBS 1X frío, se rasparon y se lisaron en 800 µL de tampón de inmunoprecipitación (tampón IP) (150 mM de NaCl, 50 mM de Tris-

HCl [pH 8.0], 1% (v/v) de NP-40 y cOmplete™ EDTA-free Protease Inhibitor Cocktail (Sigma-Aldrich), y los extractos de proteínas se obtuvieron como se especificó anteriormente. Los extractos de proteínas totales se rotaron suavemente durante 2 h a 4 °C con 30 µL de microesferas de sefarosa (Protein G Sepharose® Fast Flow) (Sigma-Aldrich) equilibradas en tampón IP, 0.5 mg/mL de RNasa A, DNasa y libre de proteasas (Thermo Fisher Scientific), con o sin 5 µg de anticuerpo Anti GFP (FL). La mezcla se giró suavemente durante 2 h a 4 °C. Las micfroesferas de sefarosa se lavaron cinco veces más con 1 mL de tampón IP frío, incubando durante 15 min en hielo entre cada lavado. Las Co-IP se analizaron mediante SDS-PAGE al 10% y Western blot. Se realizaron ensayos de Western blot para la detección de las variantes de empalme E6*I y E6*II (utilizando el anticuerpo anti-GFP-HRP) y las isoformas de p53 (utilizando los anticuerpos DO-1, PAb1801 y HR231).

VIII.8 Ensayos de apoptosis.

Se sembraron 3 x 10^5 células H1299, SiHa y HeLa por placa, en placas de cultivo de 60 mm por triplicado. Todas las líneas celulares se transfectaron transitoriamente con 1 µg de plásmidos de expresión de las isoformas de p53 o el vector pSV vacío y se incubaron durante 24 h a 37 °C con un 5% de CO_2. Posteriormente, las células transfectadas se trataron con cisplatino (Accocit, Accord Farma, S.A. De C.V., CDMX, Mx). La concentración inhibitoria media (IC50) del cisplatino se determinó mediante el ensayo colorimétrico de 4,5-dimetiltiazol-2-il)-2,5-difeniltetrazolio (MTT). Se utilizó una IC50 de 46 µg/mL de cisplatino para las células H1299 y una IC50 de 23 µg/mL para las células SiHa y HeLa y se incubaron además

durante 24 h a 37 °C con un 5% de CO_2. Las células transfectadas tratadas con cisplatino se cosecharon para determinar el nivel de apoptosis. Se utilizó Alexa Fluor® 647 Annexin V (Thermo Fisher Scientific) para las células H1299 y Alexa Fluor™ 488 Annexin V/Dead cell Kit (Thermo Fisher Scientific) para las células SiHa y HeLa, según las instrucciones del fabricante. Tras la inducción de la apoptosis, las células se lavaron una vez con 1X PBS y se separaron con 500 µL de EDTA al 0.02% (v/v). Se utilizaron células H1299, SiHa y HeLa sometidas a ebullición como controles de tinción positivos. Las células se recogieron y se centrifugaron a 3000 rpm durante 5 min a temperatura ambiente y los sobrenadantes se desecharon. Los paquetes de células se lavaron de nuevo con PBS 1X y se centrifugaron a 3000 rpm durante 5 min y se resuspendieron en tampón de unión a anexina 1X y anexina V con 100 µg/ml de yoduro de propidio. Las células se incubaron a temperatura ambiente durante 15 min protegidas de la luz. Después del periodo de incubación, se añadieron 350 µL de tampón de unión a anexina 1X y las células se mezclaron suavemente. Inmediatamente, las células teñidas se analizaron en un citómetro de flujo FACSCalibur™ (BD Biosciences, Franklin Lakes, NJ, EE.UU.).

Los niveles de apoptosis de las células transfectadas con isoformas de p53 se calcularon restando el porcentaje total de apoptosis de las células no transfectadas del porcentaje de apoptosis de las células transfectadas. Se registraron 10.000 eventos para cada tratamiento. Para el análisis de datos se utilizó el software FlowJo versión 10.1.

VIII.9 Análisis estadístico.

El análisis estadístico se realizó con GraphPad Prism v6.0 (GraphPad Software). Se empleó el análisis de ANOVA de una vía seguido del *post hoc* de Dunnett para determinar las diferencias significativas. Los datos se presentan como media ± error estándar de la media (SEM), y los valores con $p<0.05$ se consideraron estadísticamente significativos.

IX. RESULTADOS

*IX.1 E6 y E6*II del VPH-16 mostraron un efecto aparente sobre los niveles relativos de p53 y sus isoformas.*

La línea celular nula para p53 H1299 co-transfectada con plásmidos de expresión de las isoformas de E6 y los plásmidos de expresión de las isoformas de p53, se utilizó como un modelo para estudiar los efectos que $E6^{SD}$, E6, E6*I y E6*II del VPH-16 ejercen sobre los niveles relativos de p53, Δ40p53, y Δ133p53. La expresión ectópica de las isoformas de E6 del VPH-16 (Fig. 5, A y B), así como de las isoformas p53 (Fig. 5, C y D) se corroboró mediante Western blot. Se observó una disminución significativa de los niveles relativos de p53 debido a la expresión de E6 de longitud completa ($p=0.0006$) y $E6^{SD}$ ($p=0.0008$). Además, E6*II, una forma corta de la oncoproteína E6 fusionada con GFP [11, 50], también disminuyó significativamente el nivel de p53 ($p=0.0003$) (Fig. 5E). Por otro lado, los niveles relativos de Δ40p53 sólo se redujeron en presencia de E6 ($p= 0.0085$) y E6*II ($p=0.0003$) (Fig. 5F). En cambio, E6, E6*I o E6*II no afectaron los niveles relativos de Δ133p53 (Fig. 5G).

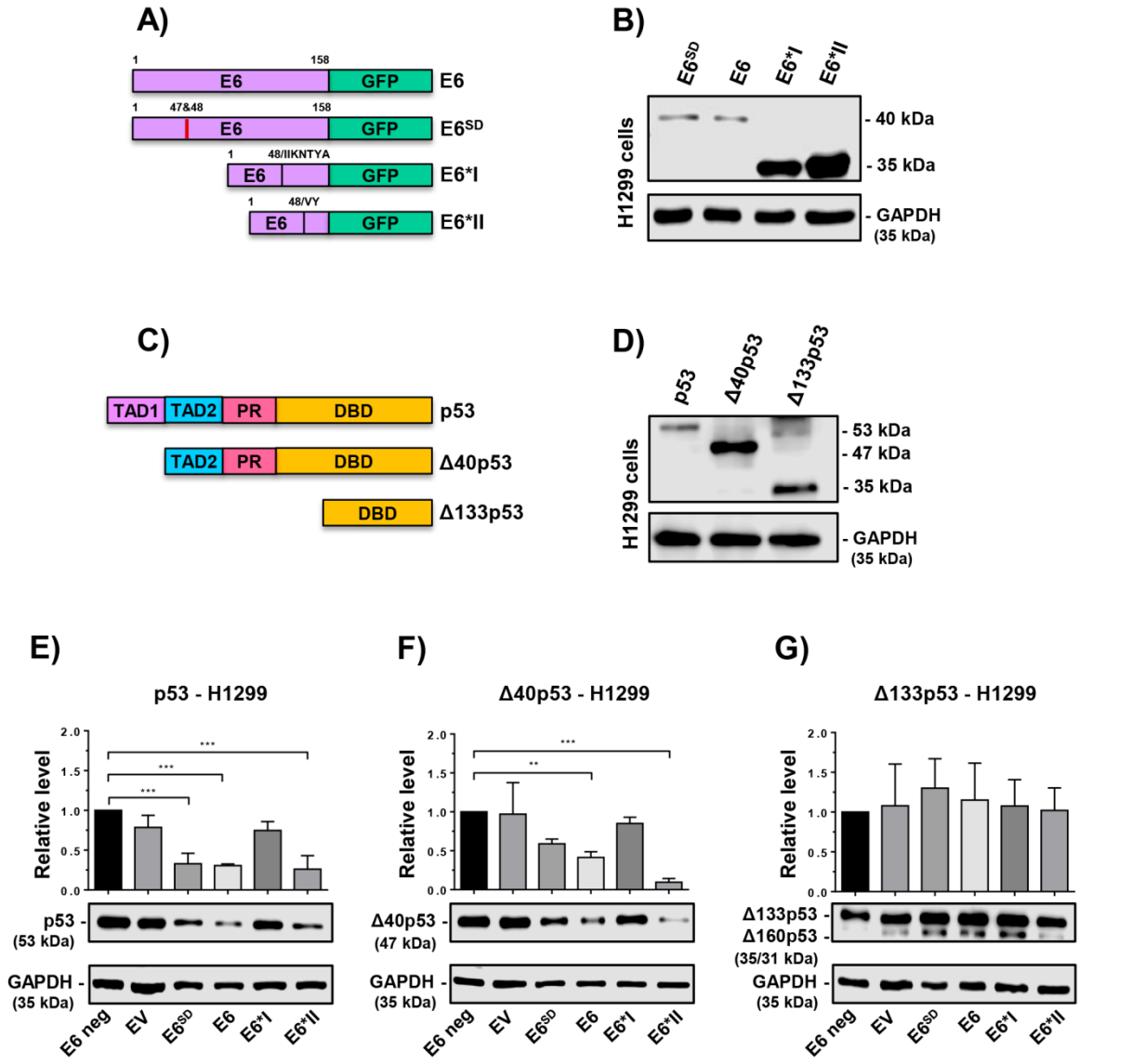

Figura 5. Niveles relativos de las isoformas de p53 en células H1299 co-transfectadas con diferentes versiones de E6 del VPH-16. (A) Representación esquemática de las proteínas de fusión E6-GFP, E6SD-GFP, E6*I-GFP y E6*II-GFP expresadas por los plásmidos donados por el Dr. Nicolás Villegas Sepúlveda [11, 50]; una línea roja vertical en $E6^{SD}$ indica las mutaciones aminoacídicas R47E y E48F; las isoformas E6*I y E6*II comparten los primeros 48 aminoácidos y se diferencian entre sí por los últimos aminoácidos; **(B)** la expresión de dichas proteínas de fusión se verificó por Western blot; **(C)** representación esquemática de las proteínas p53, Δ40p53 y Δ133p53 expresadas por los plásmidos donados por el Dr. Jean-Christophe Bourdon [13] y **(D)** la expresión de dichas proteínas se verificó por Western blot. Las células H1299 fueron co-transfectadas con 1 µg de los plásmidos de expresión de las isoformas de p53 y 2 µg de los plásmidos de expresión de las isoformas de E6 y se realizaron ensayos de inmunotransferencia para determinar los niveles relativos de **(E)** p53**, (F)** Δ40p53 y **(G)** Δ133p53**.** Se muestra un experimento representativo de tres experimentos independientes. E6 neg, son células H1299 transfectadas solo con p53, Δ40p53 o Δ133p53**;**

EV, es el vector vacío pEGFP-N1 y; $E6^{SD}$, es una mutante del sitio donante de empalme que no genera las variantes de empalme de E6. **p<0.01, ***p<0.001 *versus células* H1299 transfectadas sólo con p53 o Δ40p53.

*IX.2 E6*II pero no E6*I induce una disminución de los niveles relativos de p53.*

Es ampliamente conocido que E6 del VPH-16 induce la degradación de p53 por la vía dependiente de la ubiquitina-proteasoma [3-5], pero se desconoce si E6*I y E6*II provocan el mismo efecto a través de un mecanismo similar. Sin embargo, dado que nuestros hallazgos descritos anteriormente mostraron que $E6^{SD}$, E6 y E6*II inducen la degradación sólo de p53 y Δ40p53, co-transfectamos las células H1299 tanto con $E6^{SD}$, E6*I y E6*II del VPH-16 con p53 como con $E6^{SD}$, E6*I y E6*II del VPH-16 con Δ40p53 y posteriormente tratamos las células con el inhibidor MG-132 para bloquear la degradación mediante el proteasoma. Se observó un cambio notable en la proteína p53 en presencia de $E6^{SD}$ y E6*II cuando las células fueron tratadas con MG-132 (Fig. 6A). No se observaron cambios aparentes en p53 en presencia de la E6*I cuando el inhibidor MG-132 estaba presente (Fig. 6A). Tampoco se observaron cambios notables en la proteína Δ40p53 en las células H1299 co-transfectadas con E6*I y E6*II tratadas y no tratadas con MG132, lo que sugiere que Δ40p53 no es degradada por E6*I y E6*II a través de la vía dependiente de la ubiquitina-proteasoma (Fig. 6B).

Dado que $E6^{SD}$ mostró el mismo efecto aparente que E6 en la inducción de la disminución de los niveles de p53 y Δ40p53, se decidió excluir a $E6^{SD}$ de los análisis posteriores.

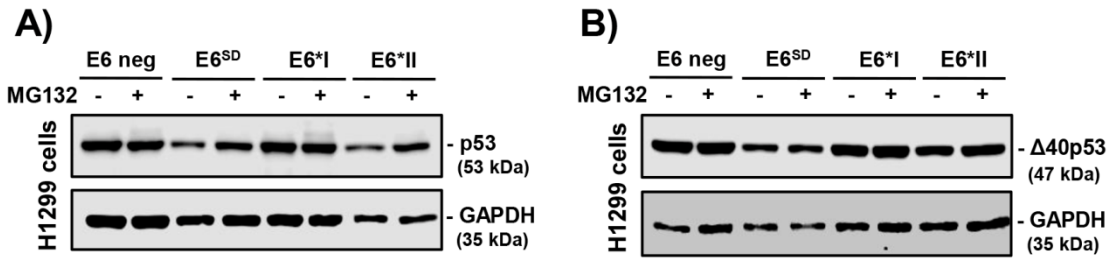

Figura 6. Expresión ectópica de p53 y Δ40p53 en la línea celular H1299 cotransfectada con isoformas de E6 del VPH-16 (+) tratada y (-) no tratada con el inhibidor del proteasoma MG132. Las células H1299 fueron co-transfectadas con 1 µg de p53 o Δ40p53 y con 2 µg de $E6^{SD}$, E6*I o E6*II. Inmunoblots representativos de tres experimentos independientes para **(A)** p53 y **(B)** Δ40p53 en células H1299 co-transfectadas. Las células H1299 transfectadas sólo con p53 o Δ40p53, denominadas E6 neg, se utilizaron como controles negativos. $E6^{SD}$: mutante del sitio donante de empalme que no genera las variantes de empalme E6*I y E6*II.

*IX.3 E6 y E6*II del VPH-16 se asocian con niveles reducidos de p53 pero no de Δ40p53 ni de Δ133p53.*

A continuación se realizaron ensayos de *Renilla* para descartar diferencias en la eficiencia de transcripción que interfirieran con los primeros hallazgos. Para ello, co-transfectamos células H1299 con plásmidos de expresión de las isoformas de p53 y plásmidos de expresión de las isoformas de E6, donde se analizaron los niveles de p53, Δ40p53 y Δ133p53 utilizando actividades RLuc equivalentes y se observó que los niveles de p53 disminuyeron en presencia de E6 y E6*II pero no en presencia de E6*I (Fig. 7, A y B), este resultado coincide con el observado en la Fig. 5E. Curiosamente y contrario a lo observado en la Fig. 5F, fue notorio que los niveles de Δ40p53 disminuyeron sólo en presencia de E6 (Fig. 7, A y C) y además, los niveles de Δ133p53 no mostraron cambios aparentes en presencia de E6, E6*I o E6*II (Fig. 7, A y D).

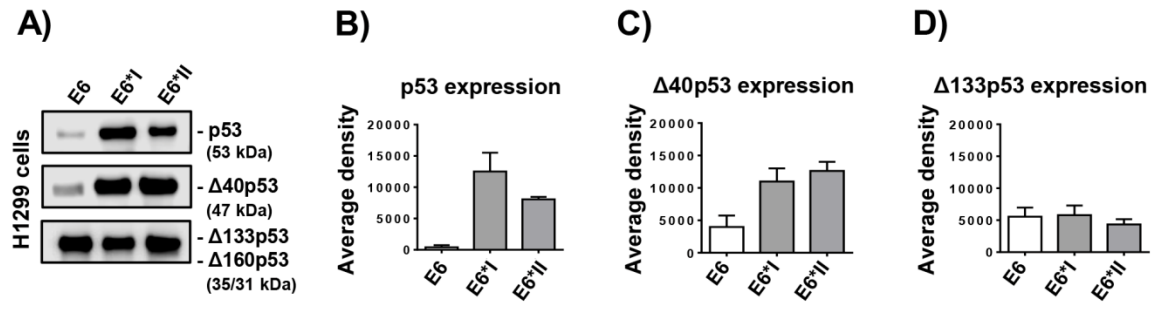

Figura 7. Densidad media de los niveles de las isoformas p53 en células H1299 co-transfectadas con diferentes proteínas E6. Las células H1299 fueron co-transfectadas con 1 µg de plásmidos de expresión de p53, Δ40p53 o Δ133p53, junto con 2 µg de plásmidos de expresión de E6, E6*I o E6*II y 50 ng de pRL-CMV *Renilla*. **(A)** La expresión ectópica de las proteínas p53, Δ40p53 y Δ133p53 se detectó mediante Western blot. Se muestra un experimento representativo de tres experimentos independientes. **(B, C y D)** Densidad media ± error estándar de la media (SEM) de las bandas de Western blot para p53, Δ40p53 o Δ133p53.

*IX.4 E6*II del VPH-16 interactúa con p53 pero no con Δ40p53 ni Δ133p53.*

Debido a los diferentes efectos promovidos por E6*I y E6*II del VPH-16 sobre los niveles relativos de las isoformas de p53, se utilizaron células H1299 co-transfectadas con E6*I o E6*II y con p53, Δ40p53 o Δ133p53 para realizar ensayos de co-inmunoprecipitación seguidos de Western blot, para analizar si E6*I y E6*II interactuaban con p53 o sus isoformas. Estos resultados revelaron que E6*I del VPH-16 no interactuó con p53, Δ40p53 o Δ133p53 (Fig. 8, A-C), de acuerdo con lo observado en la Fig. 7, A-D, donde los niveles relativos de p53, Δ40p53 y Δ133p53 no disminuyeron en presencia de E6*I. Por el contrario, E6*II del VPH-16 interactuó con p53 (Fig. 8D) pero no interactuó con Δ40p53 ni con Δ133p53 (Fig. 8, E y F).

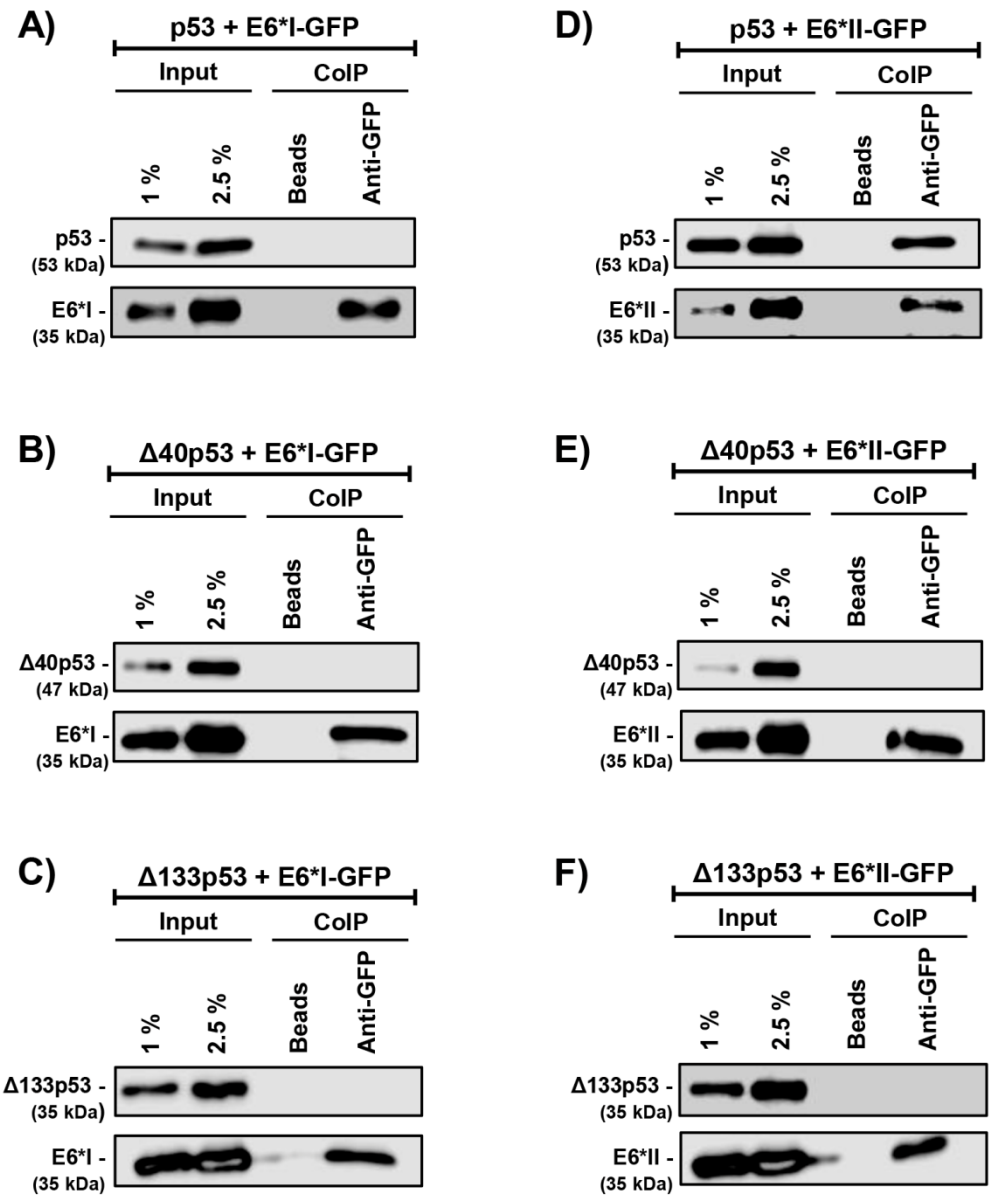

Figura 8. Ensayos de co-inmunoprecipitación (Co-IP) en células H1299 co-transfectadas con E6*I o E6*II del VPH-16 e isoformas de p53. Ensayo de Co-IP en células H1299 co-transfectadas con plásmidos de expression de **(A)** p53 y E6*I, **(B)** Δ40p53 y E6*I, **(C)** Δ133p53 y E6*I, **(D)** p53 y E6*II, **(E)** Δ40p53 y E6*II, y **(F)** Δ133p53 y E6*II. Los extractos de proteínas (input) se analizaron mediante Western blot utilizando el anticuerpo anti-GFP-HRP para la detección de E6*I y E6*II y los anticuerpos DO-1, Pab1801 y HR231 para la detección de p53, Δ40p53 y Δ133p53, respectivamente. Para todos los ensayos de Co-IP se muestra un experimento representativo de tres experimentos independientes.

IX.5 p53, Δ40p53 y Δ133p53 expresadas ectópicamente y en combinación con cisplatino aumentan la apoptosis en células H1299.

Para explorar el efecto de las diferentes isoformas de p53 en la inducción de la apoptosis y eliminar el fuerte efecto antiapoptótico ejercido por E6 [51-55], se transfectaron células H1299 con plásmidos de expresión de las isoformas de p53 y se evaluó la apoptosis mediante citometría de flujo. Se observó que la expresión ectópica de p53, Δ40p53 y Δ133p53 indujo un aumento de células apoptóticas (9.30%, p<0.0001; 9.12%, p<0.0001 y 6.84%, p=0.0005, respectivamente). Sin embargo, el porcentaje de células apoptóticas mostró un mayor incremento cuando las células H1299 fueron transfectadas con las isoformas de p53 y luego tratadas con cisplatino (Cis): p53+Cis (14.06%, p<0.0001), Δ40p53+Cis (11.03%, p<0.0001), y Δ133p53+Cis (7.34%, p=0.0195) (Fig. 9. A y B).

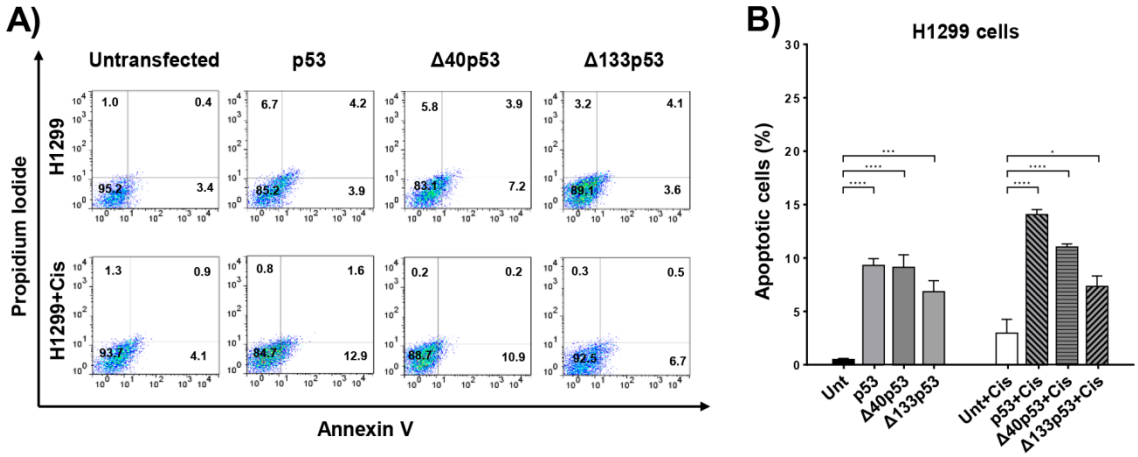

Figura 9. Detección de apoptosis mediante el ensayo de anexina V y yoduro de propidio (PI) en células H1299 transfectadas con p53, Δ40p53 o Δ133p53 tratadas y no tratadas con cisplatino. (A) Análisis de citometría de flujo representativo de la apoptosis en células H1299 transfectadas transitoriamente con isoformas de p53 tratadas y no tratadas con cisplatino (Cis). **(B)** Porcentaje de células apoptóticas. Las células apoptóticas se calcularon

como el porcentaje de células apoptóticas en la parte superior derecha y en la parte inferior derecha en relación con el número total de células (registrando 10.000 eventos). Los datos se presentan como la media ± el error estándar de tres experimentos independientes. ***p<0.001 y ****p<0.0001 frente al control (células H1299 no transfectadas con o sin Cis).

IX.6 La expresión ectópica de p53, Δ40p53 y Δ133p53 induce niveles diferentes de apoptosis en las líneas celulares SiHa y HeLa tratadas con cisplatino.

La pérdida de función de p53 en las células tumorales se asocia con la resistencia al tratamiento con cisplatino [56, 57], donde las células tumorales con p53 disfuncional no logran activar el programa de muerte celular apoptótica [57, 58]. El presente estudio evaluó el efecto apoptótico después de la expresión ectópica de las isoformas de p53 sola o en combinación con cisplatino, un fármaco convencional utilizado regularmente en la terapia del cáncer de cuello uterino [39], en células cancerosas que han perdido la función de p53 debido a la E6 del VPH-16 (SiHa) y del VPH-18 (HeLa). Estos resultados revelaron un efecto apoptótico significativo en las células SiHa con las combinaciones p53+Cis (14.19%, p=0.0006) y Δ40p53+Cis (13.35%, p=0.0014) (Fig. 10, A y B) y un efecto apoptótico significativo con la combinación p53+Cis (21.94%, p=0.0065) en las células HeLa (Fig. 10, C y D). No se observaron diferencias significativas en la apoptosis con la expresión ectópica de p53, Δ40p53 y Δ133p53 en las células SiHa y HeLa en ausencia de cisplatino (Fig. 10, A-D).

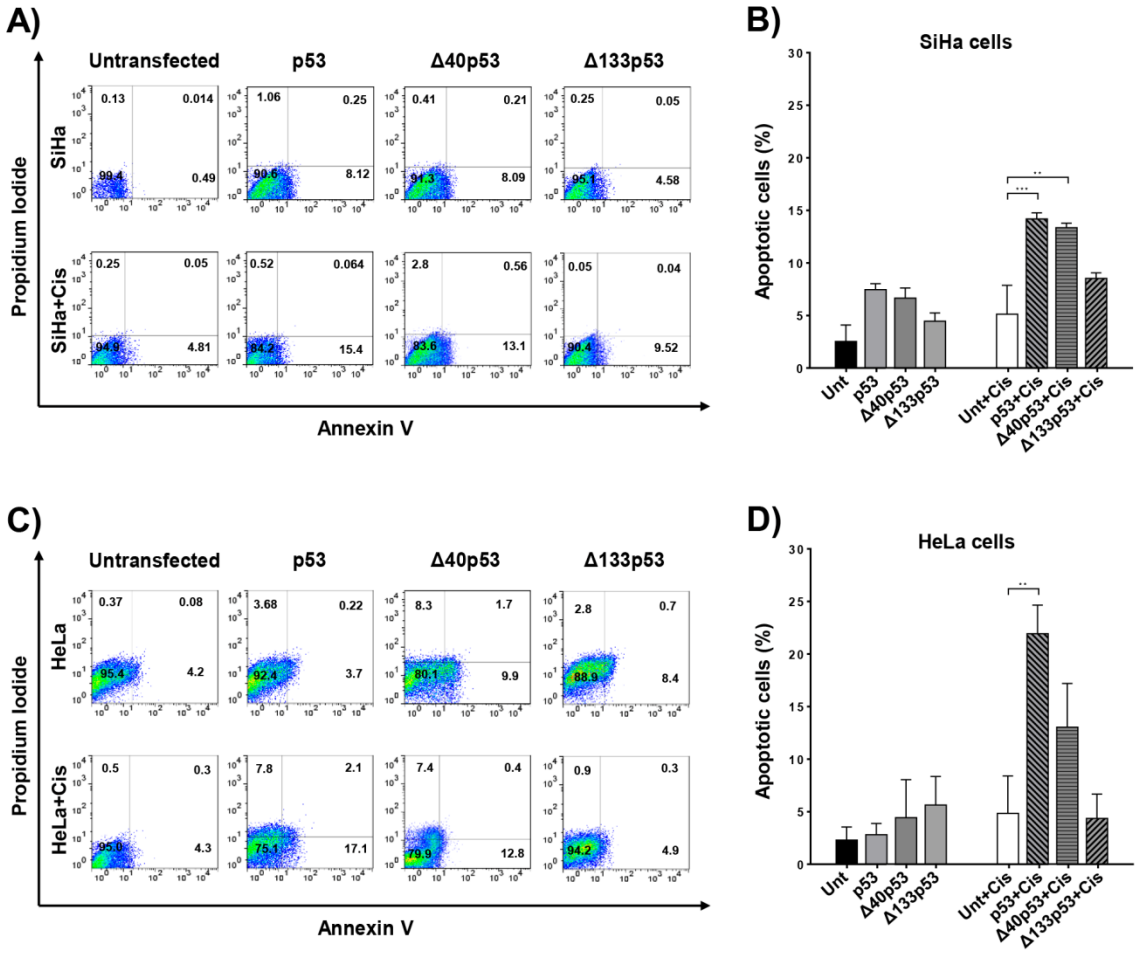

Figura 10. Detección de la apoptosis mediante el ensayo de anexina V y yoduro de propidio (PI) en líneas celulares SiHa y HeLa transfectadas con p53, Δ40p53 y Δ133p53 tratadas y no tratadas con cisplatino. Análisis de citometría de flujo representativo de la apoptosis en **(A)** células SiHa y **(C)** células HeLa transfectadas con isoformas de p53 tratadas y no tratadas con cisplatino (Cis). Porcentaje de células apoptóticas en **(B)** SiHa y **(D)** HeLa. Las células apoptóticas se calcularon como el porcentaje de células apoptóticas en la parte superior derecha y en la parte inferior derecha en relación con el número total de células (registrando 10.000 eventos). Los datos se presentan como la media ± el error estándar de tres experimentos independientes. **p<0.01 y ***p<0.001 frente al control (células SiHa y HeLa no transfectadas o células SiHa y HeLa no transfectadas + Cis).

X. DISCUSIÓN

La expresión y caracterización de las proteínas E6, E6*I y E6*II del VPH-16 está ampliamente establecida [59, 60] y se ha reportado su efecto sobre los niveles relativos de p53 en un modelo de células C33-A [11]. Sin embargo, no se han reportado los efectos de las diferentes proteínas E6 sobre las isoformas de p53. En el presente estudio, se evaluó el impacto de las proteínas E6, E6*I y E6*II del VPH-16 sobre los niveles relativos de p53, Δ40p53 y Δ133p53 y el efecto de estas isoformas de p53 en la apoptosis de líneas celulares de cáncer de pulmón y CaCu.

Los resultados obtenidos en este estudio muestran que E6 y E6*II, pero no E6*I del VPH-16, indujeron una disminución de los niveles de p53 (Fig. 5E) en el modelo de células H1299. El efecto de E6*II observado en los niveles de p53 en el presente estudio fue consistente con lo reportado por del Moral-Hernández, *et al*. [11].

En otro estudio, Camus, *et al.* reportan que la proteína E6 del VPH-16 no induce la degradación de Δ133p53α, Δ133p53β, y Δ133p53ɣ [61]. De forma similar, nuestros resultados muestran que E6, E6*I y E6*II del VPH 16 no afectaron a los niveles relativos de Δ133p53. Se ha sugerido que la falta de efecto de E6 sobre los niveles de las isoformas Δ133p53 (α, β y ɣ) puede deberse a la pérdida de los primeros 132 aminoácidos observada en dichas isoformas comparado con la p53 canónica [13], ya que dichos aminoácidos abarcan una región importante del DBD, región implicada en la interacción de E6 con E6AP, necesaria para la degradación posterior de p53 por la vía dependiente de la ubiquitina-proteasoma [4, 5]. No obstante, otro estudio sugiere que aunque la vía principal de degradación de p53 promovida por la oncoproteína E6 de los VPH-AR es dependiente del sistema ubiquitina-proteasoma, estos virus pueden

utilizar una vía independiente para promover la degradación de p53 [2]. Con base en las diferencias observadas en los efectos de E6*I y E6*II del VPH-16 en los niveles de p53, Δ40p53 y Δ133p53, se investigó la posible interacción de las variantes de empalme de E6 del VPH-16 con p53, Δ40p53 y Δ133p53. No se detectó ninguna interacción de E6*I del VPH-16 con p53, Δ40p53 o Δ133p53 utilizando ensayos de Co-IP, consistente con la falta de efecto en los niveles de proteína de las isoformas de p53 observadas en presencia de E6*I del VPH-16 (Fig. 5, E-G). En cambio, se detectó la interacción entre p53 y E6*II del VPH 16 (Fig. 8D), que está relacionada con la disminución de los niveles de p53 (Fig. 5E y Fig. 7, A y B). Curiosamente, no se observó la formación de un complejo entre E6*II y Δ40p53, lo que concuerda con la ausencia de cambios en los niveles de Δ40p53 en presencia de E6*II y del inhibidor del proteasoma MG132 (Fig. 6B) y con los hallazgos obtenidos con los ensayos de *Renilla* en los que analizamos los niveles de proteína Δ40p53 utilizando actividades RLuc equivalentes para realizar Western blot (Fig. 7, A y C).

Yin, *et al*. reportan que la isoforma Δ40p53 (también conocida como p53/p47, p47 y ΔNp53) podría inducir la apoptosis en las células H1299 (p53 nulas) [26]. Sin embargo, Δ40p53 puede actuar de forma dominante negativa inhibiendo la actividad transcripcional inducida por p53 y la apoptosis [24] y Δ40p53 por sí sola no induce la apoptosis en las células H1299 o Saos-2, ambas nulas para p53 [25]. En este studio, cuando se evaluó la apoptosis en las células H1299 transfectadas con p53, Δ40p53 o Δ133p53, fue observado un aumento considerable del porcentaje de apoptosis, especialmente cuando las células H1299 transfectadas fueron tratadas con cisplatino. No obstante, se observó que la expresión ectópica de p53 y Δ40p53 aumentó

significativamente los niveles de apoptosis en las células SiHa tratadas con cisplatino, pero en las células HeLa los niveles de apoptosis sólo aumentaban significativamente en presencia de p53 y cisplatino, lo que sugiere que el tipo de infección por VPH puede ser un factor determinante.

Se ha reportado que en las células C33A, una línea de CaCu negativa al VPH y que posee una versión alterada de p53 (mutación en el codón 273), E6*I y E6*II ectópicas ejercen efectos opuestos sobre la apoptosis [50]. En este caso, E6*II muestra un mayor efecto apoptótico que E6*I en presencia del tratamiento con cisplatino. La característica clave de nuestras células modelo de CaCu es la presencia de p53 de tipo silvestre que puede estar influyendo en las diferencias observadas. Curiosamente, nuestros hallazgos sugieren que Δ133p53 no indujo ningún efecto apoptótico significativo en las células tratadas con cisplatino, lo que fue más notable en las células HeLa que en las células SiHa. El efecto de Δ133p53 sobre la apoptosis de las células derivadas de CaCu no se había reportado. Sin embargo, utilizando la línea celular de osteosarcoma U2OS que expresa p53, Aoubala, *et al.* reportan que Δ133p53α inhibe la apoptosis mediada por p53 y la detención del ciclo celular en G1 pero no en G2 [17].

En este estudio se observaron diferencias en el efecto apoptótico en las células SiHa y HeLa tratadas con cisplatino. Varios informes apoyan la idea de que p53 no está totalmente inactivada en las líneas celulares de CaCu, en particular, las células HeLa muestran una mayor actividad transcripcional basal de p53 que las células SiHa [62], además de que ambas líneas celulares de cáncer poseen un número diferente de copias de VPH, lo que sugiere que la capacidad de inducir apoptosis entre los

tratamientos farmacológicos podría explicarse por estas diferencias. Con base en ésto, sugerimos que los tratamientos farmacológicos cuyo efecto dependen de la actividad de p53 pueden ser contrarrestados en presencia de las isoformas de p53 [63].

En el presente estudio se muestra el efecto de la expresión ectópica de la oncoproteína E6 del VPH-16 y de las isoformas E6*I y E6*II sobre los niveles relativos de las isoformas de p53, la interacción entre E6*II del VPH-16 y p53 y que la combinación de p53 o Δ40p53 con cisplatino induce un aumento de la apoptosis de las células cancerosas. Son necesarios más estudios para evaluar este efecto en modelos *in vivo* y esclarecer su papel en el tratamiento de los tumores asociados al VPH-16. Además, dado que los hallazgos sugieren que la combinación de p53 o Δ40p53 con cisplatino induce un aumento en la apoptosis de las células cancerosas que expresan las isoformas E6 del VPH-16, valdría la pena evaluar los niveles de las isoformas E6 y las isoformas p53 en pacientes con tumores positivos al VPH-16 para argumentar una posible respuesta antineoplásica. Es de gran interés el desarrollo de estrategias terapéuticas moleculares que aporten conocimientos para superar no sólo los problemas asociados a la fármacorresistencia, sino para mejorar la eficacia del cisplatino contra el cáncer.

XI. CONCLUSIÓN

Los hallazgos de este estudio muestran el efecto diferente de la expresión ectópica de la oncoproteína E6 y las variantes de empalme E6*I y E6*II del VPH-16 sobre los niveles relativos de las isoformas de p53, la interacción entre E6*II del VPH-16 y p53 y la inducción del aumento de la apoptosis de las células de cáncer que expresan dichas variantes de empalme en respuesta a la expresión ectópica de p53 o Δ40p53 sumada al tratamiento con cisplatino.

XII. REFERENCIAS

1. de Martel, C., et al., *Global burden of cancer attributable to infections in 2018: a worldwide incidence analysis.* Lancet Glob Health, 2020. **8**(2): p. e180-e190.
2. Camus, S., et al., *Ubiquitin-independent degradation of p53 mediated by high-risk human papillomavirus protein E6.* Oncogene, 2007. **26**(28): p. 4059-70.
3. Massimi, P., et al., *HPV E6 degradation of p53 and PDZ containing substrates in an E6AP null background.* Oncogene, 2008. **27**(12): p. 1800-4.
4. Scheffner, M., et al., *The HPV-16 E6 and E6-AP complex functions as a ubiquitin-protein ligase in the ubiquitination of p53.* Cell, 1993. **75**(3): p. 495-505.
5. Scheffner, M., et al., *The E6 oncoprotein encoded by human papillomavirus types 16 and 18 promotes the degradation of p53.* Cell, 1990. **63**(6): p. 1129-36.
6. Stewart, D., A. Ghosh, and G. Matlashewski, *Involvement of nuclear export in human papillomavirus type 18 E6-mediated ubiquitination and degradation of p53.* J Virol, 2005. **79**(14): p. 8773-83.
7. Martinez-Zapien, D., et al., *Structure of the E6/E6AP/p53 complex required for HPV-mediated degradation of p53.* Nature, 2016. **529**(7587): p. 541-5.
8. Filippova, M., et al., *The large and small isoforms of human papillomavirus type 16 E6 bind to and differentially affect procaspase 8 stability and activity.* J Virol, 2007. **81**(8): p. 4116-29.
9. Pim, D., V. Tomaic, and L. Banks, *The human papillomavirus (HPV) E6* proteins from high-risk, mucosal HPVs can direct degradation of cellular proteins in the absence of full-length E6 protein.* J Virol, 2009. **83**(19): p. 9863-74.
10. Filippova, M., et al., *The small splice variant of HPV16 E6, E6, reduces tumor formation in cervical carcinoma xenografts.* Virology, 2014. **450-451**: p. 153-164.
11. Del Moral-Hernandez, O., et al., *The HPV-16 E7 oncoprotein is expressed mainly from the unspliced E6/E7 transcript in cervical carcinoma C33-A cells.* Arch Virol, 2010. **155**(12): p. 1959-70.
12. Filippova, M., et al., *Complexes of human papillomavirus type 16 E6 proteins form pseudo-death-inducing signaling complex structures during tumor necrosis factor-mediated apoptosis.* J Virol, 2009. **83**(1): p. 210-27.
13. Bourdon, J.C., et al., *p53 isoforms can regulate p53 transcriptional activity.* Genes Dev, 2005. **19**(18): p. 2122-37.
14. Marcel, V., et al., *Delta160p53 is a novel N-terminal p53 isoform encoded by Delta133p53 transcript.* FEBS Lett, 2010. **584**(21): p. 4463-8.
15. Joruiz, S. M. and Bourdon, J.C., *p53 Isoforms: Key Regulators of the Cell Fate Decision*. Cold Spring Harb Perspect Med, 2016. **6**(8), a026039: p. 1-20.
16. Anbarasan, T. and J.C. Bourdon, *The Emerging Landscape of p53 Isoforms in Physiology, Cancer and Degenerative Diseases.* Int J Mol Sci, 2019. **20**(24).
17. Aoubala, M., et al., *p53 directly transactivates Delta133p53alpha, regulating cell fate outcome in response to DNA damage.* Cell Death Differ, 2011. **18**(2): p. 248-58.
18. Bourougaa, K., et al., *Endoplasmic reticulum stress induces G2 cell-cycle arrest via mRNA translation of the p53 isoform p53/47.* Mol Cell, 2010. **38**(1): p. 78-88.

19. Fujita, K., et al., *p53 isoforms Delta133p53 and p53beta are endogenous regulators of replicative cellular senescence.* Nat Cell Biol, 2009. **11**(9): p. 1135-42.
20. Surget, S., M.P. Khoury, and J.C. Bourdon, *Uncovering the role of p53 splice variants in human malignancy: a clinical perspective.* Onco Targets Ther, 2013. **7**: p. 57-68.
21. Khoury, M.P. and J.C. Bourdon, *p53 Isoforms: An Intracellular Microprocessor?* Genes Cancer, 2011. **2**(4): p. 453-65.
22. Takahashi, R., et al, *Dominant effects of Delta40p53 on p53 function and melanoma cell fate.* J Invest Dermatol, 2014. **134**(3): p. 791-800.
23. Marcel, V. and P. Hainaut, *p53 isoforms - a conspiracy to kidnap p53 tumor suppressor activity?* Cell Mol Life Sci, 2009. **66**(3): p. 391-406.
24. Courtois, S., et al., *DeltaN-p53, a natural isoform of p53 lacking the first transactivation domain, counteracts growth suppression by wild-type p53.* Oncogene, 2002. **21**(44): p. 6722-8.
25. Ghosh, A., D. Stewart, and G. Matlashewski, *Regulation of human p53 activity and cell localization by alternative splicing.* Mol Cell Biol, 2004. **24**(18): p. 7987-97.
26. Yin, Y., et al., *p53 Stability and activity is regulated by Mdm2-mediated induction of alternative p53 translation products.* Nat Cell Biol, 2002. **4**(6): p. 462-7.
27. Sharathchandra, A., A. Katoch, and S. Das, *IRES mediated translational regulation of p53 isoforms. Wiley Interdiscip Rev RNA,* 2013 **5**(1): p. 131–139.
28. Hafsi, H., D. Santos-Silva, S. Courtois-Cox, et al., *Effects of Δ40p53, an isoform of p53 lacking the N-terminus, on transactivation capacity of the tumor suppressor protein p53*. BMC Cancer, 2013. **13**(134): p 1-10.
29. Kitayner, M., H. Rozenberg, N. Kessler, et al., *Structural Basis of DNA Recognition by p53 Tetramers*. Molecular Cell, 2006. **22**(6): p. 741–753.
30. Horikawa, I., K. Park, K. Isogaya, et al., *Δ133p53 represses p53-inducible senescence genes and enhances the generation of human induced pluripotent stem cells.* Cell Death Differ, 2017. **24**(6): p. 1017-1028.
31. Fujita K., *p53 Isoforms in cellular senescence- and ageing-associated biological and physiological functions.* Int J Mol Sci., 2019. **20**(23), 6023: p. 1-19.
32. Avery-Kiejda, K.A., et al., *Small molecular weight variants of p53 are expressed in human melanoma cells and are induced by the DNA-damaging agent cisplatin.* Clin Cancer Res, 2008. **14**(6): p. 1659-68.
33. Fragou, A., et al., *Increased Delta133p53 mRNA in lung carcinoma corresponds with reduction of p21 expression.* Mol Med Rep, 2017. **15**(4): p. 1455-1460.
34. Hofstetter, G., et al., *The N-terminally truncated p53 isoform Delta40p53 influences prognosis in mucinous ovarian cancer.* Int J Gynecol Cancer, 2012. **22**(3): p. 372-9.
35. Hofstetter, G., et al., *Delta133p53 is an independent prognostic marker in p53 mutant advanced serous ovarian cancer.* Br J Cancer, 2011. **105**(10): p. 1593-9.

36. Nutthasirikul, N., et al., *Ratio disruption of the 133p53 and TAp53 isoform equilibrium correlates with poor clinical outcome in intrahepatic cholangiocarcinoma.* Int J Oncol, 2013. **42**(4): p. 1181-8.
37. Takahashi, R., et al., *p53 isoform profiling in glioblastoma and injured brain.* Oncogene, 2013. **32**(26): p. 3165-74.
38. Boldrup, L., et al., *Expression of p53 isoforms in squamous cell carcinoma of the head and neck.* Eur J Cancer, 2007. **43**(3): p. 617-23.
39. WHO, *WHO (World Health Organization) Model List of Essential Medicines, 20th List (April 2017, amended August 2017).* 2017: p. https://www.who.int/publications/i/item/eml-20.
40. Dasari, S. and Tchounwou, P.B., *Cisplatin in cancer therapy: molecular mechanisms of action.* Eur J Pharmacol. 2014. **5**(740): 364-78.
41. Ghosh, S., *The first metal based anticancer drug. Bioorg Chem.* 2019. **88**,102925: p. 1-20.
42. Bhattacharjee, R., et al., *Cellular landscaping of cisplatin resistance in cervical cancer.* Biomed Pharmacother. 2022. **153**:113345.
43. Giaccone, G., et al., *Neuromedin B is present in lung cancer cell lines.* Cancer Res, 1992. **52**(9 Suppl): p. 2732s-2736s.
44. Fries, K.L., W.E. Miller, and N. Raab-Traub, *Epstein-Barr virus latent membrane protein 1 blocks p53-mediated apoptosis through the induction of the A20 gene.* J Virol, 1996. **70**(12): p. 8653-9.
45. Tsai, C.M., et al., *Correlations between intrinsic chemoresistance and HER-2/neu gene expression, p53 gene mutations, and cell proliferation characteristics in non-small cell lung cancer cell lines.* Cancer Res, 1996. **56**(1): p. 206-9.
46. Diao, M.K., et al., *Integrated HPV genomes tend to integrate in gene desert areas in the CaSki, HeLa, and SiHa cervical cancer cell lines.* Life Sci, 2015. **127**: p. 46-52.
47. Meissner, J.D., *Nucleotide sequences and further characterization of human papillomavirus DNA present in the CaSki, SiHa and HeLa cervical carcinoma cell lines.* J Gen Virol, 1999. **80 (Pt 7)**: p. 1725-1733.
48. Pater, M.M. and A. Pater, *Human papillomavirus types 16 and 18 sequences in carcinoma cell lines of the cervix.* Virology, 1985. **145**(2): p. 313-8.
49. Yaginuma, Y. and H. Westphal, *Analysis of the p53 gene in human uterine carcinoma cell lines.* Cancer Res, 1991. **51**(24): p. 6506-9.
50. Vaisman, C.E., et al., *C33-A cells transfected with E6*I or E6*II the short forms of HPV-16 E6, displayed opposite effects on cisplatin-induced apoptosis.* Virus Res, 2018. **247**: p. 94-101.
51. DeFilippis, R.A., et al., *Endogenous human papillomavirus E6 and E7 proteins differentially regulate proliferation, senescence, and apoptosis in HeLa cervical carcinoma cells.* J Virol, 2003. **77**(2): p. 1551-63.
52. Duerksen-Hughes, P.J., J. Yang, and S.B. Schwartz, *HPV 16 E6 blocks TNF-mediated apoptosis in mouse fibroblast LM cells.* Virology, 1999. **264**(1): p. 55-65.

53. Filippova, M., et al., *The human papillomavirus 16 E6 protein binds to tumor necrosis factor (TNF) R1 and protects cells from TNF-induced apoptosis.* J Biol Chem, 2002. **277**(24): p. 21730-9.
54. Shimada, M., et al., *The human papillomavirus E6 protein targets apoptosis-inducing factor (AIF) for degradation.* Sci Rep, 2020. **10**(1): p. 14195.
55. Thomas, M. and L. Banks, *Inhibition of Bak-induced apoptosis by HPV-18 E6.* Oncogene, 1998. **17**(23): p. 2943-54.
56. Chao, C.C., *Decreased accumulation as a mechanism of resistance to cis-diamminedichloroplatinum(II) in cervix carcinoma HeLa cells: relation to DNA repair.* Mol Pharmacol, 1994. **45**(6): p. 1137-44.
57. Siddik, Z.H., *Cisplatin: mode of cytotoxic action and molecular basis of resistance.* Oncogene, 2003. **22**(47): p. 7265-79.
58. Minagawa, Y., et al., *Cisplatin-resistant HeLa cells are resistant to apoptosis via p53-dependent and -independent pathways.* Jpn J Cancer Res, 1999. **90**(12): p. 1373-9.
59. Doorbar, J., et al., *Detection of novel splicing patterns in a HPV16-containing keratinocyte cell line.* Virology, 1990. **178**(1): p. 254-62.
60. Smotkin, D., H. Prokoph, and F.O. Wettstein, *Oncogenic and nononcogenic human genital papillomaviruses generate the E7 mRNA by different mechanisms.* J Virol, 1989. **63**(3): p. 1441-7.
61. Camus, S., et al., *The p53 isoforms are differentially modified by Mdm2.* Cell Cycle, 2012. **11**(8): p. 1646-55.
62. Hietanen, S., et al., *Activation of p53 in cervical carcinoma cells by small molecules.* Proc Natl Acad Sci U S A, 2000. **97**(15): p. 8501-6.
63. Chen, J., et al., *p53 isoform delta113p53 is a p53 target gene that antagonizes p53 apoptotic activity via BclxL activation in zebrafish.* Genes Dev, 2009. **23**(3): p. 278-90.

XIII. ANEXOS

XIII.1 Artículo científico original: Antonio-Véjar, et al. Pathology- Research and Practice. 2022.

Pathology - Research and Practice 234 (2022) 153890

Contents lists available at ScienceDirect

Pathology - Research and Practice

journal homepage: www.elsevier.com/locate/prp

New insights into the interactions of HPV-16 E6*I and E6*II with p53 isoforms and induction of apoptosis in cancer-derived cell lines

Verónica Antonio-Véjar [a,b,e], Elizabeth Ortiz-Sánchez [c], Pedro Rosendo-Chalma [a,e], Carlos C. Patiño-Morales [e,1], Miriam C. Guido-Jiménez [e], Eduardo Alvarado-Ortiz [d,e], Greco Hernández [c], Alejandro García-Carrancá [e,*]

[a] Programa de Doctorado en Ciencias Biomédicas, Universidad Nacional Autónoma de México (UNAM), Ciudad de México, 10450, Mexico
[b] Laboratorio de Biomedicina Molecular, Facultad de Ciencias Químico Biológicas, Universidad Autónoma de Guerrero, Chilpancingo, 39090, Guerrero, Mexico
[c] Subdirección de Investigación Básica, Instituto Nacional de Cancerología, Ciudad de México, 14080, Mexico
[d] Programa de Posgrado en Ciencias Biológicas. Universidad Nacional Autónoma de México (UNAM), Ciudad de México, 04510, Mexico
[e] Unidad de Investigación Biomédica en Cáncer, Instituto de Investigaciones Biomédicas, Universidad Nacional Autónoma de México and Instituto Nacional de Cancerología, Ciudad de México, 14080, Mexico

ARTICLE INFO

Keywords:
Cervical cancer
Human Papillomavirus
E6
p53
Apoptosis

ABSTRACT

An important characteristic of cancers associated with high-risk human papillomaviruses (HR-HPV) is the inability of p53 to activate apoptosis due to the effect of the oncoprotein E6. However, the effect of HPV-16 E6 splice variant isoforms (namely E6*I and E6*II), their interaction with the existing p53 isoforms, and their influence on apoptosis is unclear. Here, we report the outcome of ectopic expression of HPV-16 E6, E6*I, and E6*II on the relative levels of p53 and p53 isoforms Δ40p53 and Δ133p53 and their interactions with these proteins. Additionally, we evaluated the effect of ectopic expression of p53, Δ40p53, and Δ133p53 on apoptosis in a p53 null pulmonary cell line (H1299) co-transfected with E6 isoforms and $p53^{+/+}$ cell lines with HR-HPV (SiHa and HeLa), transfected with p53 isoforms and treated with cisplatin, a conventional drug used to treat cervical cancer. Our results show that E6 and E6*II induced a significant decrease in p53, but only E6 triggered a Δ40p53 decrease and that E6*II interacts with p53 but not with Δ40p53 and Δ133p53. On the other hand, E6*I did not show any effect or interaction with the p53 isoforms. We found that apoptosis was elevated in H1299 cells transfected with p53 ($p = 0.0001$) and Δ40p53 ($p = 0.0001$). A weak apoptotic effect was observed when Δ133p53 was ectopically expressed ($p = 0.0195$). We observed that both p53 ($p = 0.0006$) and Δ40p53 ($p = 0.0014$) induced apoptosis in cisplatin-treated SiHa cells; however in cisplatin-treated HeLa cells, only p53 induced apoptosis ($p = 0.0029$). No significant differences in apoptosis were observed upon ectopic expression of p53, Δ40p53, and Δ133p53 in SiHa and HeLa cells. Our findings suggest a possible therapeutic application for the combining of p53 or Δ40p53 with cisplatin to induce an increased apoptosis of cancer cells expressing E6 isoforms from HPV-16.

1. Introduction

A recent study based on the GLOBOCAN 2018 database reported that high-risk human papillomavirus (HR-HPV) types 16 and 18 cause 72% of all HPV-attributable cancers and that types 31, 33, 45, 52, and 58 are detected in an additional 17% of cervical cancer incidence [1]. It is well established that HR-HPV oncoprotein E6 binds to p53 via E6-AP and promotes its degradation through a ubiquitin-proteasome-dependent pathway that contributes to the oncogenicity of these viruses [2–7].

A bicistronic pre-mRNA encodes HPV-16 E6 and E7 oncoproteins. In

* Correspondence to: Laboratorio de Virus y Cáncer, Unidad de Investigación Biomédica en Cáncer, Instituto Nacional de Cancerología, Secretaría de Salud, Avenida San Fernando No. 22, Colonia Sección XVI, Delegación Tlalpan, CP 14080, Ciudad de México, México.
E-mail addresses: 11335@uagro.mx (V. Antonio-Véjar), eortizs@incan.edu.mx (E. Ortiz-Sánchez), peterchalma@hotmail.com (P. Rosendo-Chalma), cpatino@cua.uam.mx (C.C. Patiño-Morales), mguido@iibiomedicas.unam.mx (M.C. Guido-Jiménez), eduralv.o@gmail.com (E. Alvarado-Ortiz), ghernandezr@incan.edu.mx (G. Hernández), carranca@biomedicas.unam.mx (A. García-Carrancá).
[1] Laboratorio de Investigación en Biología del Desarrollo y Teratogénesis Experimental, Hospital Infantil de México Federico Gómez, Ciudad de México, CP 06720, México

https://doi.org/10.1016/j.prp.2022.153890
Received 8 January 2022; Received in revised form 4 April 2022; Accepted 6 April 2022
Available online 9 April 2022
0344-0338/

addition to generating the mature E6 transcript, this pre-mRNA generates alternatively spliced transcripts encoding E6*I, E6*II, and E6^E7 [8,9]. Protein products generated from the HPV-16 E6*I and E6*II transcripts are quite similar, differing only in at least 7 amino acids [10]. Some studies suggest that the HPV-16 E6 splice variants might play different cellular roles. For example, E6*I has been attributed with partial or similar functions to E6. It can also play an antagonistic role by inhibiting the oncogenic activities of E6 [10–12]. The effect of HPV-16 E6*II on the carcinogenesis of the uterine cervix has not been well elucidated.

In humans, the *TP*53 gene can express up to nine different messenger RNA isoforms encoding 12 different functional p53 variants [13,14], generated either by alternative splicing, alternative promoters or, alternative translation initiation sites [13,15]. p53 isoforms are involved in a variety of diverse functions, including response against cellular stress, DNA damage repair mechanisms, cell cycle arrest, apoptosis, and cellular senescence [16–20].

p53 isoforms differ from full-length p53 by the absence of structural and functional domains that can alter the essential biochemical properties for the suppressor function of p53, and only one region of the DNA-binding domain (DBD) (residues 133–257) is common for all isoforms [21]. Δ40p53 and Δ133p53 isoforms lack amino acids 1–39 and 1–132, respectively. Furthermore, Δ40p53 lacks the first N-terminal transactivation domain (TADI) but maintains the TADII and the DBD, whereas Δ133p53 lacks both TADs and a conserved region of the DBD [13,22–24]. In addition, all isoforms have α, β, and γ C-terminal versions [13]. This suggests that the p53 isoforms exert their effects either through their autonomous functional properties, different from p53, and or by modulating p53 activity [21]. Moreover, p53 isoform expression is tissue-specific, and anomalous expression patterns have been observed in several malignant diseases [13,25]. Δ40p53 and Δ133p53 expression has been studied in melanoma, colorectal cancer, ovarian cancer, cholangiocarcinoma, glioblastoma, lung cancer, and squamous cell carcinoma of the head and neck [18,26–32], suggesting a key role for the abnormal expression of these isoforms in the development and progression of cancer.

Since the role of HPV-16 E6*I and E6*II during uterine cervix carcinogenesis, as well as their interplay with p53 isoforms, has not been analyzed, the aim of the present study was to determine the effect of ectopic expression of HPV-16 E6 and the E6*I and E6*II splice variants on the relative levels of p53 isoforms and their interaction with these proteins. Additionally, the effect of ectopic expression of p53, Δ40p53, and Δ133p53 on apoptosis was evaluated in a p53 null cell line, derived from non-small cell lung cancer (H1299), and in $p53^{+/+}$ cell lines positive for HPV-16 (SiHa) and HPV-18 (HeLa) and that were additionally treated with cisplatin, a conventional drug commonly used for cervical cancer therapy [33].

2. Materials and methods

2.1. Cell culture conditions

The human cell lines H1299 (ATCC® CRL-5803™) derived from non-small cell lung cancer [34] and null for p53 [35,36], SiHa (ATCC® HTB-35™) derived from grade II cervical squamous cell carcinoma with HPV-16 [37–39] and wild-type p53 ($p53^{+/+}$) [40], and HeLa (ATCC® CRM-CCL-2) derived from uterine cervical adenocarcinoma with HPV-18 [37–39] and wild-type $p53^{+/+}$ [40] were obtained from the American Type Culture Collection (ATCC, Manassas, VA, USA). H1299 cells were cultured in RPMI (Thermo Fisher Scientific, Inc., USA), and SiHa and HeLa cell lines were cultured in DMEM (Thermo Fisher Scientific, Inc., USA). All cells were supplemented with 10% fetal bovine serum (Thermo Fisher Scientific, Inc., USA) and 100 U/mL penicillin/streptomycin (Thermo Fisher Scientific, Inc., USA), and were incubated at 37 °C in a humidified atmosphere with 5% CO_2.

2.2. Plasmids

The empty pSV vector and plasmids expressing p53 (pSV-p53) and p53 isoforms (pSV-Δ40p53, pSV-Δ133p53), subsequently referred to as plasmids expressing p53 isoforms, were kindly donated by Dr. Jean-Christophe Bourdon (Dundee Cancer Center, University of Dundee, UK) [13]. Plasmids expressing HPV-16 E6-GFP fusion proteins ($E6^{SD}$-GFP, E6-GFP, E6*I-GFP, E6*II-GFP), subsequently referred to as plasmids expressing E6 isoforms, and the empty vector pEGFP-N1 were kindly provided by Dr. Nicolás Villegas Sepúlveda (Departamento de Biomedicina Molecular, Centro de Investigación y de Estudios Avanzados-IPN (CINVESTAV-IPN), Ciudad de México). The plasmid pRL-CMV (*Renilla* luciferase reporter vector) (Promega) was used for normalization of transfection in Western blot assay.

2.3. Transfections and co-transfections

A total of 4×10^5 H1299 cells per dish were seeded on 60 mm dishes in triplicate, and transient transfections and co-transfections were performed using Lipofectamine® Reagent and Plus™ Reagent (Thermo Fisher Scientific) according to the manufacturer's protocol. For transient transfections, 1 μg of plasmids expressing p53 isoforms or empty pSV vector, as transfection control, were used. For co-transfection, 2 or 4 μg of each of the plasmids expressing E6 isoforms or the empty pEGFP-N1 vector were used in combination with 1 μg of plasmids expressing p53 isoforms or empty pSV vector. Transfected and co-transfected H1299 cells were further incubated for 24 h at 37 °C with 5% CO_2. Additionally, co-transfected H1299 cells were treated with 20 μM of MG-132 proteasome inhibitor (Sigma-Aldrich) and were further incubated for 4 h at 37 °C with 5% CO_2. Subsequently, protein extraction for the transfected and co-transfected H1299 cells was performed.

On the other hand, a total of 4×10^5 SiHa and HeLa cells were seeded in 60 mm dishes in triplicate, and transient transfections were performed using Lipofectamine® Reagent and Plus™ Reagent (Thermo Fisher Scientific) according to the manufacturer's recommendations. For transfections, 1 μg of plasmids expressing p53 isoforms or empty pSV vector, as a transfection control, were used. Cells were further incubated for 4 h at 37 °C with 5% CO_2.

2.4. Renilla luciferase activity

Renilla luciferase (RLuc) activity was used as an internal normalization standard for SDS-PAGE as follows: a total of 2×10^5 H1299 cells were seeded on 6-well plates with complete medium and co-transfected with 1 μg of plasmids expressing p53 isoforms, 2 μg of the plasmids expressing E6 isoforms and 50 ng of pRL-CMV *Renilla*. Co-transfections were performed using Lipofectamine™ 3000 Transfection Reagent (Thermo Fisher Scientific) according to the manufacturer's protocol. 24 h after transfection H1299 cells were vigorously scrapped with 150 μl of PBL (Passive lysis buffer, Promega) with a rubber policeman. 100 μl of lysate were transfer onto a tube with cOmplete™ EDTA-free Protease Inhibitor Cocktail (Sigma-Aldrich) and 10 μl were transfer to another tube to measure RLuc activity using the Dual-Luciferase® Reporter Assay System (Promega). RLuc activities were determined using a Glo-Max® 20/20 Luminometer (Promega). Extract volumes representing equivalent RLuc activities to RLU (Relative Units of Light) were loaded on SDS-PAGE gels. All assays were carried out in triplicate.

2.5. Protein extraction

For transient transfection and co-transfection assays, total protein was obtained from cell cultures at 70–80% confluency using a lysis buffer solution containing 150 mM NaCl, 50 mM Tris-HCl [pH 8], 1% (v/v) Triton X-100, 5 mM EDTA, 1X PMSF, and 1.2 mg/mL cOmplete™ EDTA-free Protease Inhibitor Cocktail (Sigma-Aldrich). Protein extracts were forced repeatedly through a 22-gauge needle and were centrifuged

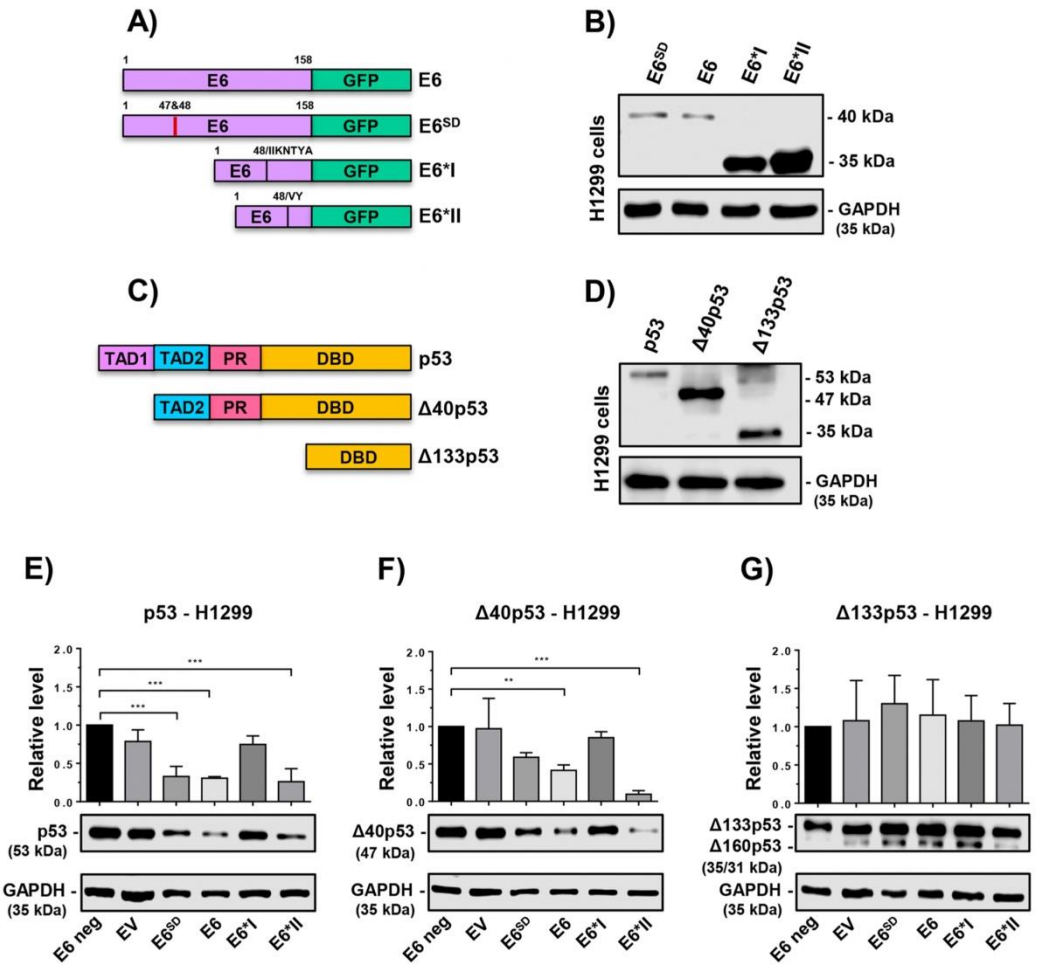

Fig. 1. Relative levels of p53 isoforms in H1299 cells co-transfected with different versions of HPV-16 E6. (A) Schematic representation of the fusion proteins E6-GFP, E6SD-GFP, E6*I-GFP and E6*II-GFP expressed by the plasmids kindly donated by Dr. Nicolás Villegas Sepúlveda [11,41]; a vertical red line in $E6^{SD}$ indicates amino acid mutations R47E and E48F; isoforms E6*I and E6*II share the first 48 amino acids and differ from each other by the last amino acids; (B) the expression of such fusion proteins was verified by Western blot. (C) Schematic representation of the proteins p53, Δ40p53, and Δ133p53 expressed by the plasmids kindly donated by Dr. Jean-Christophe Bourdon [13] and (D) the expression of such proteins was verified by Western blot. H1299 cells were co-transfected with 1 μg of plasmids expressing p53 isoforms and 2 μg of plasmids expressing E6 isoforms and immunoblot assays were done to determine relative protein levels of (E) p53, (F) Δ40p53 and (G) Δ133p53. E6 neg, are H1299 cells transfected only with p53 or Δ40p53; EV, is empty vector pEGFP N1 and; $E6^{SD}$, is a splice donor site mutant that does not generate the short forms of E6. $^{**}p < 0.01$, $^{***}p < 0.001$ versus H1299 cells E6 neg.

for 10 min at 13,000 rpm at 4 °C, the supernatant was recovered in a previously cooled tube and either used immediately or stored at − 80 °C until analysis. Protein lysates were quantified by Pierce BCA Protein Assay Kit (Thermo Fisher Scientific).

2.6. Antibodies

We used the DO-1(sc-126) antibody, that recognizes residues 21–25 (TADI epitope) of p53; Pab1801 (sc-98), that recognizes residues 46–55 (TADII epitope) of p53 and Δ40p53; and HR231 (sc-65226), that recognizes residues 371–380 (epitope in the BR) of Δ133p53. For detection of the different versions of E6-GFP fusion proteins, the anti-GFP antibody (B-2) (sc-9996 HRP) was used. In addition, actin antibody (I-19) (sc-1616), GAPDH antibody (L-18) (sc-48167), and the secondary antibodies goat anti-mouse IgG-HRP (sc-2005) and donkey anti-goat IgG-HRP (sc-2020) were used. All antibodies were purchased from Santa Cruz Biotechnology.

2.7. Western blot

Thirty micrograms of total cell lysates were resolved on 12% SDS-PAGE gels followed by transfer to nitrocellulose membranes and were

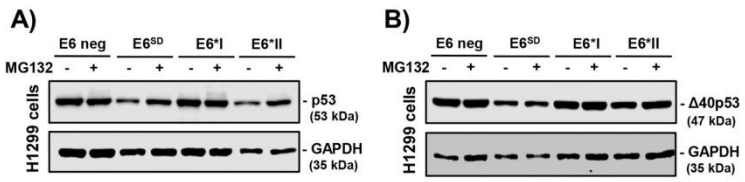

Fig. 2. Ectopic expression of p53 and Δ40p53 in the H1299 cell line co-transfected with HPV-16 E6 isoforms (+) treated and (-) untreated with MG132 proteasome inhibitor. H1299 cells were co-transfected with 1 μg of p53 or Δ40p53 and with 2 μg of $E6^{SD}$, E6*I or E6*II. Representative immunoblots for (A) p53 and (B) Δ40p53 in H1299 cells co-transfected. H1299 cells transfected only with p53 or Δ40p53, denominated as E6 neg, were used as negative controls. $E6^{SD}$: splice donor site mutant that does not generate the short forms of E6.

blocked with 5% milk and TBS 1X-Tween 20 for 1 h. Antibodies against p53 (DO-1, 1:1000), Δ40p53 (PAb1801, 1:1000), Δ133p53 (HR231, 1:1000), GAPDH (L-18, 1:10000) and actin (I-19, 1:10000) were incubated overnight at 4 °C. Subsequently, membranes were incubated with secondary antibodies anti-mouse IgG-HRP (1:10000) or anti-goat IgG-HRP (1:5000) for 2 h at room temperature. For the detection of different versions of E6-GFP fusion proteins, the anti-GFP Antibody (B-2) conjugated to HRP (1:1000) was incubated for 1 h at room temperature. The signal was detected by chemiluminescence according to the manufacturer's instructions (Millipore). The images were captured using a C-DiGit Chemiluminescence Western Blot Scanner (LI-COR Biotechnology) and were analyzed and processed in the Image Studio™ Lite version 5.2 software (LI-COR Biotechnology). Densitometric analysis to quantify protein expression levels was performed using ImageJ 1.50i software (National Institutes of Health, USA).

2.8. Co-immunoprecipitation assays

Co-immunoprecipitation (Co-IP) assays were performed in triplicate. A total of 4×10^5 H1299 cells per dish were seeded on 60 mm dishes and co-transfection assays were performed using 1 μg of plasmids expressing p53 isoforms in combination with plasmids expressing E6 isoforms. After co-transfection, cells were washed with cold 1X PBS, scraped and lysed in 800 μl of immunoprecipitation buffer (IP buffer) (150 mM NaCl, 50 mM Tris-HCl [pH 8.0], 1% (v/v) NP-40, and cOmplete™ EDTA-free Protease Inhibitor Cocktail (Sigma-Aldrich) and protein extracts were obtained as specified above. Total protein extracts were gently rotated during 2 h at 4 °C with 30 μl of Protein G Sepharose® Fast Flow bead slurry (Sigma-Aldrich) equilibrated in IP buffer, 0.5 mg/mL RNase A, DNase and protease-free (Thermo Scientific), with or without 5 μg of AntiGFP(FL) antibody. The mixture was gently rotated during 2 h at 4 °C. Beads were further washed 5 times with 1 mL of cold IP buffer, resting for 15 min on ice between each wash. Co-IPs were analyzed by 10% SDS-PAGE and Western blot. Western blot analyses were performed for the detection of short forms of E6 (using anti-GFP-HRP antibody) and the p53 isoforms (using antibodies DO-1, PAb1801 and HR231).

2.9. Apoptosis assays

A total of 3×10^5 H1299, SiHa and HeLa cells were seeded on 60 mm culture dishes in triplicate. All cell lines were transiently transfected with 1 μg of plasmids expressing p53 isoforms or the empty pSV vector and incubated for 24 h at 37 °C with 5% CO_2. Subsequently, the transfected cells were treated with cisplatin (CDDP) (Accord Farm). IC[50] 46 μg/mL of cisplatin for H1299 cells and IC[50] 23 μg/mL for SiHa and HeLa cells were used and further incubated for 24 h at 37 °C with 5% CO_2. Cisplatin-treated transfected cells were harvested to determine the level of apoptosis. Alexa Fluor® 647 Annexin V (Thermo Fisher Scientific) was used for H1299 cells and Alexa Fluor™ 488 Annexin V/Dead cell Kit (Thermo Fisher Scientific) was used for SiHa and HeLa cells, according to the manufacturer's instructions. Briefly, after the induction of apoptosis, the cells were washed once with 1X PBS and detached with 500 μl of 0.02% (v/v) EDTA. Boiled H1299, SiHa and HeLa cells were used as a positive staining control. Cells were collected and centrifuged at 3000 rpm for 5 min at room temperature and the supernatant discarded. Cell pellets were further washed with 1X PBS and centrifuged at 3000 rpm for 5 min and resuspended in 1X annexin-binding buffer and annexin V with 100 μg/mL propidium iodide. Cells were incubated at room temperature for 15 min protected from light. After the incubation period, 350 μl of 1X annexin-binding buffer was added and cells were mixed gently. Immediately, the stained cells were analyzed using a FACSCalibur™ flow cytometer (BD Bioscience). The apoptosis levels of cells transfected with p53 isoforms was calculated by the subtraction of the total percent apoptosis of un-transfected cells from the percent apoptosis of transfected cells. 10,000 events were recorded for each treatment. FlowJo software version 10.1 was used for data analysis.

2.10. Statistical analyses

Statistical analyses were performed using GraphPad Prism v6.0 (GraphPad Software). One-way ANOVA followed by Dunnett post hoc was employed to determine the significant differences. Data are presented as mean ± standard error of the mean (SEM), and values with $p < 0.05$ were considered statistically significant.

3. Results

3.1. HPV-16 E6 and E6*II shown an apparent effect on the relative levels of p53 and its isoforms

The p53 null cell line H1299 co-transfected with plasmids expressing E6 isoforms and plasmids expressing p53 isoforms was used as a model to study the effects that $E6^{SD}$, E6, E6*I and E6*II, of HPV-16 exert on the relative levels of p53, Δ40p53, and Δ133p53. The ectopic expression of HPV-16 E6 isoforms (Fig. 1 A and B) as well as p53 isoforms (Fig. 1, C and D) were corroborated by Western blot. A significant decrease in the relative levels of p53 was observed due to full-length E6 ($p = 0.0006$) and $E6^{SD}$ ($p = 0.0008$). Additionally, E6*II, a short form of the E6 oncoprotein fused with GFP [11,41], also decreased significantly ($p = 0.0003$) the level of p53 (Fig. 1E). Furthermore, the relative levels of Δ40p53 only reduced in the presence of E6 ($p = 0.0085$) and E6*II ($p = 0.0003$) (Fig. 1 F). In contrast, E6, E6*I, or E6*II did not affect the relative levels of Δ133p53 (Fig. 1 G).

3.2. E6*II but not E6*I induces a decrease in the relative levels of p53

It is widely known that HPV-16 E6 induces the degradation of p53 by the ubiquitin-proteasome-dependent pathway [3–5], but it is unknown whether E6*I and E6*II elicit the same effect via the same mechanism. However, given that our findings reported above show that E6*I and E6*II induce degradation only in p53 and D40p53, we co-transfected H1299 cells with both the HPV-16 E6*I and E6*II with p53 and HPV-16 E6*I and E6*II with Δ40p53 and were subsequently treated with the MG-132 inhibitor to block proteasome degradation. A noticeable change in p53 protein was observed in the presence of $E6^{SD}$ and E6*II when the cells were treated with MG-132 (Fig. 2 A). No apparent

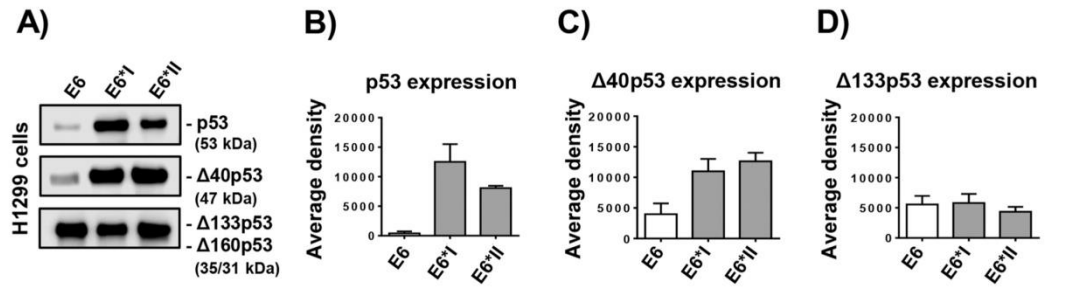

Fig. 3. Average density of levels p53 isoforms in H1299 cells co-transfected with different E6 proteins. H1299 cells were co-transfected with 1 μg of plasmids expressing p53, Δ40p53, or Δ133p53, along with 2 μg of plasmids expressing E6, E6*I or E6*II, and 50 ng of pRL-CMV *Renilla*. (A) The ectopic expression of p53, Δ40p53, and Δ133p53 proteins was detected by Western blot. (B, C and D) Average density ± standard error of the mean (SEM) of bands of Western blot for p53, Δ40p53, or Δ133p53.

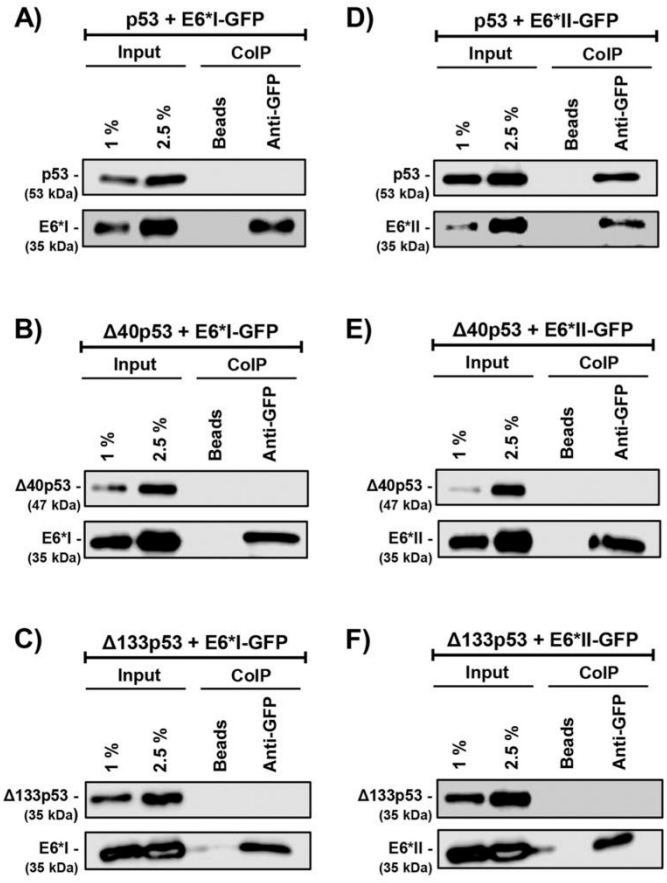

Fig. 4. Co-immunoprecipitation (Co-IP) assays of H1299 cells co-transfected with HPV-16 E6 * I, or E6 * II and p53 isoforms. Co-IP assay in H1299 cells co-transfected with expression plasmids (A) p53 and E6*I, (B) Δ40p53 and E6*I, (C) Δ133p53 and E6*I, (D) p53 and E6*II, (E) Δ40p53 and E6*II, and (F) Δ133p53 and E6*II. Protein extracts (input) were detected by immunoblotting using anti-GFP-HRP antibodies for detection of E6*IE6 * I and E6*II,E6 * II, and DO-1, Pab1801 and HR231 antibodies for the detection of p53, Δ40p53 and Δ133p53, respectively. For all Co-IP assays, a representative experiment out of three independent experiments is shown.

changes were observed in p53 in the presence of the E6 * I when MG-132 was present (Fig. 2 A). No noticeable changes in Δ40p53 protein were observed in H1299 cells co-transfected with E6 * I and E6*II treated and untreated with MG132, suggesting that Δ40p53 is not degraded by E6*I and E6*II through the ubiquitin-proteasome-dependent pathway (Fig. 2B), Since $E6^{SD}$ shows

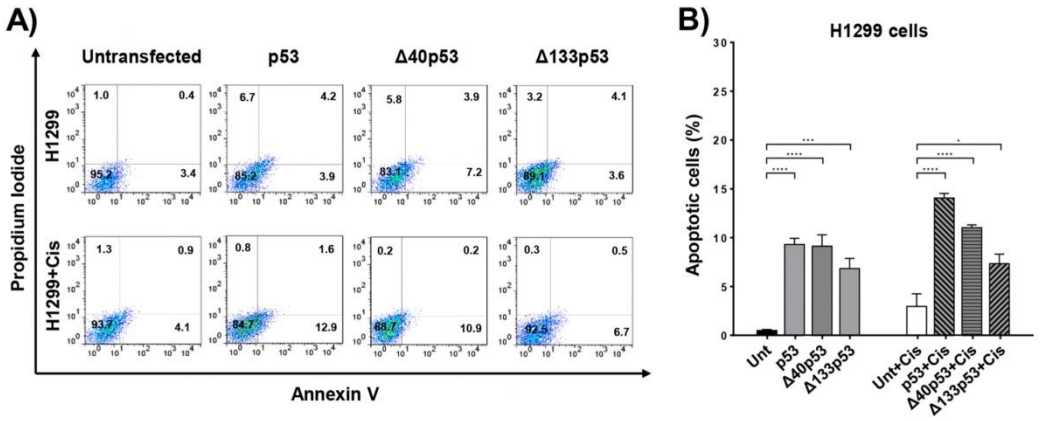

Fig. 5. Apoptosis detection by annexin V-propidium iodide (PI) assay in H1299 cells transfected with p53, Δ40p53 or Δ133p53 treated and untreated with cisplatin. (A) Representative flow cytometric analysis of apoptosis in H1299 cells transiently transfected with p53 isoforms treated and untreated with cisplatin (Cis). (B) Percentage of apoptotic cells. Apoptotic cells were calculated as the percentage of apoptotic cells in the upper right portion and the lower right portion relative to the total number of cells (recording 10,000 events). Data are presented as the means ± standard error of three independent experiments. *** $p < 0.001$ and *** * $p < 0.0001$ versus control (un-transfected H1299 cells with or without Cis).

the same apparent effect as E6 in inducing a decrease in p53 and Δ40p53 levels, we decided to exclude $E6^{SD}$ from further analysis.

*3.3. HPV-16 E6 and E6*II are associated with decreased levels of p53 but not Δ40p53 nor Δ133p53*

We next performed *Renilla* assays to rule out transcription deficiencies that interfered with our first findings. For that purpose, we co-transfected H1299 cells with plasmids expressing p53 isoforms with plasmids expressing E6 isoforms where p53, Δ40p53 and Δ133p53 levels were analyzed using equivalent RLuc activities and observed that p53 levels are decreased in the presence of E6 and E6*II but not in the presence of E6*I (Fig. 3, A and B), this result is in agreement with that observed in Fig. 1E. Interestingly, and contrary to what was observed in the Fig. 1 F, we observed that Δ40p53 levels decreased only in the presence of E6 (Fig. 3, A and C), and Δ133p53 levels show no apparent changes in the presence of either E6, E6*I, or E6*II (Fig. 3, A and D).

*3.4. HPV-16 E6*II interacts with p53 but not with Δ40p53 nor Δ133p53*

Due to the different effects promoted by HPV-16 E6*I and E6*II on the relative levels of p53 isoforms, H1299 cells co-transfected with either E6*I or E6*II and with p53, Δ40p53, or Δ133p53 were used to perform co-immunoprecipitation assays followed by Western blot, to analyze whether E6*I and E6*II interacted with p53, or its isoforms. These results revealed that E6*I did not interact with p53, Δ40p53 or Δ133p53 (Fig. 4, A-C), in agreement with what we observed in Fig. 3, A-D where p53, Δ40p53 and Δ133p53 did not decrease in the presence of HPV-16 E6*I. In contrast, HPV-16 E6*II interacted with p53 (Fig. 4D) but did not interact with Δ40p53 or Δ133p53 (Fig. 4, E and F).

3.5. p53, Δ40p53 and Δ133p53 ectopically expressed in combination with cisplatin increase apoptosis in H1299 cells

To explore the effect of different p53 isoforms on induction of apoptosis, and removing the strong anti-apoptotic effect exerted by E6 [42–46], H1299 cells were transfected with plasmids expressing p53 isoforms and apoptosis was evaluated by flow cytometry. We observed that ectopic expression of p53, Δ40p53 and Δ133p53 induced an increase in apoptotic cells (9.30%, $p < 0.0001$; 9.12%, $p < 0.0001$; and 6.84%, $p = 0.0005$, respectively). However, the percentage of apoptotic cells showed a bigger increase when H1299 cells were transfected with the p53 isoforms and then treated with cisplatin (Cis): p53 + Cis (14.06%, $p < 0.0001$), Δ40p53 +Cis (11.03%, $p < 0.0001$), and Δ133p53 +Cis (7.34%, $p = 0.0195$) (Fig. 5, A and B).

3.6. The ectopic expression of p53, Δ40p53, and Δ133p53 in combination with cisplatin induces different levels of apoptosis in SiHa and HeLa cell lines

p53 loss of function in tumor cells is associated with resistance to cisplatin treatment [47,48], where tumor cells with dysfunctional p53 fail to activate the apoptotic cell death program [48,49]. The present study evaluated the apoptotic effect of the ectopic expression of p53 isoforms alone or in combination with cisplatin, a conventional drug used regularly in cervical cancer therapy [33], in cancer cells that have lost p53 function due to the E6 of HPV-16 (SiHa) and HPV-18 (HeLa). These results revealed a significant apoptotic effect on SiHa cells with the combinations p53 + Cis (14.19%, $p = 0.0006$) and Δ40p53 +Cis (13.35%, $p = 0.0014$) (Fig. 6, A and B), and a significant apoptotic effect with the combination p53 + Cis (21.94%, $p = 0.0065$) in HeLa cells (Fig. 6, C and D). No significant differences in apoptosis were observed with the ectopic expression of p53, Δ40p53, and Δ133p53 in SiHa and HeLa cells in the absence of cisplatin (Fig. 6, A-D).

4. Discussion

The expression and characterization of HPV-16 E6, E6*I, and E6*II is widely established [50,51] and their effect on p53 relative levels has been reported in a C33-A cell model [11]. However, the effects of the different E6 proteins on p53 isoforms has not been reported. In the present study, we evaluated the impact of HPV-16 E6, E6*I, and on the relative levels of p53, Δ40p53, and Δ133p53.

Our results show that E6 and E6*II, but not E6*I induced a decrease in the levels of p53 (Fig. 1E) in an H1299 cell model. The effect of E6*II observed on p53 levels in the present study was consistent with that reported by del Moral-Hernandez, et al. Camus et al. demonstrated that HPV-16 E6 did not induce the degradation of Δ133p53α, Δ133p53β, and Δ133p53γ [52]. Similarly, our results show that HPV-16 E6, E6*I, and E6*II did not affect the relative levels of Δ133p53. It has been suggested

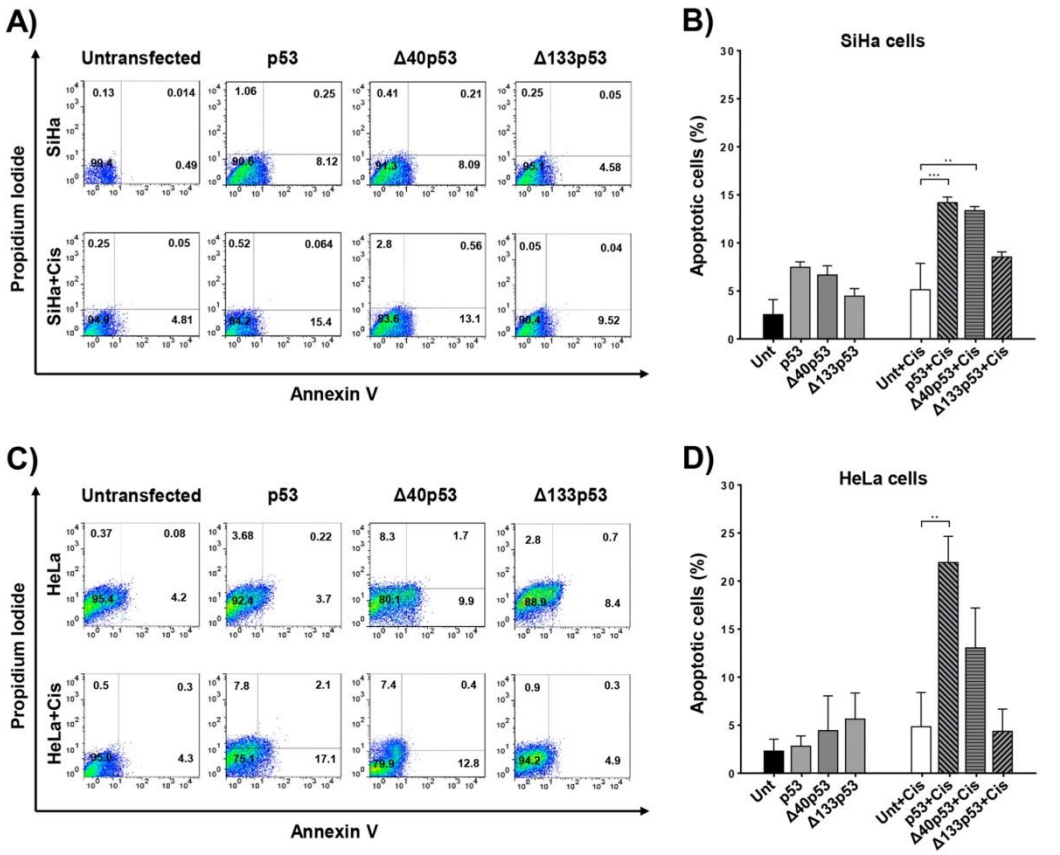

Fig. 6. Apoptosis detection by annexin V-propidium iodide (PI) assay in SiHa and HeLa cell lines transfected with p53, Δ40p53 and Δ133p53 treated and untreated with cisplatin. Representative flow cytometric analysis of apoptosis in (A) SiHa and (C) HeLa cells transfected with p53 isoforms treated and untreated with cisplatin (Cis). Percentage of apoptotic cells in (B) SiHa and (D) HeLa. Apoptotic cells were calculated as the percentage of apoptotic cells in the upper right portion and the lower right portion relative to the total number of cells (recording 10,000 events). Data are presented as the means ± standard error of three independent experiments. ** $p < 0.01$ and *** $p < 0.001$ versus control (un-transfected SiHa and HeLa cells or un-transfected SiHa and HeLa cells + Cis).

that the lack of effect of E6 on the Δ133p53 (α, β, and γ) levels may be due to the lack of the first 132 amino acids found in p53 [13], which includes an important region of the DBD and, therefore, a region involved in the interaction with E6-E6AP required for the subsequent degradation of p53 by the ubiquitin-proteasome-dependent pathway [4, 5]. Nevertheless, another report suggested that although the main pathway for p53 degradation promoted by E6 HR-HPVs is ubiquitin-proteasome-dependent, these viruses may use an independent pathway to promote p53 degradation [2]. Based on the observed differences between HPV-16 E6*I, and E6*II effects on the levels of p53, Δ40p53, and Δ133p53, we investigated the possible interaction of the E6 splice variants of HPV-16 with p53, Δ40p53, and Δ133p53. No interaction of HPV-16 E6*I was detected with p53, Δ40p53, or Δ133p53 using Co-IP assays, consistent with the lack of effect on the protein levels of the p53 isoforms observed in the presence of HPV-16 E6*I (Fig. 1, E-G). In contrast, we detected an interaction between p53 and HPV-16 E6*II (Fig. 3D), which is related with the decreased levels of p53 (Fig. 1 F and Fig. 3, A and B). Interestingly, a complex between E6*II and Δ40p53 was not observed, consistent with the lack of changes in Δ40p53 levels in the presence of E6*II and proteasome inhibitor MG132 (Fig. 2B) and the findings obtained with *Renilla* assays in which we analyzed Δ40p53 protein levels using equivalent RLuc activities to perform Western blot (Fig. 3, A and C).

Yin et al. reported that Δ40p53 (also known as p53/p47, p47, and ΔNp53) might induce apoptosis in H1299 cells (p53 null) [24]. However, Δ40p53 can act in a negative dominant manner by inhibiting p53-induced transcriptional activity and apoptosis [22], and Δ40p53 alone does not induce apoptosis in H1299 or Saos-2 cells, both null for p53 [23]. When we evaluated apoptosis in H1299 cells transfected with p53, Δ40p53, or Δ133p53, we observed a considerable increase in apoptosis percentage, especially when the transfected H1299 cells were treated with cisplatin. In contrast, we observed that the ectopic expression of p53 and Δ40p53 significantly increased the levels of apoptosis in SiHa cells treated with cisplatin, while in HeLa cells, apoptosis levels only increased significantly in the presence of p53 and cisplatin, suggesting that the type of HPV infection may be a determining factor. In C33A, a cervical cancer line HPV-negative and possessing an altered p53 version (mutation in 273 codon), E6*I and E6*II

exert an opposite effect on apoptosis [41]. In this case, E6*II show an increased apoptotic effect than E6*I among cisplatin treatment. The key feature of our model cells is the presence of wild-type p53, which can be influencing the differences observed. Interestingly, our findings suggest that Δ133p53 did not induce a significant apoptotic effect in cisplatin-treated cells, which is more remarkable in HeLa cells than in SiHa cells. The effect of Δ133p53 on apoptosis of cervical cancer-derived cells has not been reported previously. The effect of Δ133p53 on apoptosis of cells derived from cervical cancer has not been previously reported. However, using the U2OS osteosarcoma cell line expressing p53, Aoubala et al. reported that Δ133p53α inhibits p53-mediated apoptosis and cell cycle arrest in G1 but not in G2 [16]. Differences of apoptotic effect on SiHa and HeLa cancer cells were observed among cisplatin treatments. Various reports support the notion that p53 is not entirely inactivated in cervical cancer cell lines; particularly, HeLa cells show a higher basal transcriptional activity of p53 than SiHa cells [53] even though both cancer cell lines possess different number of copies of HPV, suggesting that the capacity of induce apoptosis among pharmacological treatments can be explained by these differences. Based on this, pharmacological treatments whose effect depend of p53 activity can be counteracted in the presence of p53 isoforms [54].

We show the effect of ectopic expression of the HPV-16 E6 oncoprotein and the E6*I and E6*II isoforms on the relative levels of p53 isoforms, the interaction between E6*II of HPV-16, and p53 and that the combination of p53 or Δ40p53 with cisplatin induces an increase in cancer cell apoptosis. Further studies are necessary to evaluate this effect in in vivo models to clarify its role in treating HPV-16-associated tumors. Furthermore, since our findings suggest that the combination of p53 or Δ40p53 with cisplatin induces increased apoptosis of cancer cells expressing HPV-16 E6 isoforms, it would be worthwhile to evaluate the levels of E6 isoforms and p53 isoforms in patients with HPV-16 positive tumors to argue for a possible antineoplastic response.

Funding

This work was supported by Consejo Nacional de Ciencia y Tecnología (CONACYT), grants Nr. 0253804 to A.G-C., and Nr.179894 to E.O. S., and by the intramural funding program of Instituto Nacional de Cancerología to A.G.C. and G.H.

CRediT authorship contribution statement

Verónica Antonio-Véjar: Investigation, Methodology, Writing – original draft. **Elizabeth Ortiz-Sánchez:** Investigation, Methodology, Writing – review & editing, Visualization, Funding acquisition. **Pedro Rosendo-Chalma:** Investigation, Methodology, Writing – review & editing. **Carlos C. Patiño-Morales:** Investigation, Methodology. **Miriam C. Guido-Jiménez:** Investigation, Methodology. **Eduardo Alvarado-Ortiz:** Investigation, Methodology. **Greco Hernández:** Methodology, Visualization, Writing – review & editing. **Alejandro García-Carrancá:** Conceptualization, Methodology, Resources, Writing – review & editing, Funding acquisition.

Acknowledgements

Verónica Antonio Véjar is a doctoral student from the Programa de Doctorado en Ciencias Biomédicas, Universidad Nacional Autónoma de México (UNAM) and received a fellowship from Consejo Nacional de Ciencia y Tecnología (CONACYT; grant Nr. 269673). We thank Nicolás Villegas Sepúlveda and Jean-Christophe Bourdon for plasmids. We thank the anonymous reviewers' for their valuable criticism and suggestions, which significantly improved the manuscript during the revision process. We also thank Prof. Elizabeth Langley for English language editing.

Conflict of interest

Authors declare that they have no conflict of interest.

References

[1] C. de Martel, et al., Global burden of cancer attributable to infections in 2018: a worldwide incidence analysis, Lancet Glob. Health 8 (2) (2020) e180–e190.
[2] S. Camus, et al., Ubiquitin-independent degradation of p53 mediated by high-risk human papillomavirus protein E6, Oncogene 26 (28) (2007) 4059–4070.
[3] P. Massimi, et al., HPV E6 degradation of p53 and PDZ containing substrates in an E6AP null background, Oncogene 27 (12) (2008) 1800–1804.
[4] M. Scheffner, et al., The HPV-16 E6 and E6-AP complex functions as a ubiquitin-protein ligase in the ubiquitination of p53, Cell 75 (3) (1993) 495–505.
[5] M. Scheffner, et al., The E6 oncoprotein encoded by human papillomavirus types 16 and 18 promotes the degradation of p53, Cell 63 (6) (1990), 1129-36.
[6] D. Stewart, A. Ghosh, G. Matlashewski, Involvement of nuclear export in human papillomavirus type 18 E6-mediated ubiquitination and degradation of p53, J. Virol. 79 (14) (2005) 8773–8783.
[7] D. Martinez-Zapien, et al., Structure of the E6/E6AP/p53 complex required for HPV-mediated degradation of p53, Nature 529 (7587) (2016) 541–545.
[8] M. Filippova, et al., The large and small isoforms of human papillomavirus type 16 E6 bind to and differentially affect procaspase 8 stability and activity, J. Virol. 81 (8) (2007), 4116-29.
[9] D. Pim, V. Tomaic, L. Banks, The human papillomavirus (HPV) E6* proteins from high-risk, mucosal HPVs can direct degradation of cellular proteins in the absence of full-length E6 protein, J. Virol. 83 (19) (2009) 9863–9874.
[10] M. Filippova, et al., The small splice variant of HPV16 E6, E6, reduces tumor formation in cervical carcinoma xenografts, Virology 450–451 (2014) 153–164.
[11] O. del Moral-Hernandez, et al., The HPV-16 E7 oncoprotein is expressed mainly from the unspliced E6/E7 transcript in cervical carcinoma C33-A cells, Arch. Virol. 155 (12) (2010) 1959–1970.
[12] M. Filippova, et al., Complexes of human papillomavirus type 16 E6 proteins form pseudo-death-inducing signaling complex structures during tumor necrosis factor-mediated apoptosis, J. Virol. 83 (1) (2009) 210–227.
[13] J.C. Bourdon, et al., p53 isoforms can regulate p53 transcriptional activity, Genes Dev. 19 (18) (2005), 2122-37.
[14] V. Marcel, et al., Delta160p53 is a novel N-terminal p53 isoform encoded by Delta133p53 transcript, FEBS Lett. 584 (21) (2010) 4463–4468.
[15] T. Anbarasan, J.C. Bourdon, The emerging landscape of p53 isoforms in physiology, cancer and degenerative diseases, Int. J. Mol. Sci. 20 (24) (2019).
[16] M. Aoubala, et al., p53 directly transactivates Delta133p53alpha, regulating cell fate outcome in response to DNA damage, Cell Death Differ. 18 (2) (2011) 248–258.
[17] K. Bourougaa, et al., Endoplasmic reticulum stress induces G2 cell-cycle arrest via mRNA translation of the p53 isoform p53/47, Mol. Cell 38 (1) (2010) 78–88.
[18] K. Fujita, et al., p53 isoforms Delta133p53 and p53beta are endogenous regulators of replicative cellular senescence, Nat. Cell Biol. 11 (9) (2009), 1135-42.
[19] M.P. Khoury, J.C. Bourdon, p53 isoforms: an intracellular microprocessor? Genes Cancer 2 (4) (2011), 453-65.
[20] R. Takahashi, S.N. Markovic, H.J. Scrable, Dominant effects of Delta40p53 on p53 function and melanoma cell fate, J. Investig. Dermatol. 134 (3) (2014) 791–800.
[21] V. Marcel, P. Hainaut, p53 isoforms - a conspiracy to kidnap p53 tumor suppressor activity? Cell Mol. Life Sci. 66 (3) (2009) 391–406.
[22] S. Courtois, et al., DeltaN-p53, a natural isoform of p53 lacking the first transactivation domain, counteracts growth suppression by wild-type p53, Oncogene 21 (44) (2002) 6722–6728.
[23] A. Ghosh, D. Stewart, G. Matlashewski, Regulation of human p53 activity and cell localization by alternative splicing, Mol. Cell Biol. 24 (18) (2004) 7987–7997.
[24] Y. Yin, et al., p53 Stability and activity is regulated by Mdm2-mediated induction of alternative p53 translation products, Nat. Cell Biol. 4 (6) (2002) 462–467.
[25] S. Surget, M.P. Khoury, J.C. Bourdon, Uncovering the role of p53 splice variants in human malignancy: a clinical perspective, Oncol. Targets Ther. 7 (2013) 57–68.
[26] K.A. Avery-Kiejda, et al., Small molecular weight variants of p53 are expressed in human melanoma cells and are induced by the DNA-damaging agent cisplatin, Clin. Cancer Res. 14 (6) (2008), 1659-68.
[27] A. Fragou, et al., Increased Delta133p53 mRNA in lung carcinoma corresponds with reduction of p21 expression, Mol. Med. Rep. 15 (4) (2017) 1455–1460.
[28] G. Hofstetter, et al., The N-terminally truncated p53 isoform Delta40p53 influences prognosis in mucinous ovarian cancer, Int. J. Gynecol. Cancer 22 (3) (2012) 372–379.
[29] G. Hofstetter, et al., Delta133p53 is an independent prognostic marker in p53 mutant advanced serous ovarian cancer, Br. J. Cancer 105 (10) (2011) 1593–1599.
[30] N. Nutthasirikul, et al., Ratio disruption of the 133p53 and TAp53 isoform equilibrium correlates with poor clinical outcome in intrahepatic cholangiocarcinoma, Int. J. Oncol. 42 (4) (2013) 1181–1188.
[31] R. Takahashi, et al., p53 isoform profiling in glioblastoma and injured brain, Oncogene 32 (26) (2013), 3165-74.
[32] L. Boldrup, et al., Expression of p53 isoforms in squamous cell carcinoma of the head and neck, Eur. J. Cancer 43 (3) (2007), 617-23.
[33] WHO, WHO (World Health Organization) Model List of Essential Medicines, 20th List (April 2017, amended August 2017)ſ. 2017: p. https://www.who.int/publications/i/item/eml-20.

[34] G. Giaccone, et al., Neuromedin B is present in lung cancer cell lines, Cancer Res. 52 (9 Suppl) (1992) 2732s–2736s.
[35] K.L. Fries, W.E. Miller, N. Raab-Traub, Epstein-Barr virus latent membrane protein 1 blocks p53-mediated apoptosis through the induction of the A20 gene, J. Virol. 70 (12) (1996) 8653–8659.
[36] C.M. Tsai, et al., Correlations between intrinsic chemoresistance and HER-2/neu gene expression, p53 gene mutations, and cell proliferation characteristics in non-small cell lung cancer cell lines, Cancer Res. 56 (1) (1996) 206–209.
[37] M.K. Diao, et al., Integrated HPV genomes tend to integrate in gene desert areas in the CaSki, HeLa, and SiHa cervical cancer cell lines, Life Sci. 127 (2015) 46–52.
[38] J.D. Meissner, Nucleotide sequences and further characterization of human papillomavirus DNA present in the CaSki, SiHa and HeLa cervical carcinoma cell lines, J. Gen. Virol. 80 (Pt 7) (1999) 1725–1733.
[39] M.M. Pater, A. Pater, Human papillomavirus types 16 and 18 sequences in carcinoma cell lines of the cervix, Virology 145 (2) (1985) 313–318.
[40] Y. Yaginuma, H. Westphal, Analysis of the p53 gene in human uterine carcinoma cell lines, Cancer Res 51 (24) (1991) 6506–6509.
[41] C.E. Vaisman, et al., C33-A cells transfected with E6*I or E6*II the short forms of HPV-16 E6, displayed opposite effects on cisplatin-induced apoptosis, Virus Res 247 (2018) 94–101.
[42] R.A. DeFilippis, et al., Endogenous human papillomavirus E6 and E7 proteins differentially regulate proliferation, senescence, and apoptosis in HeLa cervical carcinoma cells, J. Virol. 77 (2) (2003), 1551-63.
[43] P.J. Duerksen-Hughes, J. Yang, S.B. Schwartz, HPV 16 E6 blocks TNF-mediated apoptosis in mouse fibroblast LM cells, Virology 264 (1) (1999) 55–65.
[44] M. Filippova, et al., The human papillomavirus 16 E6 protein binds to tumor necrosis factor (TNF) R1 and protects cells from TNF-induced apoptosis, J. Biol. Chem. 277 (24) (2002) 21730–21739.
[45] M. Shimada, et al., The human papillomavirus E6 protein targets apoptosis-inducing factor (AIF) for degradation, Sci. Rep. 10 (1) (2020) 14195.
[46] M. Thomas, L. Banks, Inhibition of Bak-induced apoptosis by HPV-18 E6, Oncogene 17 (23) (1998) 2943–2954.
[47] C.C. Chao, Decreased accumulation as a mechanism of resistance to cis-diamminedichloroplatinum(II) in cervix carcinoma HeLa cells: relation to DNA repair, Mol. Pharm. 45 (6) (1994) 1137–1144.
[48] Z.H. Siddik, Cisplatin: mode of cytotoxic action and molecular basis of resistance, Oncogene 22 (47) (2003), 7265-79.
[49] Y. Minagawa, et al., Cisplatin-resistant HeLa cells are resistant to apoptosis via p53-dependent and -independent pathways, Jpn. J. Cancer Res. 90 (12) (1999) 1373–1379.
[50] J. Doorbar, et al., Detection of novel splicing patterns in a HPV16-containing keratinocyte cell line, Virology 178 (1) (1990), 254-62.
[51] D. Smotkin, H. Prokoph, F.O. Wettstein, Oncogenic and nononcogenic human genital papillomaviruses generate the E7 mRNA by different mechanisms, J. Virol. 63 (3) (1989) 1441–1447.
[52] S. Camus, et al., The p53 isoforms are differentially modified by Mdm2, Cell Cycle 11 (8) (2012) 1646–1655.
[53] S. Hietanen, et al., Activation of p53 in cervical carcinoma cells by small molecules, Proc. Natl. Acad. Sci. USA 97 (15) (2000) 8501–8506.
[54] J. Chen, et al., p53 isoform delta113p53 is a p53 target gene that antagonizes p53 apoptotic activity via BclxL activation in zebrafish, Genes Dev. 23 (3) (2009) 278–290.

XIII.2 Coautora en artículo científico publicado en International Journal of Oncology. 2020.

INTERNATIONAL JOURNAL OF ONCOLOGY 57: 301-313, 2020

CDH1 and SNAI1 are regulated by E7 from human papillomavirus types 16 and 18

PEDRO ROSENDO-CHALMA[1,2], VERÓNICA ANTONIO-VEJAR[2,3], GABRIELE DAVIDE BIGONI-ORDÓÑEZ[2], CARLOS CÉSAR PATIÑO-MORALES[2], AMPARO CANO-GARCÍA[4,5] and ALEJANDRO GARCÍA-CARRANCÁ[2]

[1]Programa de Doctorado en Ciencias Biomédicas, Instituto de Investigaciones Biomédicas (IIB), Universidad Nacional Autónoma de México (UNAM), Mexico City 10450; [2]Laboratorio de Virus y Cáncer, Unidad de Investigación Biomédica en Cáncer of Instituto de Investigaciones Biomédicas-Universidad Nacional Autónoma de México (IIB-UNAM) and División de Investigación Básica of Instituto Nacional de Cancerología-Secretaría de Salud (INCan-SSA), Mexico City 14080; [3]Laboratorio de Biomedicina Molecular, Unidad Académica de Ciencias Químico Biológicas (UACQB), Universidad Autónoma de Guerrero (UAGro), Chilpancingo, Guerrero 39090, Mexico; [4]Departamento de Bioquímica, Universidad Autónoma de Madrid (UAM), Instituto de Investigaciones Biomédicas 'Alberto Sols' (CSIC-UAM), Instituto de Investigación Sanitaria del Hospital Universitario La Paz (IdiPAZ); [5]Centro de Investigación Biomédica en Red de Cáncer (CIBERONC), Madrid 28029, Spain

Received January 11, 2019; Accepted October 24, 2019

DOI: 10.3892/ijo.2020.5039

Abstract. A common characteristic of cancer types associated with viruses is the dysregulated expression of the *CDH1* gene, which encodes E-cadherin, in general by activation of DNA methyltransferases (Dnmts). In cervical cancer, E7 protein from high risk human papillomaviruses (HPVs) has been demonstrated to interact with Dnmt1 and histone deacetylase type 1 (HDAC1). The present study proposed that E7 may regulate the expression of *CDH1* through two pathways: i) Epigenetic, including DNA methylation; and ii) Epigenetic-independent, including the induction of negative regulators of *CDH1* expression, such as Snail family transcriptional repressor Snai1 and Snai2. To test this hypothesis, HPV16- and HPV18-positive cell lines were used to determine the methylation pattern of the *CDH1* promoter and its expression in association with its negative regulators. Different methylation frequencies were identified in the *CDH1* promoter in HeLa (88.24%) compared with SiHa (17.65%) and Ca Ski (0%) cell lines. Significant differences in the expression of *SNAI1* were observed between these cell lines, and an inverse association was identified between the expression levels of *SNAI1* and *CDH1*. In addition, suppressing E7 not only increased the expression of *CDH1*, but notably decreased the expression of *SNAI1* and modified the methylation pattern of the *CDH1* promoter. These results suggested that the expression of *CDH1* was dependent on the expression of *SNAI1* and was inversely associated with the expression of E7. The present results indicated that E7 from HPV16/18 regulated the expression of *CDH1* by the two following pathways in which Snai1 is involved: i) Hypermethylation of the *CDH1* promoter region and increasing expression of *SNAI1*, as observed in HeLa; and ii) Hypomethylation of the *CDH1* promoter region and expression of *SNAI1*, as observed in SiHa. Therefore, the suppression of *CDH1* and expression of *SNAI1* may be considered to be biomarkers of metastasis in uterine cervical cancer.

Correspondence to: Dr Alejandro García-Carrancá, Virus and Cancer Laboratory, Biomedical Research Unit on Cancer, National Cancer Institute, Ministry of Health, 22 San Fernando Avenue, Section XVI, Tlalpan, Mexico City 14080, Mexico
E-mail: carranca@biomedicas.unam.mx

Key words: epigenetic, human papillomavirus, E7, SNAI1, SNAIL/SNAIL1, SNAI2, SLUG/SNAIL2, CDH1, E-cadherin

Introduction

According to current research, 15-20% of all cases of cancer can be attributed to infectious agents, including *Helicobacter pylori* and human papillomavirus (HPV), followed by hepatitis B virus (HBV), hepatitis C virus (HCV) and the Epstein-Barr virus (EBV) (1-3). In HPV, specifically types 16, 18, 31, 33, 35, 39, 45, 51, 52, 56, 58 and 59 that are commonly referred to as high-risk (HR), are not only associated with cervical cancer (CC), the third most prevalent type of cancer worldwide in women in 2017, but also with other tumor types, including anal, penile, vulvar, vaginal and head and neck cancer (1,4).

Persistent infections with HR-HPVs are necessary, but not sufficient to cause cancer, indicating the existence of multistep actions in viral carcinogenesis that contribute to the characteristic hallmarks underlying the phenotype of tumors (3,5). Thus, it has been of great interest to study mechanisms by which persistent infections with these viruses contribute to cancer development. HPV has been demonstrated to induce a series of mechanisms that contribute to the evasion of the immune response and apoptosis-activated cell death, and finally the transformation, proliferation and cellular immortalization of the host cell (6,7).

HPV life cycle disruption due to integration of the viral genome into the cellular genome (8,9) and activation of the cell methylation machinery have been demonstrated to be involved in the carcinogenic process of CC among other factors (10-12). Specifically, the HR-HPV E7 oncoprotein has been reported to serve a crucial role in oncogenic transformation due to its ability to form complexes with members of the retinoblastoma protein (pRB) family and destabilize them (13,14), in addition to the ability to interact with other proteins, including histone deacetylase 1 (HDAC1) (15) and DNA methyltransferase 1 (Dnmt1) (16).

E7 binds to HDAC1 via its zinc finger-like motif through an intermediary protein Mi2β, which is a component of the nucleosome remodeling and histone deacetylation (NURD) complex that has the ability to modify chromatin structure trough both deacetylation of histones and ATP-dependent nucleosome repositioning (17,18). The formation of this complex is necessary for the maintenance of viral episomes, controlling cell proliferation and extending cell life (15,17). Consistent with this, a chromatin immunoprecipitation assay in Ca Ski cells demonstrated that E7 and HDACs are associated with the major histocompatibility complex (MHC) class I promoter and histone deacetylation (19), as well as chromatin repression and the downregulation of *MHC* class I genes and MHC class I heavy chain, and repression of the genes encoding the transporter associated with antigen processing subunit 1 (TAP1) and low molecular weight protein 2 (LMP2) (20). Furthermore, an association with Dnmt1 is directed and mediated by the conserved region 3 (CR3) zinc-finger region of E7, which is known to contribute to E7 transformation functions and stimulate the methyltransferase activity of Dnmt1, which may lead to aberrant genome methylation and cellular transformation as a consequence of the silencing of tumor-suppressor genes (16). Another study has demonstrated that in samples of normal cervix and cervical cancer, HPV types 16 and 18 activate the cell methylation machinery to methylate viral DNA, as well as the promoter regions of cellular genes, including cyclin A1, Rubicon-like autophagy enhancer, retinoic acid receptor β2, cadherin 1 (*CDH1*), death-associated protein kinase 1, human telomerase reverse transcriptase 1 (*hTERT1*), *hTERT2*, hypermethylated in cancer 1 and Twist Family BHLH Transcription Factor 1 (21). Therefore, previous evidence suggests that HR-HPV *E7* serves an important role in the activation of the cellular methylation machinery, which regulates the transcription of viral and cellular genes either during their productive infection during its life cycle or during the carcinogenic process.

The mechanisms by which E7 is involved in the regulation of gene expression at the chromatin level are not well understood. It has been observed that a common characteristic of several cancer types associated with viruses is the decreased expression of *CDH1*, which encodes E-cadherin, through epigenetic mechanisms (22-24). In the case of cancer types associated with HPV infections, it has been demonstrated that HPV16 *E7* suppresses the transcription of *CDH1*, which reduces protein expression of E-cadherin (25,26). In addition, HPV16 *E7* has been reported to increase the amount and activity of Dnmt1 in NIKS cells, which are derived from foreskin keratinocytes transfected with HPV16 *E7* or NIKS bearing episomal HPV16 DNA (26); however, NIKS cells not infected with HPV16 and NIKS bearing episomal HPV16 DNA did not exhibit any differences in the CpG methylation status of the *CDH1* promoter regions, as all CpG sites were unmethylated (26). It is evident that HPV activates the methylation machinery via E7/Dnmt1; however, it is not clear how HPV induces *CDH1* repression by epigenetic mechanisms.

Since HR-HPVs E7 has been demonstrated to interact with Dnmt1 and HDAC1, the aim of the current study was to determine the methylation pattern of the *CDH1* promoter region in HeLa, SiHa and Ca Ski cell lines positive for HPV16 and HPV18. Additionally, associations with transcription factors Snai1 and Snai2, which are negative regulators of *CDH1* expression and inducers of the epithelial-mesenchymal transition (EMT) process (27), were evaluated. HeLa, SiHa and Ca Ski cell lines were selected for the present study, as they are representative of the most frequent cancer types of the uterine cervix with positive HR-HPV infection with different viral loads and epithelial origins, including cervical adenocarcinoma, cervical squamous cell carcinoma and cervical epidermoid carcinoma (28-34).

Materials and methods

Cell lines. As reported by the American type culture collection, HeLa cells are derived from a female African-American patient with uterine cervical adenocarcinoma and are reported to contain 10-50 integrated copies of HPV18 per cell (30-36). SiHa cells are derived from a female Asian patient with grade II cervical squamous cell carcinoma and are reported to contain 1-2 integrated copies of HPV16 per cell (29,30,33,36). Ca Ski cells are derived from a female Caucasian patient with cervical epidermoid carcinoma and are reported to contain 500-600 integrated copies of HPV16 per cell (28,30,36). HaCaT is a non-tumorigenic immortalized human epidermal cell line derived from skin keratinocytes. All cell lines were authenticated through STR DNA profiling (ID no. DP0297) by the University of Colorado DNA Sequencing & Analysis Core. HeLa, SiHa and HaCaT cell lines (ATCC) were cultured in DMEM (cat. no. 12800-058; Gibco; Thermo Fisher Scientific, Inc.); Ca Ski cells were cultured in RPMI medium (cat. no. 31800-014; Gibco; Thermo Fisher Scientific, Inc.). All cell lines were supplemented with 10% fetal bovine serum (FBS; cat. no. 16000-044; Gibco; Thermo Fisher Scientific, Inc.) and 1X penicillin-streptomycin (cat. no. 15140122; Gibco; Thermo Fisher Scientific, Inc.) and were incubated in a humidified chamber at 37˚C with 5% CO_2.

Untransfected MCF-7 cells and MCF-7 cell stable clones transfected with a pcDNA 3.1 expression vector (Invitrogen; Thermo Fisher Scientific, Inc) with the bicistronic E6/E7 region from HPV18 (MCF-7 pE6/E7) were kindly provided by Dr Erick de la Cruz Hernández (Juarez Autonomous University of Tabasco, Villahermosa, Mexico) and were cultured with 800 μg/ml Geneticin in DMEM/F12 for 3 weeks as previously described (37-39). Untransfected C33-A cells and C33-A cell stable clones transfected with a pcDNAE7 plasmid (C33-A pE7/HPV16) were kindly provided by Dr Patricio Gariglio (CINVESTAV-IPN, Mexico City, Mexico) and were cultured with 800 μg/ml Geneticin in DMEM for 2 weeks as previously described (40).

Treatments with 5-aza-2'-deoxycytidine (5-AzadC) and trichostatin A (TSA). 5-AzadC causes DNA demethylation or hemi-demethylation that results in gene activation by inhibiting Dnmt activity (41). TSA has been used as a histone deacetylase inhibitor, which causes histone hyperacetylation that leads to chromatin relaxation and modulation of gene expression (42). 5-AzadC and TSA were obtained from Sigma-Aldrich; Merck KGaA (cat. nos. A3656 and T8552, respectively) and resuspended in DMSO (Sigma-Aldrich; Merck KGaA; cat. no. D8418) to obtain working stock solutions (10.0 mM 5-AzadC and 1.0 mM TSA). The 5-AzadC and TSA stock solutions were aliquoted, protected from light and stored at -80˚C for later use. A total of $4.5x10^5$ HeLa and $5x10^5$ SiHa cells were seeded in p60 boxes in triplicate and were treated with 5 and 10 μM 5-AzadC and 200 and 500 nM TSA. Untreated cells or cells treated with DMSO were used as controls. The total volume of culture medium was 3 ml, which was supplemented with 10% FBS and did not contain any antibiotics. Assays were performed protected from light and the cells were incubated for 48 h at 37˚C with 5% CO_2. The culture medium was replaced after 24 h due to the half-life of 5-AzadC and TSA.

Transfection with short interfering RNA (siRNA). siRNAs targeting HPV16 and HPV18 E7 were designed as previously described (43,44) and obtained from Ambion (Thermo Fisher Scientific, Inc.; cat. nos. s237642 and s237640). Silencer® Select *GAPDH* siRNA (Hs, Mm, Rn) (cat. no. 4390849; Ambion; Thermo Fisher Scientific, Inc.) was used as a positive transfection control to select the transfection agent (Lipofectamine® 2000 or siPORT™ NeoFX™) and to optimize gene silencing without affecting cell viability according to the manufacturer's protocol and as previously described (45-50). siRNAs were resuspended in UltraPure™ DNase/RNase-free distilled water (cat. no. 10977-015; Thermo Fisher Scientific, Inc.) to obtain a working stock of 10 μM. siRNAs were then aliquoted and stored at -80˚C for later use.

Transfection with siRNA was performed in triplicate using the siPORT™ NeoFX™ kit (cat. no. AM4511; Ambion; Thermo Fisher Scientific, Inc.) according to the manufacturer's protocol. A total of $7.5x10^4$ HeLa and $8.0x10^4$ SiHa cells/well were seeded in a 12-well plate. HeLa cells were transfected with 30 nM siRNA against HPV18 E7, whereas SiHa cells were transfected with 30 nM siRNA against HPV16 E7. In addition, 30 nM siRNA targeting *GAPDH* was transfected as a positive control in both cell lines. Cells subjected to treatment with siPORT™ NeoFX™ Transfection Agent with Opti-MEM® I (cat. no. 31985070; Thermo Fisher Scientific, Inc.) were used as a reference control to obtain the relative values, and untransfected cells were used as a reference control for statistical comparisons. Culture medium supplemented with 12% FBS and no antibiotics was added to make up a final transfection volume of 1.2 ml. Cells were incubated for 48 h at 37˚C with 5% CO_2 and subsequently the extraction of nucleic acids and proteins was performed. Transfection efficiency was determined by measuring the expression of E7 and GAPDH at the mRNA level.

Bisulfite conversion and DNA methylation analysis. Total genomic DNA was isolated from the treated and transfected cell lines using the Wizard® Genomic DNA Purification kit (cat. no. A1120; Promega Corporation) and 1.5 μg genomic DNA was treated with bisulfite according to the manufacturer's protocol of the EZ DNA Methylation-Gold™ kit (cat. no. D5006; Zymo Research Corp.). Methylation of CpG sites at the *CDH1* promoter region was analyzed by the bisulfite sequencing PCR (BSP) protocol (Fig. 1A) (10-12,51,52) or using oligonucleotides for MSP-protocol provided by Dr Alfonso Dueñas-Gonzalez (INCan-UNAM, Mexico City, Mexico); the PCR conditions for MSP-protocol were the same as those used for the BSP protocol. PCR was performed with a total volume of 25 μl, containing 1X PCR Gold Buffer, 1 mM dNTP, 2 mM $MgCl_2$, 10 pMol forward *CDH1*-BSP (5'-TTTTAGTAATTTTAGGTTAGAGGGTTAT-3') and reverse *CDH1*-BSP (5'-AAACTCACAAATACTTTACAATTCC-3') oligonucleotides, 1 U AmpliTaq Gold® DNA Polymerase (cat. no. 4338856; Applied Biosystems; Thermo Fisher Scientific, Inc.) and 300 ng bisulfite-treated DNA. The thermocycling conditions were as follows: 95˚C for 7 min, followed by 35 cycles of 95˚C for 35 sec, 57˚C for 35 sec and 72˚C for 60 sec, and a final extension at 72˚C for 7 min. PCR products were treated using *Exo*I (cat. no. EN0581; Thermo Fisher Scientific, Inc.) and *SAP* (cat. no. EF0651; Thermo Fisher Scientific, Inc.) enzymes. The treated PCR products were sequenced using the BigDye® v3.1 Cycle Sequencing kit (cat. no. 4337455; Applied Biosystems; Thermo Fisher Scientific, Inc.) according to the manufacturer's protocol in an ABI PRISM™ 3100-Avant Genetic Analyzer (Applied Biosystems; Thermo Fisher Scientific, Inc.). The BSP oligonucleotides were designed by MethPrimer v2.0 software (The Li Lab; PUMCH; Chinese Academy of Medical Sciences) using GenBank sequence DQ335132.1 for the *CDH1* gene (53). The sequencing data obtained from BSP were analyzed using Chromas v2.6.4 software (Technelysium Pty., Ltd.) and Lasergene v7 package (DNASTAR, Inc.).

RNA extraction and reverse transcription-quantitative (RT-q) PCR. Total RNA was extracted from the treated and transfected cells using TRIzol® reagent (cat. no. 15596026; Invitrogen; Thermo Fisher Scientific, Inc.). The RNA was treated with *DNase I* (cat. no. EN0521; Invitrogen; Thermo Fisher Scientific, Inc.), and purified with Direct-zol™ RNA MicroPrep (cat. no. R2060; Zymo Research Corp.) according to the manufacturer's protocol. Complementary DNA (cDNA) was obtained from the purified RNA using the SuperScript™ IV First-Strand Synthesis system (cat. no. 18091050; Invitrogen; Thermo Fisher Scientific, Inc.) according to the manufacturer's protocol. The RNA-primer mix was incubated at 65˚C for 5 min and 4˚C for 1 min, and the RT reaction mix was incubated at 55˚C for 15 min and 80˚C for 10 min to inactivate the reaction and placed on ice for subsequent use. Subsequently, 60 ng cDNA was subjected to qPCR to determine the expression levels of the genes of interest using the primers listed in Table I. qPCR conditions were as follows: 95˚C for 10 min, followed by 40 cycles of 95˚C for 20 sec, 60˚C for 30 sec and 72˚C for 35 sec, and a final extension at 72˚C for 7 min. This was followed by a melting curve analysis at 65-95˚C. All qPCR assays were analyzed using Rotor-Gene Q Series v2.1.0 software (Qiagen, Inc.).

To obtain expression levels of *CDH1*, *SNAI1*, *SNAI2*, HPV16 E7 and HPV18 *E7* in the HeLa, SiHa, Ca Ski and

Table I. Primer sequences used for the BSP and qPCR assays.

Gene	Assay	Primer sequences (5'→3')
CDH1	BSP	F: TTTTAGTAATTTTAGGTTAGAGGGTTAT R: AAACTCACAAATACTTTACAATTCC
CDH1	qPCR	F: GTCAGTTCAGACTCCAGCCC R: AAATTCACTCTGCCCAGGACG
SNAI1	qPCR	F: ACCACTATGCCGCGCTCTT R: GGTCGTAGGGCTGCTGGAA
SNAI2	qPCR	F: GACCCTGGTTGCTTCAAGGA R: TGTTGCAGTGAGGGCAAGAA
E7 HPV16	qPCR	F: CAGCTCAGAGGAGGAGGATG R: TGCCCATTAACAGGTCTTCC
E7 HPV18	qPCR	F: TGAAATTCCGGTTGACCTTC R: CACGGACACACAAAGGACAG
GAPDH	qPCR	F: AAGGTCGGAGTCAACGGATTTG R: CCATGGGTGGAATCATATTGGAA
HPRT	qPCR	F: GGACTAATTATGGACAGGACTG R: GCTCTTCAGTCTGATAAAATCTAC

BSP, bisulfite sequencing PCR; qPCR, quantitative PCR.

HaCaT cells, a commercial sample of RNA extracted from normal cervix negative for HPV (Human Cervix Total RNA; cat. no. AM6992; Ambion; Thermo Fisher Scientific, Inc.) was used as a reference. The ΔCq values for each gene were normalized to the reference gene *GAPDH* using the $2^{-\Delta\Delta Cq}$ method (54). The commercial sample of normal cervix negative for HPV was set as 1, and the results are not presented. For statistical analysis, the HaCaT cell line was used for comparison. For experiments involving the treatment of HeLa and SiHa cells with 5-AzadC and TSA, cells treated with DMSO were used as a reference, but data were not included in the graphs. For experiments involving the transfection of HeLa and SiHa cells with siRNAs, the cells treated with siPORT™ NeoFX™ Transfection Agent with Opti-MEM® I were used as a reference, but results were not included in the graphs. ΔCq values of *CDH1*, *SNAI1*, *SNAI2*, HPV16 E7 and HPV18 *E7* were normalized using the $2^{-\Delta\Delta Cq}$ method (39) with *GAPDH* as reference for 5-AzadC and TSA treatments, and *HPRT* as reference for experiments involving siRNA transfections. For statistical analysis, untreated (Unt) HeLa and SiHa cells were used for comparisons.

Protein extraction and western blot analysis. Proteins were obtained using a lysis buffer containing 5 mM EDTA, 150 mM NaCl, 5 mM Tris-HCl pH 9.0, 1% Nonidet-P40 and 1.2 mg/ml cOmplete™ protease inhibitor cocktail (Roche Applied Science). Protein extracts were forced through a 22-gauge needle 10 times and centrifuged for 10 min at 17,000 x g at 4˚C. Protein concentration was determined using the Bradford method. Subsequently, 30 mg protein was loaded and separated on 12% SDS-PAGE gels followed by transfer to nitrocellulose membranes. Membranes were blocked with 5% nonfat dry milk in 1X TBS with 0.1% Tween-20 (TBST) at 4˚C for 1 h with gentle agitation and incubated overnight at 4˚C with antibodies against E-cadherin (cat. no. sc-8426; 1:1,000), GAPDH (cat. no. sc-48167; 1:1,000), β-actin (cat. no. sc-1616; 1:1,000; all from Santa Cruz Biotechnology, Inc.), Snai1 (cat. no. L70G2; 1:1,000; Cell Signaling Technology, Inc.) and Snai2 (cat. no. C19G7; 1:1,000; Cell Signaling Technology, Inc.) diluted in TBST with 5% BSA (cat. no. 9998; Cell Signaling Technology, Inc.). Subsequently, membranes were incubated with secondary antibodies for 2 h at room temperature, including goat anti-mouse IgG-horseradish peroxidase (HRP; cat. no. sc-2005; 1;10,000), donkey anti-rabbit IgG-HRP (cat. no. sc-2313; 10,000) and donkey anti-goat IgG-HRP (cat. no. sc-2020; 1:5,000; all from Santa Cruz Biotechnology, Inc.) diluted in TBST with 5% non-fat dry milk. Immobilon Western Chemiluminescent HRP substrate (EMD Millipore) was used for protein detection, and images were acquired using C-DiGit Blot scanner equipment (Li-Cor Biosciences) and processed in the Image Studio™ Lite version 5.2 software (Li-Cor Biosciences).

Nitrocellulose membranes were incubated with two primary antibodies in the following manner: i) Incubation was performed as described against a primary antibody, including E-cadherin, Snai1 or Snai2 with their respective secondary antibody; ii) images were acquired; iii) membranes were washed 3x5 min with TBST at room temperature; iv) membranes were re-probed with a second primary antibody, including GAPDH or β-actin with their respective secondary antibody; and v) images were acquired.

Statistical analysis. Statistical analysis was performed using GraphPad Prism v4.0 (GraphPad Software, Inc.). One-way ANOVA with Turkey's post hoc test were used to evaluate significant differences in gene expression and methylation levels, and results were presented as the mean ± SD. $P<0.05$ was considered to indicate a statistically significant difference.

Results

Different methylation patterns in the CDH1 promoter region are present in HPV16- and HPV18-positive cancer cell lines. A common site-specific methylation pattern in certain CpG islands (-160, -150, -131 and -122) of the *CDH1* promoter region was detected in HeLa and SiHa cells, whereas other CpG islands (-45, -136, -105, -103, -83, -57, -52, -45, -36, -13, +6 and +9) were identified to be methylated in HeLa only (Fig. 1B). Of note, Ca Ski cells did not exhibit methylation of any of the 17 CpG sites of the *CDH1* promoter that were analyzed (Fig. 1B). Quantification of the methylation levels in the *CDH1* promoter region indicated that HeLa presented a methylation frequency of 88.24%, SiHa cells exhibited a methylation frequency of 17.65% and Ca Ski cells demonstrated no methylation (frequency, 0%; Fig. 1C).

Based on previous studies (25-28), initial experiments were conducted using the C33-A, C33-A transfected with pE7/HPV16 (C33-A pE7/HPV16), MCF-7 and MCF-7 transfected with pE6/E7 from HPV18 (MCF-7 pE6/E7) cell lines as HPV-negative cancer models. Validation of C33-A and MCF-7 cell stable clone selection with pE7/HPV16

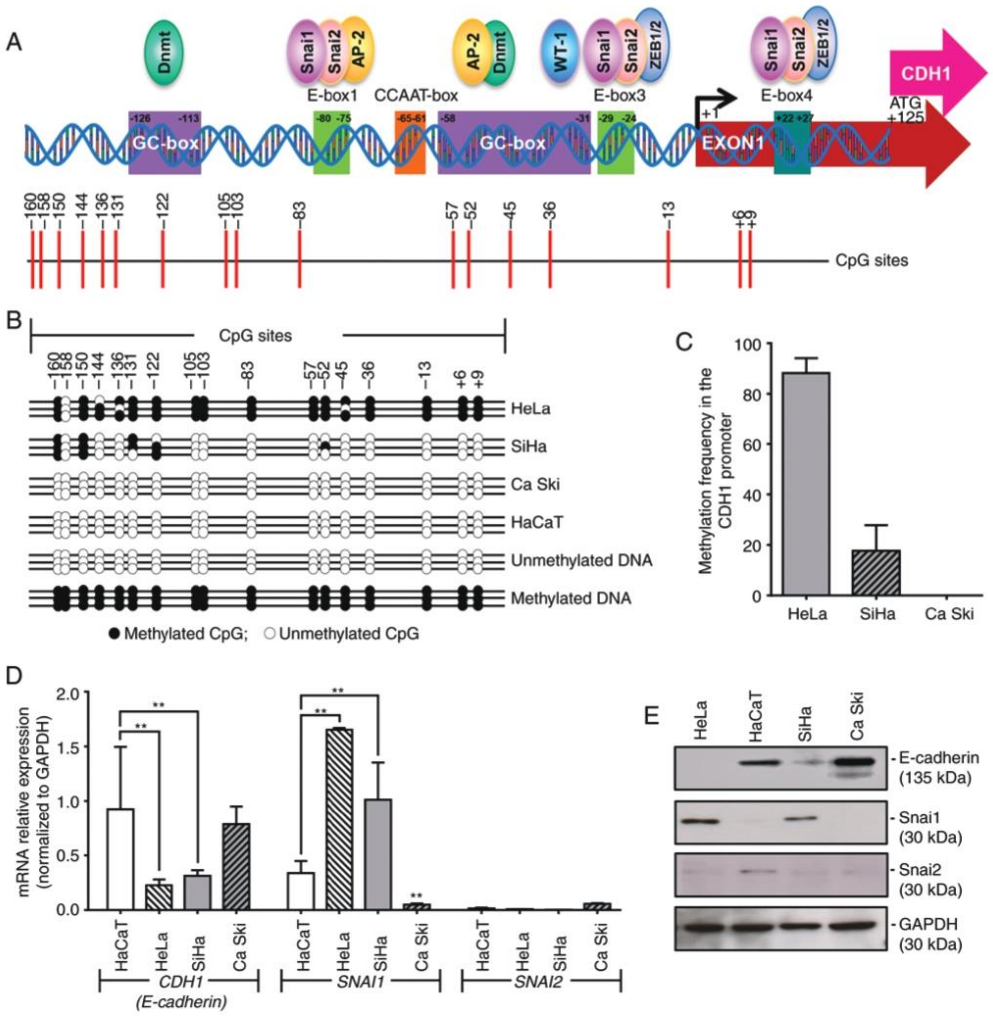

Figure 1. Methylation of the *CDH1* gene promoter region. (A) The location of different elements; the E-box and GC box motifs that regulate transcription of *CDH1*. Red vertical lines indicate each CpG site contained in the promoter region. (B) A lollipop methylation diagram of bisulfite sequencing of the *CDH1* promoter in the HeLa, SiHa, Ca Ski and HaCaT cell lines. Black indicates a methylated CpG site; white indicates an unmethylated CpG site. (C) Quantification of the methylation frequency of the *CDH1* promoter in the HeLa, SiHa and Ca Ski cell lines. (D) Quantitative PCR was performed to measure the expression levels of *CDH1*, *SNAI1* and *SNAI2* genes in the indicated cell lines. *P<0.05 and **P<0.01 vs. HaCaT. (E) Protein expression levels of E-cadherin, Snai1 and Snai2 were assessed by western blot analysis in HPV-positive cell lines. GAPDH was used as a loading control. *CDH1*, cadherin 1; Dmnt1, DNA methyltransferase 1; AP-2, activating protein 2; ZEB1/2, zinc finger E-box-binding homeobox 1/2.

and pE6/E7, respectively, was performed by evaluating E7 mRNA expression by RT-PCR (Fig. S1B). However, C33-A vs. C33-A pE7/HPV16 and MCF-7 vs. MCF-7 pE6/E7 did not exhibit any differences in the methylation of *CDH1* promoter regions (Fig. S1A) or in the expression of CDH1 at mRNA and protein levels (Fig. S1B and C). As the MCF-7 cell line is an adenocarcinoma that derives from the mammary gland and exhibits an epithelial phenotype with a high expression level of CDH1, similar to that observed in Ca Ski cells, and since the C33-A cell line originally does no express CDH1, C33-A and MCF7 cells were eliminated from the study; neither the effect of oncoprotein E7 on the suppression of *CDH1* expression, nor the methylation patterns in the *CDH1* promoter could be evaluated in these cells.

Methylation levels in the CDH1 promoter are associated with the mRNA and protein expression levels of CDH1. Analysis of *CDH1* expression in the different cell lines demonstrated a significant decrease of the *CDH1* mRNA level in the HeLa (P<0.001) and SiHa (P<0.01) cell lines compared

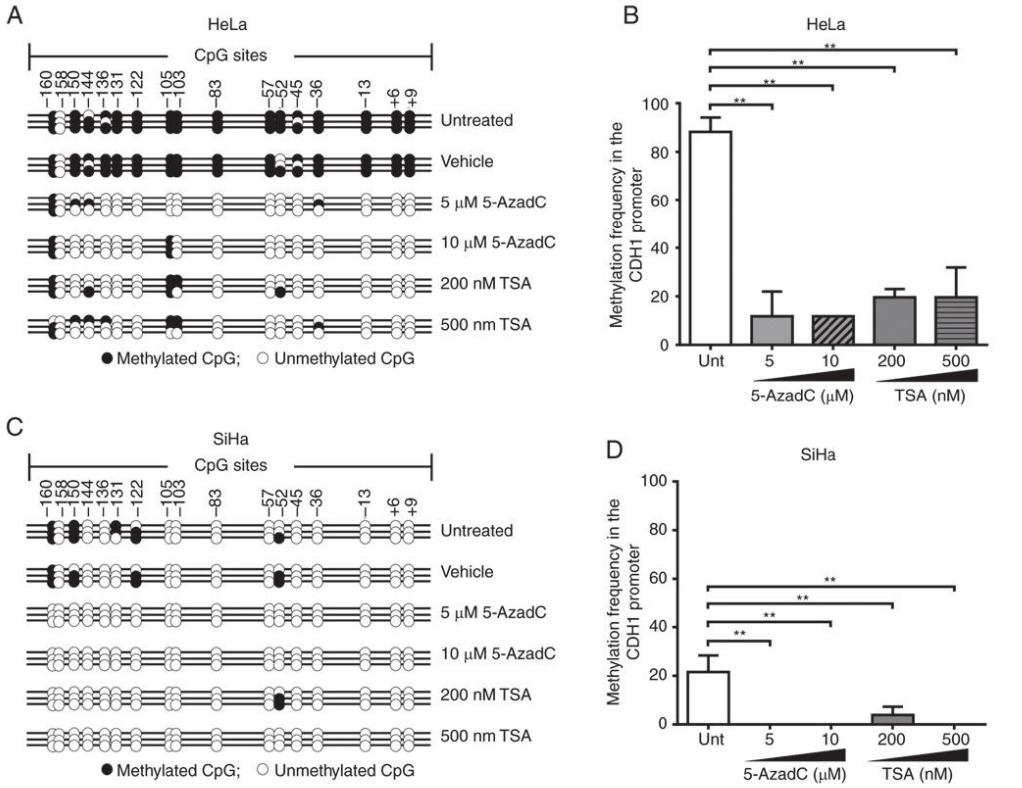

Figure 2. Changes in the methylation pattern of the *CDH1* promoter in HeLa and SiHa cell lines following treatment with 5-AzadC and TSA. (A and C) Lollipop methylation diagrams demonstrating changes in the methylation pattern in CpG sites of the *CDH1* promoter region in (A) HeLa and (C) SiHa cell lines following treatments with 5-AzadC and TSA compared with Unt and vehicle-treated cells. Black indicates a methylated CpG site; white indicates an unmethylated CpG site. (B and D) Quantification of the methylation frequency of the *CDH1* promoter in (B) HeLa and (D) SiHa cell lines following treatment with the indicated concentrations of 5-AzadC and TSA compared with untreated cells. **P<0.01 vs. untreated cells. Unt, untreated; *CDH1*, cadherin 1; 5-AzadC, 5-aza-2'-deoxycytidine; TSA, trichostatin A.

with the HaCaT cell line (Fig. 1D). A similar decrease was observed at the protein level (Fig. 1E). By contrast, the Ca Ski cell line exhibited high *CDH1* expression, similar to the control HaCaT cell line, at the mRNA and protein level (Fig. 1D and E).

CDH1 expression level is associated with the expression level of SNAI1. The present study measured the expression of *SNAI1* and *SNAI2* to test the hypothesis that the expression of *CDH1* is regulated by the transcription factors Snai1 and Snai2, which mediate EMT by negatively regulating the expression of *CDH1* (27,55-57). The results revealed that the mRNA expression level of *SNAI1* is significantly increased in HeLa (P<0.0001) and SiHa cells (P<0.001), but significantly reduced in Ca Ski cells (P<0.01) compared with HaCaT cells (Fig. 1D). This result was also reflected at the protein level (Fig. 1E). No significant differences were observed in the expression of *SNAI2* at the mRNA (Fig. 1D) and protein (Fig. 1E) level among all cell lines. Since the Ca Ski cell line exhibits a non-mesenchymal phenotype, a high expression level of E-cadherin and low expression levels of Snai1 and Snai2, this cell line was excluded from further analysis.

Treatment with 5-AzadC and TSA affect methylation and re-expression of CDH1. HeLa and SiHa cells were treated with different concentrations of 5-AzadC and TSA, followed by analysis of the expression levels of *CDH1*, *SNAI1*, and *SNAI2*. HeLa and SiHa cells treated with the vehicle (DMSO) were used for normalizing the expression values, as well for performing comparisons in statistical analysis.

The results demonstrated that in the HeLa cell line, the methylation pattern was maintained at CpG sites -103, -105, and -160 of the *CDH1* promoter region following treatment with 5-AzadC and TSA. By contrast, in the SiHa cell line, this region was completely demethylated following treatment with 5 or 10 μM 5-AzadC or 500 nM TSA, and only CpG site -52 was methylated following treatment with 200 nM TSA (Fig. 2A and C). Compared with untreated HeLa and SiHa cells, a decrease in methylation of 76.48% was observed following 5 or 10 μM 5-AzadC treatment, whereas following

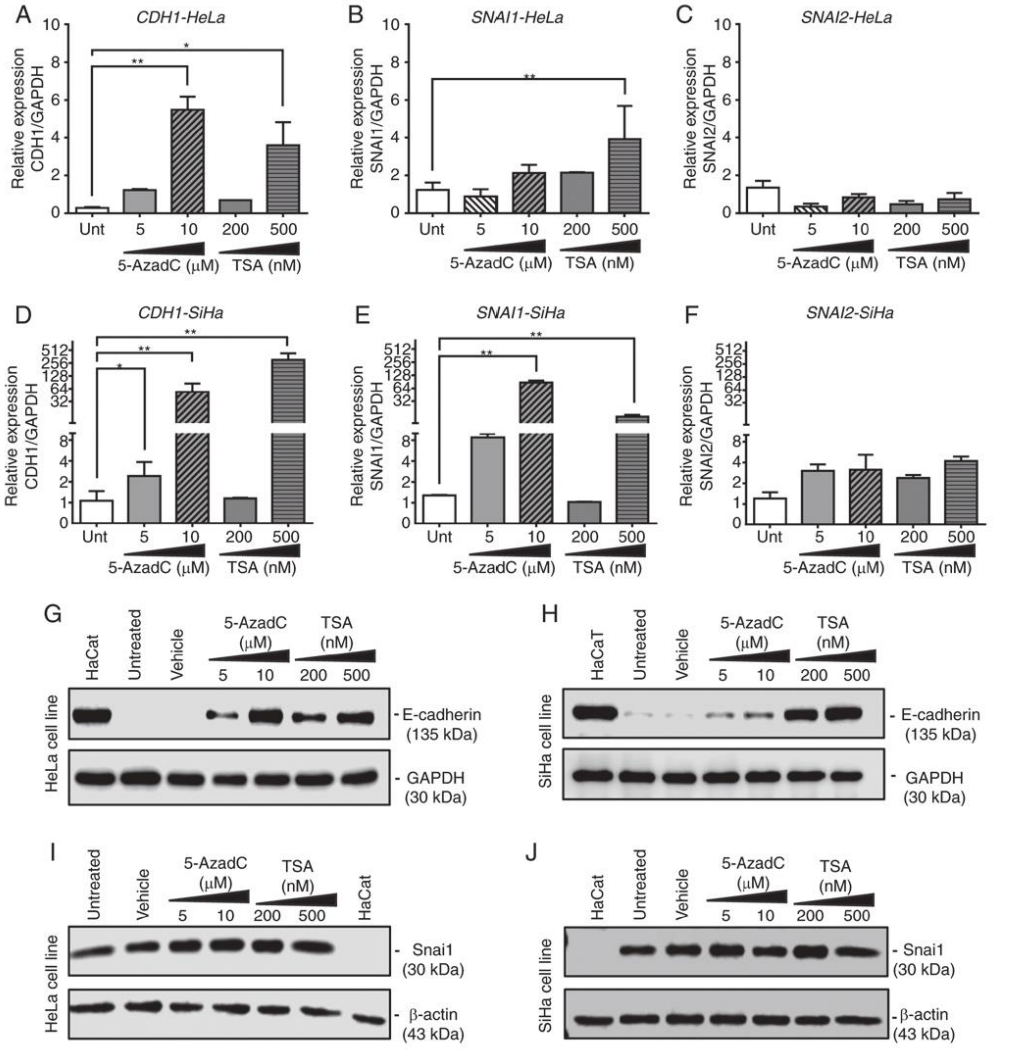

Figure 3. Changes in the expression levels of *CDH1*, *SNAI1* and *SNAI2* in HeLa and SiHa cells following treatment with 5-AzadC and TSA. (A-F) Quantitative PCR analyses of *CDH1*, *SNAI1* and *SNA2* mRNA expression levels in (A-C) HeLa and (D-F) SiHa cells following treatments with 5-AzadC and TSA compared with untreated cells; *P<0.05 and **P<0.01 vs. untreated cells. (G and H) Protein expression of E-cadherin in (G) HeLa and (H) SiHa cell lines. (I and J) Protein expression of Snai1 in (I) HeLa and (J) SiHa cell lines following the indicated treatments. Unt, untreated; *CDH1*, cadherin 1; 5-AzadC, 5-aza-2'-deoxycytidine; TSA, trichostatin A.

treatment with 200 or 500 nM TSA, a decrease in methylation of 68.63% was observed. By contrast, in SiHa cells, a decrease of 21.57% was observed following treatment with 5 or 10 μM 5-AzadC or 500 nM TSA, whereas following treatment with 200 nM TSA, a 17.65% decrease in methylation was observed. Therefore, it was demonstrated in the two cell lines that treatment with 5-AzadC or TSA significantly diminished the level of *CDH1* methylation (P<0.001; Fig. 2B and D). However, no significant differences were observed between the two treatments in diminishing the methylation levels of *CDH1*.

In the HeLa cell line, treatments with 10 μM 5-AzadC (P=0.004) and 500 nM TSA (P=0.03) significantly increased the expression of *CDH1* mRNA and protein (Fig. 3A and G). In addition, 500 nM TSA significantly increased the mRNA expression of *SNAI1* (P=0.01, Fig. 3B) in HeLa cells without notable changes in protein expression (Fig. 3I). In the SiHa cell line, the mRNA expression of *CDH1* significantly increased following treatment with 5-AzadC at 5 and 10 μM (P<0.05 and P<0.01, respectively) or 500 nM TSA (P=0.004; Fig. 3D); a similar effect was observed at the protein level (Fig. 3H).

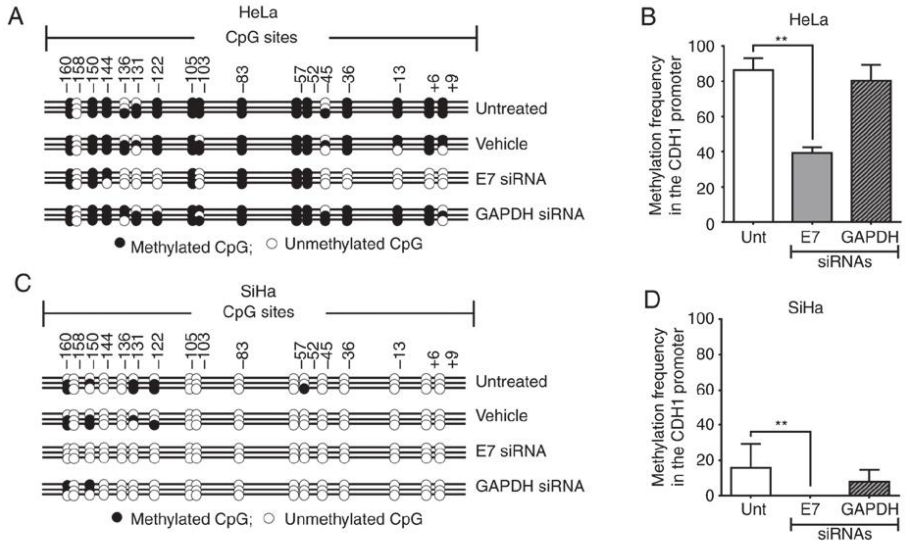

Figure 4. Silencing of E7 from HPV18 and HPV16 modifies the methylation pattern of the *CDH1* promoter in HeLa and SiHa cells. (A and C) Lollipop methylation diagrams demonstrating changes in the methylation pattern in CpG sites of the *CDH1* promoter region in (A) HeLa and (C) SiHa cell lines following transfection with siRNA targeting *E7* and *GAPDH* compared with Unt and vehicle control cells. Black indicates a methylated CpG site; white indicates an unmethylated CpG site. (B and D) Methylation frequency of the *CDH1* promoter in (B) HeLa and (D) SiHa cells following transfection with siRNA targeting *E7* from HPV18, *E7* from HPV16 and *GAPDH* compared with untreated cells. **P<0.01 vs. untreated cells. *CDH1*, cadherin 1; Unt, untreated; siRNA, small interfering RNA; HPV, human papilloma virus.

In addition, the expression of *SNAI1* mRNA was significantly increased following treatment with 10 μM 5-AzadC (P=0.004) or 500 nM TSA (P=0.01) (Fig. 3E) in SiHa cells without notable changes at the protein level (Fig. 3J), similar to that observed in HeLa.

5-AzadC and TSA also increased the mRNA expression level of *SNAI1* in the HeLa (Fig. 3B) and SiHa cell lines (Fig. 3E); however, no changes were observed in SNAI1 protein levels in the two cell lines (Fig. 3I and J). The expression of SNAI2 was not significantly modified at the mRNA level under any treatment condition in the tested cell lines (Fig. 3C and F).

Suppression of E7 by siRNA modifies the methylation patterns of the CDH1 promoter and induces CDH1 expression in HeLa and SiHa cell lines. To examine the involvement of *E7* in the *CDH1* methylation and expression patterns, HeLa and SiHa cell lines were transfected with siRNA against *E7*, which resulted in 57.9 and 42.5% reduction in the *E7* mRNA level, respectively (Fig. 5A and C). In the HeLa cell line, *E7* silencing led to demethylation of *CDH1* CpG promoter sites located between +9 and -45, as well as at -103 and between -122 and -136 (Fig. 4A). In addition, in the SiHa cell line, total demethylation of the CDH1 promoter was observed following *E7* silencing (Fig. 4C). Therefore, partial silencing of *E7* in HeLa and SiHa cells yielded a significant decrease in *CDH1* promoter methylation compared with untreated control cells (P<0.001; Fig. 4B and D). Increased *CDH1* mRNA and protein levels were observed following *E7* silencing in HeLa (Fig. 5B and F) and SiHa (Fig. 5B and G) cells. The use of Silencer® Select *GAPDH* siRNA as a positive control siRNA excluded the possibility that changes in the methylation pattern of the *CDH1* promoter were due to the siRNA transfection conditions as *GAPDH* silencing did not induce significant changes in the methylation pattern of the *CDH1* promoter in HeLa (P=0.7140; Fig. 4B) and SiHa (P=0.3248; Fig. 4D) cells; therefore, the changes in the methylation pattern were likely due to *E7* silencing.

Suppression of E7 inhibits SNAI1 and SNAI2 expression in HeLa and SiHa cells. Silencing of *E7* not only induced the expression of *CDH1*, but also significantly decreased the expression of *SNAI1* and *SNAI2* (P<0.001) in HeLa and SiHa cells (Fig. 5D, E, H and I). This suggested that E7 may be not only involved in suppressing the expression of *CDH1*, but may also regulate the expression of *SNAI1* and *SNAI2*, which negatively regulate CDH1. No significant changes were observed in the mRNA expression of *E7*, *CDH1*, *SNAI1* and *SNAI2* following *GAPDH* silencing in HeLa and SiHa cells (P>0.5; Fig. 5A, B, D and E). However, silencing of *GAPDH* with siRNA resulted in a decrease in the protein expression of Snai1 in HeLa cells (Fig. 5H).

As housekeeping genes *GAPDH* and *HPRT* were used to normalize the expression levels of the genes studied, no significant differences were noted in the reduction of *SNAI1* expression at the mRNA level (Fig. 5D). Further analysis of the expression levels of *GAPDH*, *CDH1* and *SNAI1* genes normalized against β-actin demonstrated that *GAPDH* expression was 2.6-fold higher in HaCaT, 1.6-fold higher in HeLa, 3.3-fold higher in SiHa and 3.8-fold higher in Ca Ski cells

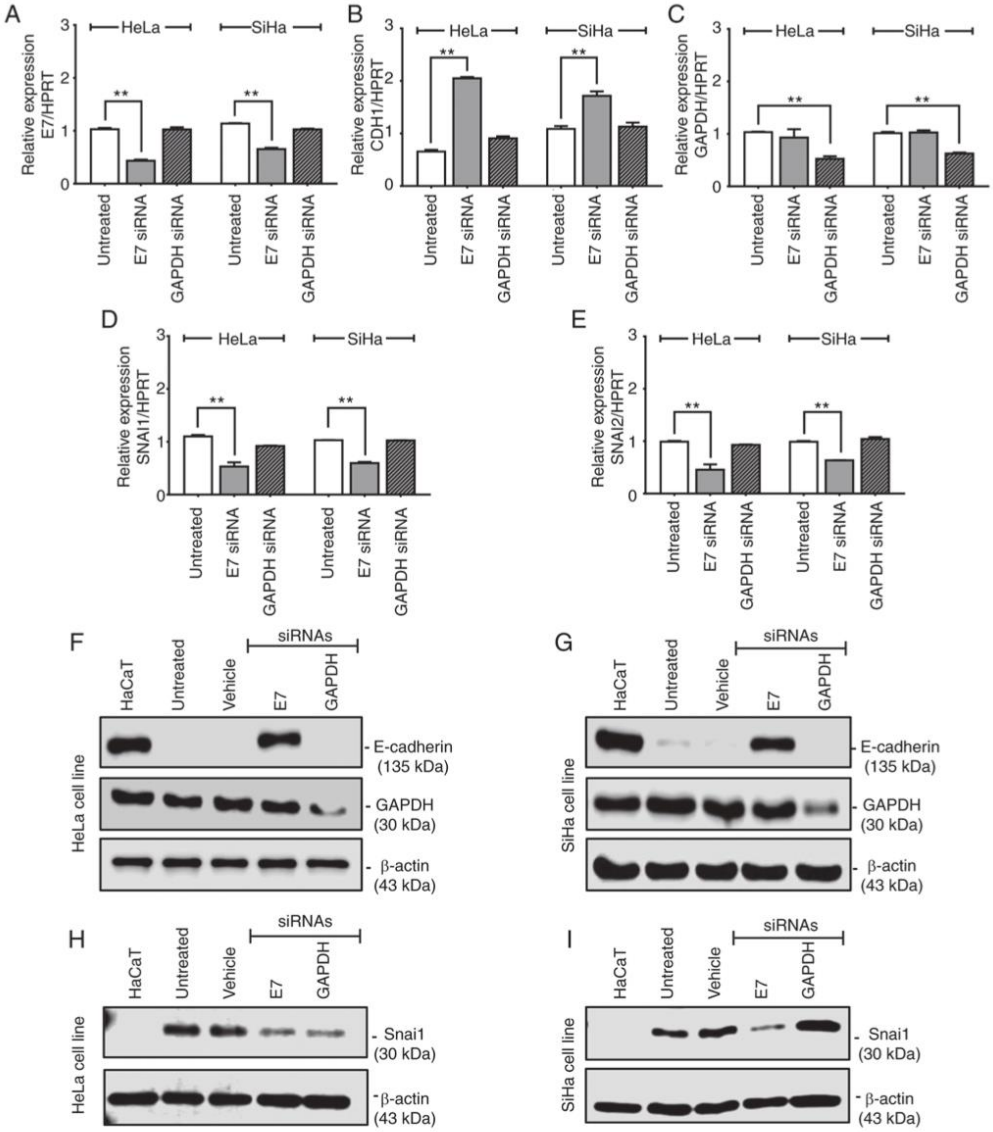

Figure 5. Silencing of E7 from HPV18 and HPV16 modifies the expression of *CDH1* and *SNAI1* genes in HeLa and SiHa cell lines. (A-E) The relative mRNA expression levels of (A) *E7*, (B) *CDH1*, (C) *GAPDH*, (D) *SNAI1* and (E) *SNAI2* in HeLa and SiHa cell lines following transfection with siRNA against *E7* and *GAPDH*. **P<0.01 vs. untreated cells. E-cadherin, Snai1, GAPDH and β-actin protein expression levels in (F and H) HeLa and (G and I) SiHa cells following transfection with siRNA targeting *E7* and *GAPDH*. *CDH1*, cadherin 1; siRNA, small interfering RNA; HPV, human papilloma virus.

compared with a commercial sample of RNA extracted from normal cervical tissue (Fig. S2).

Discussion

HR-HPV activates the cell methylation machinery, which not only methylates its own genome, but also the promoter regions of cellular genes (21). Laurson *et al* (26) have demonstrated that E7 induces the expression of Dnmt1 and suppresses the expression of *CDH1*. Reduction of E-cadherin has been reported to contribute to the persistence of HPV, which is in agreement with reports that E7 interacts with and induces the expression of Dnmt1 and triggers its *de novo* methylation activity (16) (Fig. 6A). The results of the present study agree

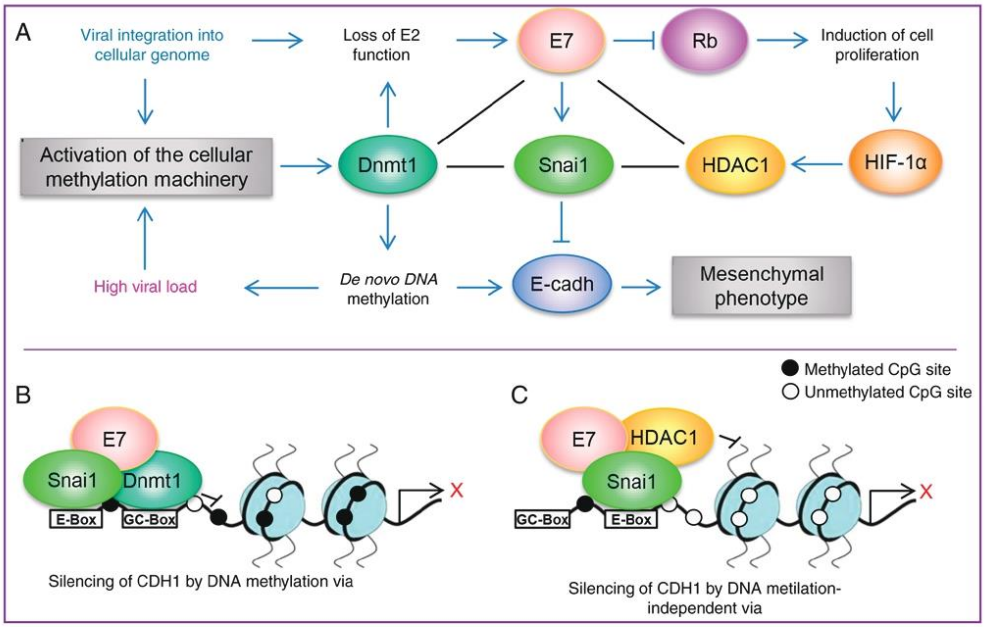

Figure 6. A schematic model demonstrating how high-risk HPV E7 may induce epithelial-mesenchymal transition via Snai1. (A) A schematic model of proteins that interact with or are induced by E7. The loss of E2 function, either from the integration or methylation of the E2 binding sites in the HPV long control region, leads to the dysregulated expression of the oncoproteins E6 and E7. E7 serves an important role in regulating several pathways; E7 induces cellular proliferation via pRB and E7 not only induces the expression of Dnmt1 and HDAC1, but also physically interacts with them, which promotes epigenetic regulation of HPV and cellular genes. The results of the present study indicated that E7 may not only suppresses the expression of *CDH1* through the methylation of its promoter region, but also induce the expression of Snai1, which is a negative regulator of *CDH1* expression. (B and C) Proposed models of how E7 may regulate the expression of *CDH1*. HPV, human papilloma virus; *CDH1*, cadherin 1; Dmnt1, DNA methyltransferase 1; HDAC1, histone deacetylase type 1; HIF-1α, hypoxia-inducible factor 1α; pRB, retinoblastoma protein.

with previous findings by Laurson *et al* (26), in which E7 from HPV16 suppressed the expression of *CDH1*. However, in this previous study, no significant differences were observed in the methylation pattern of the *CDH1* promoter of NIKS cells overexpressing E7, as the 17 CpG sites analyzed were not methylated (23). In addition, treatment with 5-AzadC re-established the expression of *CDH1* at the mRNA and protein levels (26); however, the concentration of 5-AzadC used was not stated and the changes in the expression of other cellular genes were not discussed.

The present study evaluated the re-expression of *CDH1* at the mRNA and protein levels in HeLa and SiHa cell lines treated with 5-AzadC and TSA, as well as changes in the methylation pattern of the promoter region of *CDH1*. Additionally, although TSA is not a demethylating agent, demethylation in the promoter of *CDH1* following treatment with TSA was observed. This result was an agreement with previous studies that have reported that TSA induces DNA demethylation and proposed that a change in chromatin modification, including the deacetylation of histones induced by an HDAC inhibitor, such as TSA, may render a gene susceptible to DNA demethylation (58,59).

In addition, an increase in *SNAI1* mRNA level was observed after treatment with 500 nM TSA in HeLa cells, whereas in SiHa cells an increase in *SNAI1* mRNA level was observed after treatment with 10 μM 5-AzadC and 500 nM TSA; however, no apparent changes were observed in SNAI1 protein level in the two cell lines. This result was in agreement with studies in which such treatments not only re-established the expression of *CDH1*, but also induced upregulation of *SNAI1* and *SNAI2* at the mRNA level (60,61), which was likely due to modifications in the methylation pattern in the promoter regions of *SNAI1* and *SNAI2* (62). The role of *SNAI1* regulation by epigenetic mechanisms is largely unknown. A previous study has demonstrated that the treatment with 5-AzadC in fibroblast cell IMR90, induced pluripotent stem cells from IMR90, BeWo and HTR8/SVneo cell lines induces a greater expression of *SNAI1* and *SNAI2* at the mRNA level and that the regulation of the two genes is mediated by DNA methylation of their first intron and not due to DNA methylation of their promoter region; however, this previous study did not determine the expression of these genes at the protein level (62). The present study did not determine the methylation status of the *SNAI1* promoter region as it is transcriptionally active in HeLa and SiHa cells. The differences observed in the effect on SNAI1 expression at the mRNA and protein levels by treatment with 5-AzadC and TSA indicated that other factors may regulate the expression of SNAI1 in the two cell lines.

On the other hand, the results published by Laurson *et al* (26) suggested that in the NIKS-cell model, suppression of *CDH1*

expression by E7 was independent of the methylation status of the *CDH1* promoter region, which was observed in the SiHa cell line in the current study. The previous study also suggested that repression of *CDH1* may be regulated via *SNAI2* (*SLUG*); however, it was reported that the expression of *SNAI2* was not altered by the presence of E7 (26). The results of the present study revealed that while *SNAI1* mRNA and protein was expressed in HeLa and SiHa cells, *SNAI2* mRNA expression was barely detectable in HaCaT and Ca Ski cells. *SNAI2* has been demonstrated to be upregulated in HaCaT cells during the process of cell motility and wound-healing (63).

The results of the present study demonstrated that following silencing of *E7* from HPV16 and HPV18, *CDH1* expression was recovered in HeLa and SiHa cells, which is in agreement with a previous study by Caberg *et al* (25). This previous study reported that following 24-h transfection of SiHa cells with siRNA against HPV16 *E7*, *CDH1* was upregulated and an increase of the Retinoblastoma protein (pRB), which is responsible for a major G1 check point, blocking S-phase entry and cell growth, and activating protein 2α were detected without changes in the mRNA expression levels of *SNAI1* and *SNAI2* (25). By contrast, the present study demonstrated that following 48-h transfection with siRNA against *E7*, changes in the methylation pattern of the *CDH1* promoter region were observed in HeLa and SiHa cells. In addition, an increase in the mRNA and protein expression levels of *CDH1* were identified, as well as a decrease in the mRNA and protein expression levels of *SNAI1* and *SNAI2*. Therefore, the current results suggested that E7 not only suppressed the expression of *CDH1* via the methylation of its promoter, but also regulated the expression of *SNAI1*, a negative regulator of *CDH1* involved in EMT and associated with metastasis (27,55-57). These observations are also concordant with the mechanism of action reported for other oncogenic viruses, where the X protein of HBV (HBx), core protein of HCV and latent membrane protein 1 (LMP1) of EBV promote EMT and metastasis by inducing the expression *SNAI1* and suppressing *CDH1* expression (64-67).

Following silencing *GAPDH* with siRNA, *SNAI1* expression was partially suppressed in HeLa cells at the protein level, but not at mRNA level. This was consistent with a previous study that demonstrated that the interaction of GAPDH with Sp1 resulted in increased expression of Snail, which promoted the proliferation and metastasis of cancer cells, and that suppression of *GAPDH* with shRNA resulted in a significant decrease of Snail in the HCT116 and LoVo cell lines (68). This suggested that GAPDH may serve a role in the metastasis of cervical adenocarcinoma (HeLa) by affecting EMT through the upregulation of Snail expression mediated by Sp1, similar to its role reported in colon cancer (68), but further studies are required to verify this.

It is currently unknown how HPV may activate the expression of *SNAI1*; however, it has been reported that in other cancer types associated with virus, HBx, core and LMPI proteins increased *SNAI1* expression through the activation of the PI3K/Akt and MAPK pathways by transforming growth factor-β (TGF-β) action (64,69-72), which is in agreement with a previous study by Peinado *et al* (73) suggesting that TGF-β induces *SNAI1* transcription through MAPK and PI3K.

In the present study, the signaling pathways involved in regulating *SNAI1* expression were not determined; however, previous studies have reported that HR-HPV infection activates the PI3K/Akt/mTOR pathway (74), E7 from HPV upregulates Akt activity though the pRB protein (75) and TGF-β stimulates EMT and tumor invasion in SiHa cells (76).

In summary, the results of the present demonstrated that HR-HPV E7 may regulate the expression of *CDH1* by two different pathways, in which Snail is involved. The first pathway involves hypermethylation of the *CDH1* promoter region and the expression of Snail, as observed in the HeLa cell line. The second pathway involves hypomethylation of the *CDH1* promoter region with expression of Snail as observed in SiHa cell line, suggesting that *CDH1* and *SNAI1* may be considered as biomarkers of metastasis in uterine cervical cancer. Therefore, based on the present results and previous evidence that E7 interacts with Dnmt1 and HDAC1 (15-17), it would be beneficial to determine if E7 from HR-HPV may interact with Snail to form a co-repressor complex with either Dnmt1 or HDAC1 in the *CDH1* promoter (Fig. 6B and C), which may explain the suppression of *CDH1* expression during the EMT process.

Acknowledgements

This study is part of the doctoral dissertation project of Pedro Rosendo Chalma, a Doctoral student from Programa de Doctorado en Ciencias Biomédicas (PDCB), Instituto de Investigaciones Biomédicas, Universidad Nacional Autónoma de México (UNAM) and received a fellowship from Consejo Nacional de Ciencia y Tecnología (CONACyT; grant no. 203376). The present study was supported by CONACyT (grant no. 253804 to AG-C) and MINECO (grant no. SAF2013-44739-R to AC). The authors would like to thank Ms. Miriam C. Guido Jiménez (UNAM) and Ms. Raquél López Paniagua (INCan) for their technical support, Dr Erick de la Cruz Hernández (Juarez Autonomous University of Tabasco) and Dr Patricio Gariglio (CINVESTAV-IPN) for providing the cell lines and Dr Alfonso Dueñas Gonzalez (INCan-UNAM) for providing the oligonucleotides for *CDH1* used in the MSP-Protocol.

Funding

The present study received additional support of the Fundación Miguel Alemán, A.C. to AGC. PRC received a fellowship from Programa de Movilidad Internacional de Estudiantes de la Coordinación de Estudios de Posgrado (CEP-UNAM) during his doctoral stay at the Universidad Autónoma de Madrid (UAM).

Availability of data and materials

The datasets used and analyzed during the current study are available from the corresponding author on reasonable request.

Authors' contributions

PRC performed all experiments, interpreted the data and wrote the manuscript. VAV, GDBO and CCPM performed western blot analysis and interpreted the data. AC and AGC conceived and designed the study, interpreted the data and

edited the manuscript. All authors have read and approved the final manuscript.

Ethics approval and consent to participate

Not applicable.

Patient consent for publication

Not applicable.

Competing interests

The authors declare that they have no competing interests.

References

1. Ferlay J, Soerjomataram I, Dikshit R, Eser S, Mathers C, Rebelo M, Parkin DM, Forman D and Bray F: Cancer incidence and mortality worldwide: Sources, methods and major patterns in GLOBOCAN 2012. Int J Cancer 136: E359-E386, 2015.
2. Parkin DM, Bray F, Ferlay J and Pisani P: Global cancer statistics, 2002. CA Cancer J Clin 55: 74-108, 2005.
3. zur Hausen H: Papillomaviruses in the causation of human cancers-a brief historical account. Virology 384: 260-265, 2009.
4. Bansal A, Singh MP and Rai B: Human papillomavirus-associated cancers: A growing global problem. Int J Appl Basic Med Res 6: 84-89, 2016.
5. Hanahan D and Weinberg RA: Hallmarks of cancer: The next generation. Cell 144: 646-674, 2011.
6. Doorbar J: Latent papillomavirus infections and their regulation. Curr Opin Virol 3: 416-421, 2013.
7. Schiffman M, Doorbar J, Wentzensen N, de Sanjosé S, Fakhry C, Monk BJ, Stanley MA and Franceschi S: Carcinogenic human papillomavirus infection. Nat Rev Dis Primers 2: 16086, 2016.
8. Durst M, Kleinheinz A, Hotz M and Gissmann L: The physical state of human papillomavirus type 16 DNA in benign and malignant genital tumours. J Gen Virol 66: 1515-1522, 1985.
9. Lehn H, Villa LL, Marziona F, Hilgarth M, Hillemans HG and Sauer G: Physical state and biological activity of human papillomavirus genomes in precancerous lesions of the female genital tract. J Gen Virol 69: 187-196, 1988.
10. Badal S, Badal V, Calleja-Macias IE, Kalantari M, Chuang LS, Li BF and Bernard HU: The human papillomavirus-18 genome is efficiently targeted by cellular DNA methylation. Virology 324: 483-492, 2004.
11. Fernandez AF, Rosales C, Lopez-Nieva P, Graña O, Ballestar E, Ropero S, Espada J, Melo SA, Lujambio A, Fraga MF, *et al*: The dynamic DNA methylomes of double-stranded DNA viruses associated with human cancer. Genome Res 19: 438-451, 2009.
12. Kalantari M, Lee D, Calleja-Macias IE, Lambert PF and Bernard HU: Effects of cellular differentiation, chromosomal integration and 5-aza-2'-deoxycytidine treatment on human papillomavirus-16 DNA methylation in cultured cell lines. Virology 374: 292-303, 2008.
13. Boyer SN, Wazer DE and Band V: E7 protein of human papilloma virus-16 induces degradation of retinoblastoma protein through the ubiquitin-proteasome pathway. Cancer Res 56: 4620-4624, 1996.
14. Munger K, Phelps WC, Bubb V, Howley PM and Schlegel R: The E6 and E7 genes of the human papillomavirus type 16 together are necessary and sufficient for transformation of primary human keratinocytes. J Virol 63: 4417-4421, 1989.
15. Brehm A, Nielsen SJ, Miska EA, McCance DJ, Reid JL, Bannister AJ and Kouzarides T: The E7 oncoprotein associates with Mi2 and histone deacetylase activity to promote cell growth. EMBO J 18: 2449-2458, 1999.
16. Burgers WA, Blanchon L, Pradhan S, de Launoit Y, Kouzarides T and Fuks F: Viral oncoproteins target the DNA methyltransferases. Oncogene 26: 1650-1655, 2007.
17. Longworth MS and Laimins LA: The binding of histone deacetylases and the integrity of zinc finger-like motifs of the E7 protein are essential for the life cycle of human papillomavirus type 31. J Virol 78: 3533-3541, 2004.
18. Zhang Y, LeRoy G, Seelig HP, Lane WS and Reinberg D: The dermatomyositis-specific autoantigen Mi2 is a component of a complex containing histone deacetylase and nucleosome remodeling activities. Cell 95: 279-289, 1998.
19. Li H, Ou X, Xiong J and Wang T: HPV16E7 mediates HADC chromatin repression and downregulation of MHC class I genes in HPV16 tumorigenic cells through interaction with an MHC class I promoter. Biochem Biophys Res Commun 349: 1315-1321, 2006.
20. Georgopoulos NT, Proffitt JL and Blair GE: Transcriptional regulation of the major histocompatibility complex (MHC) class I heavy chain, TAP1 and LMP2 genes by the human papillomavirus (HPV) type 6b, 16 and 18 E7 oncoproteins. Oncogene 19: 4930-4935, 2000.
21. Milutin Gasperov N, Sabol I, Planinić P, Grubišić G, Fistonić I, Ćorušić A and Grce M: Methylated host cell gene promoters and human papillomavirus type 16 and 18 predicting cervical lesions and cancer. PLoS One 10: e0129452, 2015.
22. Liu J, Lian Z, Han S, Waye MM, Wang H, Wu MC, Wu K, Ding J, Arbuthnot P, Kew M, *et al*: Downregulation of E-cadherin by hepatitis B virus X antigen in hepatocellullar carcinoma. Oncogene 25: 1008-1017, 2006.
23. McLaughlin-Drubin ME and Munger K: Viruses associated with human cancer. Biochim Biophys Acta 1782: 127-150, 2008.
24. Tsai CN, Tsai CL, Tse KP, Chang HY and Chang YS: The Epstein-Barr virus oncogene product, latent membrane protein 1, induces the downregulation of E-cadherin gene expression via activation of DNA methyltransferases. Proc Natl Acad Sci USA 99: 10084-10089, 2002.
25. Caberg JH, Hubert PM, Begon DY, Herfs MF, Roncarati PJ, Boniver JJ and Delvenne PO: Silencing of E7 oncogene restores functional E-cadherin expression in human papillomavirus 16-transformed keratinocytes. Carcinogenesis 29: 1441-1447, 2008.
26. Laurson J, Khan S, Chung R, Cross K and Raj K: Epigenetic repression of E-cadherin by human papillomavirus 16 E7 protein. Carcinogenesis 31: 918-926, 2010.
27. Cano A, Perez-Moreno MA, Rodrigo I, Locascio A, Blanco MJ, del Barrio MG, Portillo F and Nieto MA: The transcription factor snail controls epithelial-mesenchymal transitions by repressing E-cadherin expression. Nat Cell Biol 2: 76-83, 2000.
28. Pattillo RA, Hussa RO, Story MT, Ruckert AC, Shalaby MR and Mattingly RF: Tumor antigen and human chorionic gonadotropin in CaSki cells: A new epidermoid cervical cancer cell line. Science 196: 1456-1458, 1977.
29. Friedl F, Kimura I, Osato T and Ito Y: Studies on a new human cell line (SiHa) derived from carcinoma of uterus. I. Its establishment and morphology. Proc Soc Exp Biol Med 135: 543-545, 1970.
30. Diao MK, Liu CY, Liu HW, Li JT, Li F, Mehryar MM, Wang YJ, Zhan SB, Zhou YB, Zhong RG and Zeng Y: Integrated HPV genomes tend to integrate in gene desert areas in the CaSki, HeLa, and SiHa cervical cancer cell lines. Life Sci 127: 46-52, 2015.
31. Yee C, Krishnan-Hewlett I, Baker CC, Schlegel R and Howley PM: Presence and expression of human papillomavirus sequences in human cervical carcinoma cell lines. Am J Pathol 119: 361-366, 1985.
32. Schneider-Gädicke A and Schwarz E: Different human cervical carcinoma cell lines show similar transcription patterns of human papillomavirus type 18 early genes. EMBO J 5: 2285-2292, 1986.
33. Pater MM and Pater A: Human papillomavirus types 16 and 18 sequences in carcinoma cell lines of the cervix. Virology 145: 313-318, 1985.
34. Pater MM and Pater A: Expression of human papillomavirus types 16 and 18 DNA sequences in cervical carcinoma cell lines. J Med Virol 26: 185-195, 1988.
35. Spence RP, Murray A, Banks L, Kelland LR and Crawford L: Analysis of human papillomavirus sequences in cell lines recently derived from cervical cancers. Cancer Res 48: 324-328, 1988.
36. Meissner JD: Nucleotide sequences and further characterization of human papillomavirus DNA present in the CaSki, SiHa and HeLa cervical carcinoma cell lines. J Gen Virol 80: 1725-1733, 1999.
37. De la Cruz-Hernandez E, Garcia-Carranca A, Mohar-Betancourt A, Dueñas-González A, Contreras-Paredes A, Pérez-Cardenas E, Herrera-Goepfert R and Lizano-Soberón M: Differential splicing of E6 within human papillomavirus type 18 variants and functional consequences. J Gen Virol 86: 2459-2468, 2005.

38. Vazquez-Vega S, Sanchez-Suarez LP, Andrade-Cruz R, Castellanos-Juarez E, Contreras-Paredes A, Lizano-Soberon M, Garcia-Carranca A and Benitez Bribiesca L: Regulation of p14ARF expression by HPV-18 E6 variants. J Med Virol 85: 1215-1221, 2013.
39. Vazquez-Vega S, Sanchez-Suarez LP, Contreras-Paredes A, Castellanos-Juárez E, Peñarroja-Flores R, Lizano-Soberón M, Andrade-Cruz R, García-Carrancá A and Benítez-Bribiesca L: Nuclear co-expression of p14ARF and p16INK4A in uterine cervical cancer-derived cell lines containing HPV. Cancer Biomark 8: 341-350, 2010-2011.
40. Gutierrez J, Garcia-Villa E, Ocadiz-Delgado R, Cortés-Malagón EM, Vázquez J, Roman-Rosales A, Alvarez-Rios E, Celik H, Romano MC, Üren A, *et al*: Human papillomavirus type 16 E7 oncoprotein upregulates the retinoic acid receptor-beta expression in cervical cancer cell lines and K14E7 transgenic mice. Mol Cell Biochem 408: 261-272, 2015.
41. Momparler RL: Epigenetic therapy of cancer with 5-aza-2'-deoxycytidine (decitabine). Semin Oncol 32: 443-451, 2005.
42. Vigushin DM, Ali S, Pace PE, Mirsaidi N, Ito K, Adcock I and Coombes RC: Trichostatin A is a histone deacetylase inhibitor with potent antitumor activity against breast cancer in vivo. Clin Cancer Res 7: 971-976, 2001.
43. Jiang M and Milner J: Selective silencing of viral gene expression in HPV-positive human cervical carcinoma cells treated with siRNA, a primer of RNA interference. Oncogene 21: 6041-6048, 2002.
44. Lea JS, Sunaga N, Sato M, Kalahasti G, Miller DS, Minna JD and Muller CY: Silencing of HPV 18 oncoproteins with RNA interference causes growth inhibition of cervical cancer cells. Reprod Sci 14: 20-28, 2007.
45. Sledz CA, Holko M, de Veer MJ, Silverman RH and Williams BR: Activation of the interferon system by short-interfering RNAs. Nat Cell Biol 5: 834-839, 2003.
46. Makpol S, Zainuddin A and Chua KH: GAPDH expression as a measurement of transfection efficiency for p16 INK4a gene silencing (siRNA) in senescent human diploid fibroblasts. Am J Mol Biol 2: 390-397, 2012.
47. Han H: RNA interference to knock down gene expression. Methods Mol Biol 1706: 293-302, 2018.
48. Borawski J, Lindeman A, Buxton F, Labow M and Gaither LA: Optimization procedure for small interfering RNA transfection in a 384-well format. J Biomol Screen 12: 546-559, 2007.
49. Peter Hahn JD, Wolfgang Bielke and Jie Kang: Patent: EP2240582 B1-Positive controls for expression modulating experiments. European Patent Office, October 23, 2013.
50. Cheng A, Magdaleno S and Vlassov AV: Optimization of transfection conditions and analysis of siRNA potency using real-time PCR. Methods Mol Biol 764: 199-213, 2011.
51. Badal V, Chuang LS, Tan EH, Badal S, Villa LL, Wheeler CM, Li BF and Bernard HU: CpG methylation of human papillomavirus type 16 DNA in cervical cancer cell lines and in clinical specimens: Genomic hypomethylation correlates with carcinogenic progression. J Virol 77: 6227-6234, 2003.
52. Kalantari M, Calleja-Macias IE, Tewari D, Hagmar B, Lie K, Barrera-Saldana HA, Wiley DJ and Bernard HU: Conserved methylation patterns of human papillomavirus type 16 DNA in asymptomatic infection and cervical neoplasia. J Virol 78: 12762-12772, 2004.
53. Hoffmann I, Hilger M and Mueller O: Homo sapiens promoter of E-cadherin from HEK293 cells. Max-Planck-Institut fuer Molekulare Physiologie, Dortmund, 2006.
54. Livak KJ and Schmittgen TD: Analysis of relative gene expression data using real-time quantitative PCR and the 2(-Delta Delta C(T)) method. Methods 25: 402-408, 2001.
55. Peinado H, Portillo F and Cano A: Transcriptional regulation of cadherins during development and carcinogenesis. Int J Dev Biol 48: 365-375, 2004.
56. Moreno-Bueno G, Cubillo E, Sarrio D, Peinado H, Rodríguez-Pinilla SM, Villa S, Bolós V, Jordá M, Fabra A, Portillo F, *et al*: Genetic profiling of epithelial cells expressing E-cadherin repressors reveals a distinct role for Snail, Slug, and E47 factors in epithelial-mesenchymal transition. Cancer Res 66: 9543-9556, 2006.
57. Peinado H, Olmeda D and Cano A: Snail, Zeb and bHLH factors in tumour progression: An alliance against the epithelial phenotype? Nat Rev Cancer 7: 415-428, 2007.
58. Cameron EE, Bachman KE, Myöhänen S, Herman JG and Baylin SB: Synergy of demethylation and histone deacetylase inhibition in the re-expression of genes silenced in cancer. Nat Genet 21: 103-107, 1999.
59. Ou JN, Torrisani J, Unterberger A, Provençal N, Shikimi K, Karimi M, Ekström TJ and Szyf M: Histone deacetylase inhibitor Trichostatin A induces global and gene-specific DNA demethylation in human cancer cell lines. Biochem Pharmacol 73: 1297-1307, 2007.
60. Meng F, Sun G, Zhong M, Yu Y and Brewer MA: Anticancer efficacy of cisplatin and trichostatin A or 5-aza-2'-deoxycytidine on ovarian cancer. Br J Cancer 108: 579-586, 2013.
61. Liu YN, Lee WW, Wang CY, Chao TH, Chen Y and Chen JH: Regulatory mechanisms controlling human E-cadherin gene expression. Oncogene 24: 8277-8290, 2005.
62. Chen Y, Wang K, Qian CN and Leach R: DNA methylation is associated with transcription of Snail and Slug genes. Biochem Biophys Res Commun 430: 1083-1090, 2013.
63. Savagner P, Kusewitt DF, Carver EA, Magnino F, Choi C, Gridley T and Hudson LG: Developmental transcription factor slug is required for effective re-epithelialization by adult keratinocytes. J Cell Physiol 202: 858-866, 2005.
64. Arzumanyan A, Friedman T, Kotei E, Ng IO, Lian Z and Feitelson MA: Epigenetic repression of E-cadherin expression by hepatitis B virus x antigen in liver cancer. Oncogene 31: 563-572, 2012.
65. Horikawa T, Yoshizaki T, Kondo S, Furukawa M, Kaizaki Y and Pagano JS: Epstein-Barr Virus latent membrane protein 1 induces Snail and epithelial-mesenchymal transition in metastatic nasopharyngeal carcinoma. Br J Cancer 104: 1160-1167, 2011.
66. Liu H, Xu L, He H, Zhu Y, Liu J, Wang S, Chen L, Wu Q, Xu J and Gu J: Hepatitis B virus X protein promotes hepatoma cell invasion and metastasis by stabilizing Snail protein. Cancer Sci 103: 2072-2081, 2012.
67. Nie D, Shan X, Nie L, Duan Y, Chen Z, Yang Y, Li Z, Tian L, Gao Q, Shan Y and Tang N: Hepatitis C virus core protein interacts with Snail and histone deacetylases to promote the metastasis of hepatocellular carcinoma. Oncogene 35: 3626-3635, 2016.
68. Liu K, Tang Z, Huang A, Chen P, Liu P, Yang J, Lu W, Liao J, Sun Y, Wen S, *et al*: Glyceraldehyde-3-phosphate dehydrogenase promotes cancer growth and metastasis through upregulation of SNAIL expression. Int J Oncol 50: 252-262, 2017.
69. Liu Y, Xu Y, Ma H, Wang B, Xu L, Zhang H, Song X, Gao L, Liang X and Ma C: Hepatitis B virus X protein amplifies TGF-β promotion on HCC motility through down-regulating PPM1a. Oncotarget 7: 33125-33135, 2016.
70. Park GB, Kim D, Kim YS, Kim S, Lee HK, Yang JW and Hur DY: The Epstein-Barr virus causes epithelial-mesenchymal transition in human corneal epithelial cells via Syk/src and Akt/Erk signaling pathways. Invest Ophthalmol Vis Sci 55: 1770-1779, 2014.
71. Sides MD, Klingsberg RC, Shan B, Gordon KA, Nguyen HT, Lin Z, Takahashi T, Flemington EK and Lasky JA: The Epstein-Barr virus latent membrane protein 1 and transforming growth factor-β1 synergistically induce epithelial--mesenchymal transition in lung epithelial cells. Am J Respir Cell Mol Biol 44: 852-862, 2011.
72. Taniguchi H, Kato N, Otsuka M, Goto T, Yoshida H, Shiratori Y and Omata M: Hepatitis C virus core protein upregulates transforming growth factor-beta 1 transcription. J Med Virol 72: 52-59, 2004.
73. Peinado H, Quintanilla M and Cano A: Transforming growth factor beta-1 induces snail transcription factor in epithelial cell lines: Mechanisms for epithelial mesenchymal transitions. J Biol Chem 278: 21113-21123, 2003.
74. Surviladze Z, Sterk RT, DeHaro SA and Ozbun MA: Cellular entry of human papillomavirus type 16 involves activation of the phosphatidylinositol 3-kinase/Akt/mTOR pathway and inhibition of autophagy. J Virol 87: 2508-2517, 2013.
75. Menges CW, Baglia LA, Lapoint R and McCance DJ: Human papillomavirus type 16 E7 up-regulates AKT activity through the retinoblastoma protein. Cancer Res 66: 5555-5559, 2006.
76. Yi JY, Hur KC, Lee E, Jin YJ, Arteaga CL and Son YS: TGFbeta1-mediated epithelial to mesenchymal transition is accompanied by invasion in the SiHa cell line. Eur J Cell Biol 81: 457-468, 2002.

XIII.3 Coautora en artículo científico publicado en Redox Biology.

Redox Biology 28 (2020) 101320

Contents lists available at ScienceDirect

Redox Biology

journal homepage: www.elsevier.com/locate/redox

Curcumin stabilizes p53 by interaction with NAD(P)H:quinone oxidoreductase 1 in tumor-derived cell lines

Carlos César Patiño-Morales[a,b,c], Ernesto Soto-Reyes[b], Elena Arechaga-Ocampo[b], Elizabeth Ortiz-Sánchez[c], Verónica Antonio-Véjar[d], José Pedraza-Chaverri[e], Alejandro García-Carrancá[f,*]

[a] Posgrado en Ciencias Biomédicas, Instituto de Investigaciones Biomédicas, Universidad Nacional Autónoma de México, Mexico City, Mexico
[b] Departamento de Ciencias Naturales, Universidad Autónoma Metropolitana, Unidad Cuajimalpa, Mexico City, 05300, Mexico
[c] División de Investigación Básica, Instituto Nacional de Cancerología, Mexico City, 14080, Mexico
[d] Laboratorio de Biomedicina Molecular, Universidad Autónoma de Guerrero, Chilpancingo Guerrero, 39080, Mexico
[e] Facultad de Química, Universidad Nacional Autónoma de México, Mexico City, 14080, Mexico
[f] Unidad de Investigación Biomédica en Cáncer, Instituto de Investigaciones Biomédicas, Universidad Nacional Autónoma de México & Instituto Nacional de Cancerología, Secretaría de Salud, Mexico City, 14080, Mexico

ARTICLE INFO

Keywords:
P53
Curcumin
NQO1
E6AP
Tumour cell lines

ABSTRACT

Curcumin is a natural phytochemical with potent anti-neoplastic properties including modulation of p53. Targeting p53 activity has been suggested as an important strategy in cancer therapy. The purpose of this study was to describe a mechanism by which curcumin restores p53 levels in human cancer cell lines.

HeLa, SiHa, CaSki and MDA-MB-231 cells were exposed to curcumin and a pulse and chase and immunoprecipitation assays were performed. Here we showed that curcumin increases the half-life of p53 by a physical interaction between p53-NQO1 (p53 - NAD(P)H:quinone oxidoreductase 1) proteins after treatment with curcumin. Interestingly, the cell viability assay after treatment with curcumin showed that the cytotoxic activity was selectively higher in cervical cancer cells contained wild type p53 but not in breast cancer cells contained mutated p53. The cytotoxic effect of curcumin in cervical cancer cells was related to the complex p53-NQO1 that avoids the interaction between p53 and its negative regulator ubiquitin ligase E6-associated protein (E6AP). Finally, we demonstrated that in pancreatic epithelioid carcinoma cells (PANC1) that are knockout for NQO1, the reestablishment of NQO1 expression can stabilize p53 in presence of curcumin. Collectively, our findings showed that curcumin is necessary to promote the protein interaction of NQO1 with p53, therefore, it increases the half-life of p53, and permits the cytotoxic effect of curcumin in cancer cells containing wild type p53. Our findings suggest that the use of curcumin may reactivate the p53 pathway in cancer cells with p53 wild-type.

1. Introduction

Cancer is a diverse group of diseases characterized by abnormal cells growth and represents an important worldwide problem. Therefore, the search of therapeutic alternatives against tumoral cells has been a major challenge for scientific and commercial interest in the discovery of potent, safe and selective anti-cancer drugs [1]. Among them, antioxidants are molecules with therapeutic potential since they have the ability to neutralize reactive oxygen species but also have been attributed antitumor properties [2,3]. An example of these natural compounds with therapeutic potential is curcumin, a natural phenolic compound obtained from the roots of *Curcuma longa*. Structurally curcumin is a molecule with polar central and flanking regions separated by a lipophilic methionine segment. Also, it has distinct chemical properties, among these the presence of α,β–unsaturated compounds (Michael acceptor) that facilitate intermolecular interactions with another molecules [4,5]. The anti-tumor activities of curcumin have been demonstrated by some research groups [6,7]. Particularly, it has been shown that it can induce cyclin-dependent kinase inhibitors, therefore this promotes p53 restoration in wild-type and mutant p53 cancer cell lines and represses the growth of numerous cancer cell lines by the phosphatidylinositol 3-kinase pathway (PI3K, AKT), Ras, and β-catenin

* Corresponding author. Laboratory of Virus and Cancer, Instituto Nacional de Cancerología, Av. San Fernando No. 22, Sección XVI, Tlalpan, CP 14080, Mexico City, Mexico.
E-mail address: carranca@biomedicas.unam.mx (A. García-Carrancá).

https://doi.org/10.1016/j.redox.2019.101320
Received 22 May 2019; Received in revised form 27 August 2019; Accepted 3 September 2019
Available online 09 September 2019

pathways [8]. Curcumin is also a powerful antioxidant because it activates the Kelch-like ECH-associated protein 1-nuclear factor (erythroid-derived 2)-like 2 pathway (Keap1/Nrf2) under oxidative microenvironment [9]. The Nrf2 pathway is regulated by Keap1 by mediating its degradation, but when cells are exposed to electrophiles or oxidants, Nrf2 is stabilized and translocate into the nucleus, binding to the antioxidant response element (ARE) located in the promoter region of antioxidant genes and upregulates their transcription. Nrf2 functions as a transcriptional factor with multiple targets as NAD(P)H: quinone oxidoreductase 1 (NQO1) [10,11]. This protein has multiple functions including neutralization of reactive oxygen species, detoxification of quinones and stabilization proteins for example; there is a report showing that NQO1 can interact with p53 causing its stabilization [12,13]. p53 is a tumour suppressor gene product that can block cell progression through the cell cycle when deoxyribonucleic acid (DNA) is damaged [14]. It is localized into nucleus, where it functions as transcription factor of DNA sequence-specific in genes as p21. The activation of p53 can activate different gene pathways, resulting in apoptosis, cell-cycle arrest, DNA repair or senescence, among others [15]. Because of its biological importance, mutations in the *TP53* tumour suppressor gene are observed in greater than 50% of all human cancers. The vast majority of p53 mutations that are associated with human cancer occur at the region of DNA binding recognition [16]. Moreover, mutant p53 in human cancer is commonly expressed at high levels and is more stable than wild-type p53 [17].

Here, we investigated the mechanism of the activation of p53 mediated by curcumin. We showed that curcumin promotes the complex formation of NQO1-p53 leading to p53 stabilization [18]. High levels of NQO1 are not enough for the p53 stabilization; we demonstrated that the presence of curcumin is necessary to stabilize the p53-NQO1 interaction. Also, this interaction can promote the loss interactions between p53 and its negative regulators. The effect of curcumin on p53 levels is differential between the cancer cell lines because it only has effect on cell viability of HeLa, SiHa and CaSki but not in MDA-MB-231. So curcumin is a molecule with an important therapeutic potential in cancer cells with p53 wild type.

2. Materials and methods

2.1. Chemicals and reagents

3-(4,5-dimethylthiazol-2-yl)-2,5-diphenyltetrazolium bromide (MTT), dicumarol, cycloheximide (CHX), dimethyl sulfoxide (DMSO), curcumin (C1386), protease inhibitor cocktail tablets EDTA-free (S8830), protein G sepharose (GE28), Trizma base (T1503), sodium chloride (NaCl S9888) were purchased from Sigma-Aldrich (St. Louis, MO, USA). Pierce BCA Protein Assay Kit (23225) and lipofectamine plus transfection reagent (15338100) were from ThermoFisher (Waltham, MA, USA) Nonidet P-40 (CAS 68412-54-4), anti-p53 mouse monoclonal antibody (DO-1), anti-NQO1 mouse monoclonal antibody (H9), anti-E6AP (E4) mouse monoclonal antibody, anti-lamin A/C (2A1) mouse monoclonal antibody, anti-glyceraldehyde-3-phosphate dehydrogenase (GAPDH, L8) goat polyclonal antibody, donkey anti-goat IgG-HRP (sc-2020), and goat anti-mouse IgG-horse radish peroxidase (HRP, sc-2005) were purchased from Santa Cruz Biotechnology (Dallas, TX, USA). Dulbecco's Modified, Eagle Medium high glucose (DMEM 11965–084) and fetal bovine serum (10500056) were from GIBCO.

2.2. Cell lines and culture

Cell lines HeLa, SiHa and CaSki were cultured in DMEM supplemented with 10% fetal bovine serum. MDAMB-231 cells were cultured in Dulbecco's Modified Eagle Medium Nutrient Mixture (DMEM, GIBCO, 11320–033) supplemented with 10% fetal bovine serum. All cell lines were cultured at 37°C in a 5% CO_2 incubator.

2.3. Western blot

The cells samples lysates were extracted with lysis buffer composed of 50 mM Tris, pH 7.6, 150 mM NaCl, 1% Nonidet P-40, 10 mM sodium phosphate, and a complete tablet protease Inhibitor Cocktail per 100 ml of buffer, and the protein concentration in the lysates was quantified using an enhanced bicinchoninic acid protein assay kit with bovine serum albumin as a standard. The total protein extract will be used for western blot analysis. Equal amounts of total protein were subjected to 10% sodium dodecyl sulfate polyacrylamide gel electrophoresis (SDS-PAGE) and transferred into a nitrocellulose membrane, followed by incubation overnight to 4°C using the following dilution of primary antibodies: anti-p53 (1:100), anti NQO1 (1:1000), anti-MDM2 (1:500), anti-E6AP (1:1000), anti-lamin A/C (1:500), anti-GAPDH (1:1000) and following by incubation with secondary antibody in blocking solution 1 h room temperature; anti-mouse (1:10000), anti-goat (1:20000) finally protein expression levels were visualized with Li-COR C-DiGit chemiluminescence western blot scanner and UVP Imaging system.

2.4. Pulse and chase assays

The cells were seeds in p35 plates at density of 1.5×10^5 cells/plate and treated with curcumin at concentration of 20 μM for 24 h, the treatment with curcumin was removed and the cells were washed with PBS, continuing with the treatment with CHX with a concentration of 50 μg/ml as previously reported [19,20], the CHX treatment is a standard protein synthesis inhibitor and aliquots of cells were collected every then minutes starting on 0 min, 10 min, 20 min so on until 60 min immediately following addition of the compound cells were lysed with lysis buffer composed of 50 mM Tris, pH 7.6, 150 mM NaCl, 1% Nonidet P-40, 10 mM sodium phosphate, and a complete tablet protease Inhibitor Cocktail per 100 ml of buffer, p53 protein abundance at each time point was analyzed, by western blot as described.

2.5. Immunoprecipitation assays

The cells were seeded in p60 plates at density of 2.5×10^5 cells/plate and treated with 20 μM curcumin for 24 h and then lysed, after centrifugation, the clear cell lysate was separated from the pellet of cell and then incubated 2 h at 4°C with 50 μl Protein G sepharose, 1 μg of antibodies and 0.5 mg/ml RNAse A, after incubation the sepharose beads coupled to protein G were washed 20 times with lysis buffer. For western blot, the resulting immunoprecipitates were resolved by SDS-PAGE, then the gel contents were transferred to a nitrocellulose membrane and probed with specific antibodies, finally protein expression levels were visualized with Li-COR C-DiGit chemiluminescence western blot scanner (LI-COR Biosciences, Lincoln, Nebraska USA).

2.6. Cell viability assays

Cell viability was determined by the MTT (M2128) assay [21]. HeLa, SiHa, CaSki and MDA-MB-231 cells (5×10^4 cells/well) were seeded in a 96-well plate and treated with 10 μM and 20 μM curcumin (C1386) for 24 h. After addition 10 μl per well MTT (5 mg/ml) solution the cells were incubated at 37°C for 4 h, the formazan crystals were dissolved using 50 μl DMSO [41]. The cell viability was determined by measuring the absorbance at 570 nm on a Synergy H1 Hybrid Multi-Mode Microplate Reader (BioTek, Winooski, VT, USA).

2.7. Transfection of PANC1 cells with NQO1 plasmids

PANC1 cells (Null to NQO1 were obtained from American Type Culture Collection (ATCC CRL-1469) were transient transfected using Lipofectamine plus transfection reagent with 1 μg pCDNA3 NQO1 or 1 μg pCDNA3 (Empty Vector) the plasmids were obtained from addgene nonprofit plasmid repository. The results were obtained from three

separate biological replicates. The cells transfected and PANC1 wild type (non transfected) were treated with curcumin, pulse and chase assay was performed. The expression levels of p53 protein were analyzed by western blot as described above.

2.8. Statistical analysis

Results are expressed as mean ± SD. Statistical tests were performed using GraphPad PRISM version 6.0c. The ANOVA test with Tukey was applied to compare the means of groups, a $p < 0.05$ was significant.

3. Results

3.1. Curcumin treatment increases the levels of NQO1, p53 and p21

Previous studies have shown that curcumin is capable to activate the Keap1/Nrf2 pathway in order to increase the expression of phase II enzymes including NQO1 [22]. To determine the participation of curcumin on the Keap1/Nrf2 in our model, we evaluate the activation of the Keap1/Nrf2 pathway through the translocation of Nrf2 to the nucleus in Hela, CasKi and SiHa cervical cancer cells lines and MDA-MB-231 breast cancer cells in response to curcumin treatment. We confirmed the immunodetection of Nrf2 in the nuclear extract after 20 μM of curcumin treatment in all cell lines (data not shown) and observed the overexpression of NQO1 (Fig. 1A). Therefore, we determine that curcumin induces the nuclear translocation of Nrf2, an event that indicates the activation of the Keap1/Nrf2 pathway and the increased levels of NQO1 that is consistent with the Nrf2 nuclear translocation. Then, we observed that curcumin treatment also increases the p53 levels (Fig. 1B). All together, these results indicate that curcumin may have an important role in the activating the p53 pathway. To evaluate the functionality of p53 pathway in response to curcumin treatment the expression of its target p21 was evaluated. We showed that curcumin increases the expression of p21 in cervical cancer cell lines with p53 wild-type genotype (CaSki, HeLa and SiHa) meanwhile, this effect was not observed in MDA-MB-231 cell line that has mutated p53 (Fig. 2A) which has decreased p53 activity. These results indicate that curcumin activates the Keap1/Nrf2 pathway in our cellular model with wild-type p53 and leads to the activation of p53 pathway.

In order to evaluate the effect of curcumin on the cell viability a MTT assay was performed. Cells were treated with 10 μM and 20 μM of curcumin; non-treated cells (−) and cells treated with vehicle (V) were used as control. Curcumin treatment induces a significant decrease on the cell viability was observed at the p53 wild type cervical cancer cell lines. Interestingly, at the same concentrations, MDA-MB-231 cells with p53 mutated were resistant to the cytotoxic effect of curcumin. These results suggest that the cytotoxic effect is related with the activation of the p53 wild type (Fig. 2B).

3.2. Curcumin increases the half life time of p53

It is widely reported that the half-life time of p53 is 20 min in physiological conditions [23]. In order to evaluate the effect of curcumin on the half-life of p53 we analyzed its stability after treatments with curcumin or cycloheximide, a well-known inhibitor of protein synthesis [24]. It was found that p53 stability of HeLa, SiHa, CaSki and MDA-MB-231 cells without treatment with curcumin was 20 min (Fig. 3A), however when cells were treated with 20 μM curcumin, p53 protein was detected until 60 min (Fig. 3B). These results suggest that curcumin is able to enhance the p53 half-life of tumor cells.

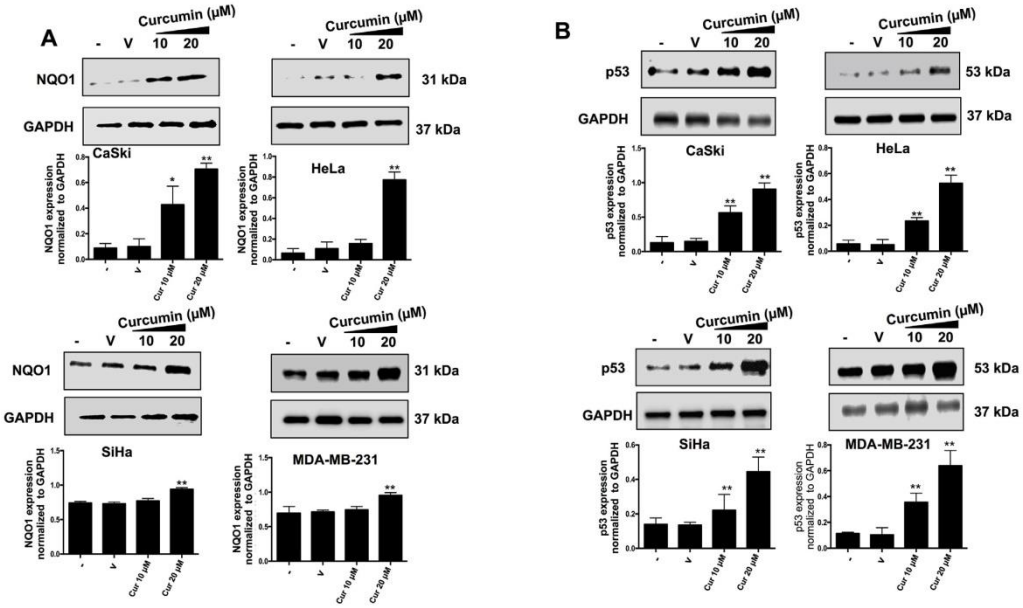

Fig. 1. Effect of curcumin (Cur) on NQO1, p53 levels in CaSki, HeLa, SiHa and MDA-MB-231 cells. CaSki, HeLa, SiHa and MDA-MB-231 cells were treated with 10 μM and 20 μM of curcumin and (A) NAD(P)H: quinone oxidoreductase 1 (NQO1, 31 kDa) and (B) p53 were detected by immunoblotting. The cells were treated for 24 h. The values are means ± SD of three independent experiments. The negative sign (−) represents without treatment, the V represents Vehicle. Statistical differences in A and B were determined using one-way ANOVA and Tukey's multiple comparison test; (*) $p < 0.005$, (**) $p < 0.001$ (−) vs V, (−) vs 10 μM of curcumin and (−) vs 20 μM of curcumin.

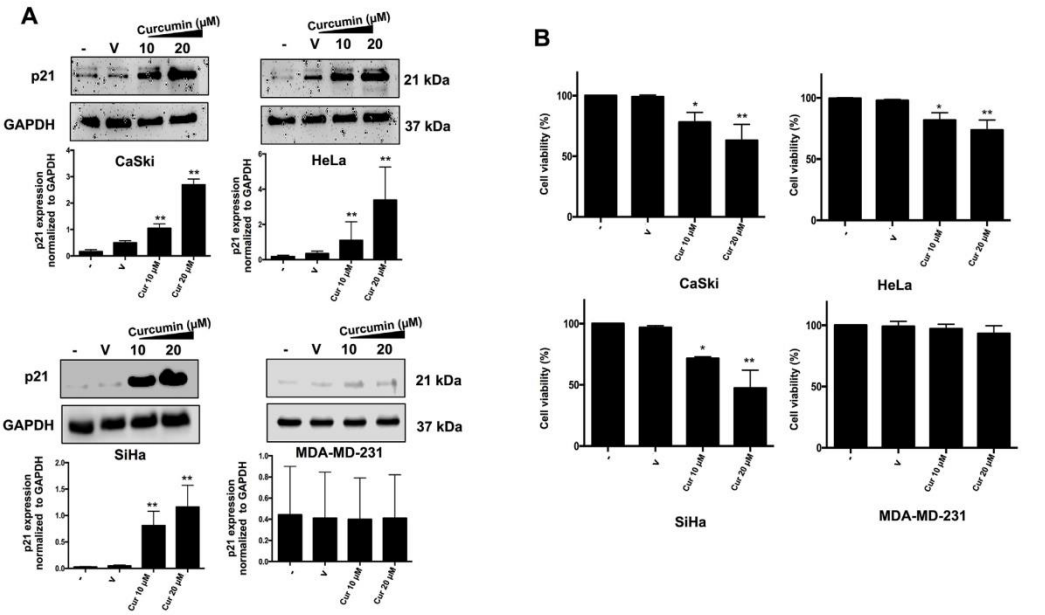

Fig. 2. Effect of curcumin (Cur) on p21 levels and cell viability in CaSki, HeLa, SiHa and MDA-MB-231 cells. CaSki, HeLa, SiHa and MDA-MB-231 cells were treated for 24 h with 10 μM and 20 μM of curcumin and (A) p21 (21 kDa) levels were detected by immunoblotting and (B) Cell viability was evaluated using MTT. The values are means ± SD of three independent experiments. The negative sign (−) represents without treatment, the V represents Vehicle. Statistical differences in A and B were determined using one-way ANOVA and Tukey's multiple comparison test; (*) $p < 0.005$, (**) $p < 0.001$ (−) vs V, (−) vs 10 μM of curcumin and (−) vs 20 μM of curcumin.

3.3. Curcumin promotes the interaction between p53 and NQO1

The NQO1 interaction with p53 under stress oxidative conditions has also been observed [25,26]. In order to evaluate whether curcumin promotes the physical interaction of p53 with NQO1, immunoprecipitation assays were performed. In these assays, p53 was inmunoprecipitated and then NQO1 was revealed by western blot assay. Non-treated cells were used as control. The input material was

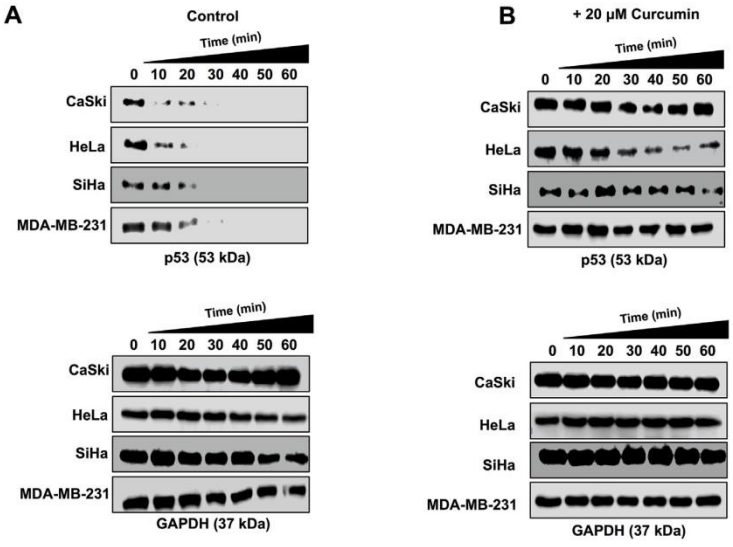

Fig. 3. Curcumin stabilizes p53. CaSki, HeLa, SiHa and MDA-MB-231 cells were treated with 20 μM of curcumin for 24 h and the half-life of p53 (53 kDa) was measured with a pulse and chase experiment with cycloheximide (50 μg/ml), the protein extraction was performed every 10 min (0–60) and revealed by immunoblot, the stability of p53 was evaluated in (A) control cells (without curcumin) and in (B) cells treated with curcumin.

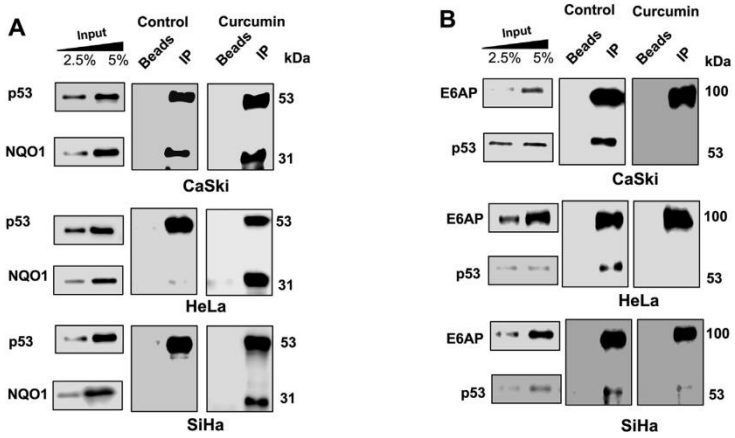

Fig. 4. Curcumin promotes interaction between p53 and NQO1. CaSki, HeLa and SiHa cells were treated with 20 μM curcumin for 24 h and NQO1 (31 kDa) was detected by immunoblot analysis following immunoprecipitation of p53 (53 kDa) from cell lysates. The input material was evaluated against p53 and NQO1 in increasing amounts of protein (2.5 and 5%). (A) The p53-NQO1 interaction after treatment with curcumin was evaluated. Cell lines were treated for 24 h with 20 μM curcumin and p53 (53 kDa) was detected by immunoblot analysis following immunoprecipitation of E6AP (100 kDa). The effect of curcumin in the interaction between E6AP-p53 is shown. (B) The input material was evaluated against p53 and E6AP in increasing amounts of protein (2.5 and 5%).

evaluated against p53 and NQO1 in increasing amounts of protein (2.5 and 5%). It was found that NQO1 physically interact with p53 when HeLa, SiHa and CaSki cells were treated with curcumin (Fig. 4A). These results suggested that NQO1-p53 complex could be stabilizing p53 in response to curcumin treatment for altered cell viability.

In order to show that the effect of curcumin could avoid the interaction between p53 and its negative regulators ubiquitin ligase E6-associated protein (E6AP) a immunoprecipitation assay was performed (Fig. 4B). In order to address this question cells with wild type p53 were used for this purpose because we did not observe any effect on cell viability in MDA-MB-231. To evaluate the change in the direct interaction between E6AP and p53 in response to curcumin treatment, E6AP protein was inmunoprecipitated and then p53 was revealed by western blot assay. Non-treated cells were used as control. The input material was evaluated against p53 and E6AP in increasing amounts of protein (2.5 and 5%). Results showed that curcumin treatment induces loss of interaction between p53 and E6AP (Fig. 4B). All together, our results showed that curcumin induces loss in the E6AP-p53 interaction and favors interaction of NQO1-p53 protein complex to promote cytotoxicity on the cervical cancer cells with p53 wild type.

3.4. Curcumin is necessary for complex NQO1-p53 and p53 stabilization

To determine whether the enzymatic activity of NQO1 is required for p53 stability when curcumin is present, the cells were treated with curcumin and after they were treated 4 h with 100 μM of dicumarol (a NQO1 activity inhibitor). To evaluate p53 stability a pulse and chase assay was performed. Results showed that p53 half-life time was less than 60 min when the cells were treated with dicumarol (Fig. 5A). This suggests that stabilization of p53 by NQO1 depends on an intact enzymatic activity of NQO1. In order to demonstrate if NQO1 is responsible for p53 stability, we used pancreatic epithelioid carcinoma cells (PANC1), a cell line null to *NQO1* gene [27,28]. We first treated wild type cells PANC1 (non-transfected) with curcumin and interestingly, observed no stabilization of p53 (Fig. 5B), suggesting that the presence of curcumin is not sufficient to increase the half-life of p53. NQO1 expression was reestablished by exogenous expression of NQO1 messenger cloned in a plasmid (PCDNA-NQO1). After 48 h of transfection, pulse and chase assay was performed in PANC1 transfected cells, but without curcumin treatment, and again the stabilization of p53 was not observed (Fig. 5C) even when NQO1 protein was expressed, suggesting that the presence of NQO1 is not enough to increase the half-life of p53. Surprisingly, when transfected cells were then treated with 20 μM curcumin, stabilization of p53 was indeed observed (Fig. 5C). This result clearly showed that curcumin is necessary to promote the stabilization of p53, via interaction with the NQO1 protein.

4. Discussion

Tumor suppressor p53 plays a central role in protecting the genome and preventing cell transformation [29]. However, normal cells must maintain p53 levels under tight control to prevent death. Despite mutations in the p53 gene occurring in 50% of all cancers, cervical cancer cells as HeLa, SiHa and CaSki cells retain functional wild-type p53 [30,31] while, MDA-MB-231 cells has a loss-of-function mutation in TP53 gene [32]. Therefore, cancer cell lines with wild type p53 can reactivate downstream pathways and consequently promote cell death and decrease cell viability [33]. Hence, p53 restoration may be a promising therapeutic strategy, however, stability of p53 is an important factor for the reactivation pathway. The main negative regulator of p53 is MDM2, however in HPV-positive cancer cell lines like HeLa, SiHa and CaSki, viral oncoprotein E6 forms a complex with E6AP and their physical interaction with wild-type p53 promotes its degradation via the ubiquitin pathway [34]. The half-life of the p53 protein is short (20 min); during periods of cellular stress, the p53 protein is regulated by a negative feedback mechanism. Here we show that curcumin increases the half-life of p53 up to 60 min and present data on the role of NQO1 in protecting p53 from degradation which are consistent with data previously reported [35]. However, in this work we demonstrated that curcumin is necessary to promote NQO1-mediated stabilization of p53. NQO1 plays an important role in this stabilization because it can physically interact with p53. NQO1 is even considered an anticancer enzyme since it protects cells from oxidative stresses [36]. Thus, the use of dietary compounds to induce the expression of NQO1 has emerged as a promising strategy for cancer prevention [37]. Compounds as curcumin had the ability to translocate Nrf2 which in turn bind to ARE in the promoter region of antioxidant enzymes and increase the expression of phase II antioxidant proteins such as NQO1 [38,39]. The increase in NQO1 levels is one of the results of the translocation of Nrf2 to the nucleus induced by curcumin. NQO1 is a protein that can form complexes with other proteins to stabilize them, including p53.

In this report, we propose that curcumin is necessary to induce NQO1 and promote its interaction with p53, which in turn results in an increase of the p53 stability, contrary to previous reports [40,41]. In 2005, Tsvetkov et al. showed that curcumin and dicoumarol destabilized p53 in M1 mouse myeloid leukemic cells transfected with a plasmid containing a temperature-sensitive p53 [135 Ala → Val] (M1-t-

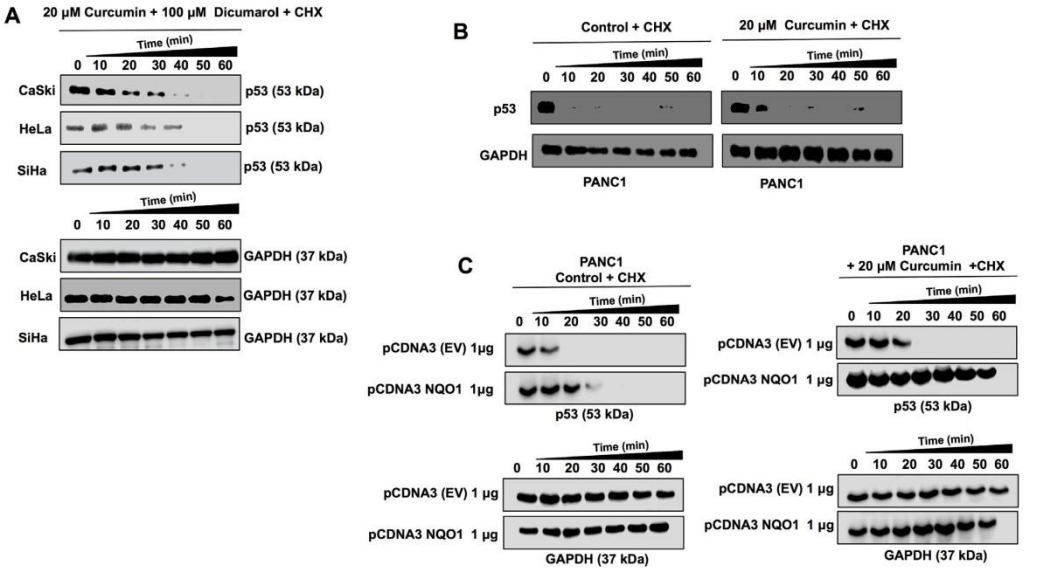

Fig. 5. Curcumin increases p53 stability in a NQO1 dependent manner. Pulse and chase analysis were performed in cell lines treated for 4 h with 20 μM curcumin 24 h and 100 μM dicumarol (NQO1 Inhibitor). (A) the effect of the inhibition of NQO1 activity by dicumarol on p53 stability is shown. Pancreatic carcinoma cells null to NQO1 (PANC1 cells) wild type and transfected with 1 μg pCDNA3 EV (empty vector) or with 1 μg of pCDNA3-NQO1 (to express the complete NQO1 protein) were treated with 20 μM for 24 h and after pulse and chase of p53 (53 kDa) was performed. The chase of proteins was performed every 10 min and revealed by immunoblot, the effect of treatment with curcumin on p53 stability in (B) absence of NQO1 (PANC1 WT or PANC1 + pCDNA3) and when (C) NQO1 levels are restored is shown. CHX = cycloheximide.

p53). M1-t-p53 protein has a wild-type conformation and activity at 32°C, but not at 37°C. In addition, they used mouse A31N-ts20 cells which had a temperature-sensitive E1 ubiquitin activating enzyme, that is inactivated at 39°C and causes accumulation of p53. They observed degradation of M1-t-p53 by low doses of curcumin (20 μM) and dicumarol (100 μM) in mouse cells growth at two different temperature conditions (39 °C or 32 °C). However, the same authors showed degradation of WT p53 in the p53-null cell line HCT116 from human colorectal cancer cells [40], In that report, cells were transfected with human WT p53 and treated with high doses of curcumin (60 μM) and dicumarol (300 μM) [40]. In our report we used cell lines derived from human cervical cancer; HeLa, SiHa, and CaSki. These cell lines exhibit a low basal wild-type p53 expression due to the presence of the Human Papillomavirus (HPV) E6 oncoprotein, therefore, in this case the mechanism for degradation of P53 is dependent on the formation of a complex between E6 and the E6AP protein. Finally, it is important to emphasize that we used low doses of curcumin (20 μM) and dicumarol (100 μM).

On the other hand, Zeekpudsa et al. in 2014 reported an increased expression of p53 when NQO1 activity is inhibited by dicoumarol. The authors used two *Opisthorchis viverrini*-related cholangiocarcinoma cell lines (KKU-100 and KKU-M214) with high and low NQO1 expression levels, respectively [41]. To decrease NQO1 levels, the authors used a specific NQO1 siRNA. On the contrary, in our work we used human cervical cancer cell lines with wild-type p53 and importantly, we use curcumin, which plays a central role in directing the interaction between NQO1 and p53 to promote its stabilization. It is worth to mention that in the report of Zeekpudsa et al., curcumin was not used. Our results indeed demonstrate that curcumin is necessary to promote the maintenance of an environment in which p53 and NQO1 can interact, and therefore increase the half-life of p53.

Finally, our data also showed that the physical interaction between NQO1 and p53 promote its loss of interaction with its negative regulator E6AP. Moreover, NQO1 exhibits catalytic enzyme properties, first reported by Ernster and Navazio in 1958 [42], that we here shown necessary for the stabilization of p53, since dicumarol, an inhibitor of NQO1 activity, inhibits the stabilization of p53, consistent with the previously reported [43,44].

We here propose a model in which p53 stability is determined by two effectors acting together: curcumin and NQO1 (Fig. 6). Curcumin activates the Keap1/Nrf2 pathway and promote the increase of NQO1 levels and, in the presence of curcumin, NQO1 can interact physically with p53 and promote its stability. Also, the formation of the NQO1-p53 complex promote the loss of interaction between p53 and its negative regulator E6AP. In cancer cells with wild-type p53, like those positive for HPV, the stabilization of p53 promotes a reactivation of the p53 pathway, and therefore decrease cell viability.

5. Conclusions

Our results demonstrate the importance of curcumin in the regulation of p53 stability. In this work we demonstrate that curcumin treatment increases p53 levels and provides an appropriate cellular environment for p53 and NQO1 to interact. At the same time this interaction promotes the loss of interaction of p53 with its negative regulator E6AP, the negative regulator of p53 when HPV E6 oncoproteins are present. In our work, HeLa, SiHa and CaSki tumor-derived cell lines that have wild-type p53 and downstream pathways intact, therefore curcumin may be a potential therapeutic agent for tumors with wild type p53.

Author's contributions

"CCPM, ESR, and AGC conceived the study, designed the

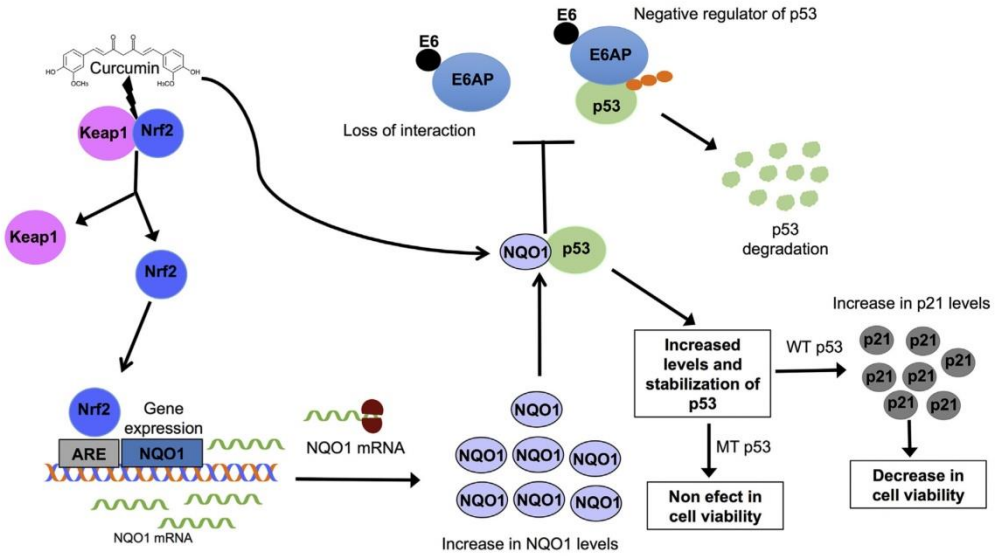

Fig. 6. Schematic model of effects of curcumin in the p53 stabilization. Curcumin activates the Kelch-like ECH-associated protein 1-nuclear factor (erythroid-derived 2)-like 2 pathway (Keap1/Nrf2) pathway; Nrf2 is translocated into the nucleus and binds to the antioxidant response element (ARE) sequences increasing the expression of NAD(P)H: quinone oxidoreductase 1 (NQO1). NQO1 is translated and binds to p53 promoting the loss of interaction between p53 and its negative regulators. Curcumin also stabilizes the interaction between NQO1-p53. In cells with wild-type p53 (WT p53) the p53 pathway is activated and has an effect on cell viability whereas in cells with mutated p53 (MT p53) there is only accumulation of p53 without effect on cell viability.

experimental strategy, analyzed the results, and drafted the manuscript. CCPM. EAO, and VAV carried out molecular biology studies and performed statistical analysis. EOS and JPC participated in drafting the discussion and helped to revise the manuscript. All authors read and approved the final manuscript."

Funding

This work was supported by Consejo Nacional de Ciencia y Tecnología (CONACyT No. 253804, to AG-C) and by Fundación Miguel Alemán, A.C. (to AG-C).

Conflicts of interest

The authors declare no conflicts of interests.

Acknowledgments

Carlos César Patiño Morales is a doctoral student from Programa de Doctorado en Ciencias Biomédicas, Universidad Nacional Autónoma de México (UNAM) and received fellowship from CONACYT. CVU 416000. We thank to the Unidad de Investigación Biomédica en Cáncer, Universidad Nacional Autónoma de México-Instituto Nacional de Cancerología (Mexico City) and to the Departamento de Ciencias Naturales, Universidad Autónoma Metropolitana, Unidad Cuajimalpa (Mexico City).

References

[1] B.P. Kanti, I.R. Syed, Plant polyphenols as dietary antioxidants in human health and disease, Oxidat. Med. Cell. Longev. 2 (5) (2009) 270–278.
[2] S. Chikara, L.D. Nagaprashantha, J. Singhal, D. Horne, S. Awasthi, S.S. Singhal, Oxidative stress and dietary phytochemicals: role in cancer chemoprevention and treatment, Cancer Lett. 413 (2018) 122–134.
[3] C.A. Houghton, R.G. Fassett, J.S. Coombes, Sulforaphane and other nutrigenomic Nrf2 activators: can the clinician's expectation Be matched by the reality? Oxidat. Med. Cell. Longev (2016) 785718 2016.
[4] M. Heger, R.F. van Golen, M. Broekgaarden, M.C. Michel, The molecular basis for the pharmacokinetics and pharmacodynamics of curcumin and its metabolites in relation to cancer, Pharmacol. Rev. 66 (1) (2013) 222–307.
[5] S.F. Nabavi, S.M. Nabavi, M. Daglia, R. Tamilselvam, A. Bishayee, H. Pazoki-toroudi, P.D. Kasi, Molecular targets of curcumin for cancer therapy: an updated review, Tumor Biol. 37 (10) (2016) 13017–13028.
[6] J.G. Devassy, I.D. Nwachukwu, P.J.H. Jones, Curcumin and cancer: barriers to obtaining a health claim, Nutr. Rev. 73 (3) (2015) 155–165.
[7] A. Goel, A.B. Kunnumakkara, B.B. Aggarwal, Curcumin as "Curecumin": from kitchen to clinic, Biochem. Pharmacol. 75 (4) (2008) 787–809.
[8] A. Mishra, B.C. Das, Curcumin as an anti-human papillomavirus and anti-cancer compound, Future Oncol. 11 (18) (2015) 2487–2490.
[9] S. Prasad, S.C. Gupta, A.K. Tyagi, B.B. Aggarwal, Curcumin, a component of golden spice: from bedside to bench and back, Biotechnol. Adv. 32 (6) (2014) 1053–1064.
[10] M. Theodore, Y. Kawai, J. Yang, Y. Kleshchenko, S.P. Reddy, F. Villalta, I.J. Arinze, Multiple nuclear localization signals function in the nuclear import of the transcription factor Nrf2, J. Biol. Chem. 283 (14) (2008) 8984–8994.
[11] B.G. Richardson, A.D. Jain, T.E. Speltz, T.W. Moore, Non-electrophilic modulators of the canonical Keap1/Nrf2 pathway, Bioorg. Med. Chem. Lett 25 (11) (2015) 2261–2268.
[12] A.L. Stefanson, M. Bakovic, Dietary regulation of Keap1/Nrf2/ARE pathway: focus on plant-derived compounds and trace minerals, Nutrients 6 (9) (2014) 3777–3801.
[13] G. Asher, J. Lotem, L. Sachs, C. Kahana, Y. Shaul, Mdm-2 and ubiquitin-independent p53 proteasomal degradation regulated by NQO1, Cell 99 (20) (2002) 13125–13130.
[14] K.D. Sullivan, C.L. Gallant-behm, R.E. Henry, J. Fraikin, M. Joaquín, The P53 Circuit Board Kelly vol. 1825, (2013), pp. 229–244 (2).
[15] C. Blattner, Regulation of p53: the next generation, Cell Cycle 7 (20) (2008) 3149–3153.
[16] J. Haller, J.S. Haller, Analysis of TP53 mutation status in human cancer cell lines: a reassessment bernard, Shadow Medicine 35 (6) (2015) 153–160.
[17] M. Scheffner, K. Munger, J.C. Byrne, P.M. Howley, The state of the p53 and retinoblastoma genes in human cervical carcinoma cell lines, Proc. Natl. Acad. Sci. 88 (13) (2006) 5523–5527.
[18] D. Siegel, A. Anwar, L.J. Tang, J.A. Pietenpol, D. Dehn, D. Ross, J.K. Kepa, Interaction of human NAD(P)H:quinone oxidoreductase 1 (NQO1) with the tumor suppressor protein p53 in cells and cell-free systems, J. Biol. Chem. 278 (12) (2003) 10368–10373.
[19] J.W. Yewdell, J.R. Lacsina, M.C. Rechsteiner, C.V. Nicchitta, Out with the old, in with the new? Comparing methods for measuring protein degradation, Cell Biol. Int. 35 (5) (2011) 457–462.
[20] M. Hochstrasser, Ubiquitin, proteasomes, and the regulation of intracellular protein

degradation, Curr. Opin. Cell Biol. 7 (2) (1995) 215–223.
[21] S.P. Langdon, Cell sensivity assays: the MTT assay, Methods Mol. Biol. 731 (2003) 237–245.
[22] M. Pulido-Moran, J. Moreno-Fernandez, C. Ramirez-Tortosa, M.C. Ramirez-Tortosa, Curcumin and health, Molecules 21 (3) (2016) 1–22.
[23] K.D. Sullivan, M.D. Galbraith, Z. Andrysik, J.M. Espinosa, Mechanisms of transcriptional regulation by p53, Cell Death Differ. 25 (1) (2018) 133–143.
[24] B.W. Buchanan, M.E. Lloyd, S.M. Engle, E.M. Rubenstein, Cycloheximide chase analysis of protein degradation in "Saccharomyces cerevisiae", J. Vis. Exp. (110) (2016) 1–9.
[25] L. Das, M. Vinayak, Long term effect of curcumin in restoration of tumour suppressor p53 and phase-II antioxidant enzymes via activation of Nrf2 signalling and modulation of inflammation in prevention of cancer, PLoS One 10 (4) (2015) 1–22.
[26] R. Kama, Y. Shaul, J. Lotem, L. Sachs, G. Asher, NQO1 stabilizes p53 through a distinct pathway, Proc. Natl. Acad. Sci. 99 (5) (2002) 3099–3104.
[27] B. Shieh, C. Yan, D. Ross, D. Siegel, J.K. Kepa, Role for NAD(P)H:quinone oxidoreductase 1 and manganese-dependent superoxide dismutase in 17-(Allylamino)-17-demethoxygeldanamycin-Induced heat shock protein 90 inhibition in pancreatic cancer cells, J. Pharmacol. Exp. Ther. 336 (3) (2010) 874–880.
[28] R.D. Traver, D. Siegel, H.D. Beall, R.M. Phillips, N.W. Gibson, W.A. Franklin, D. Ross, Characterization of a polymorphism in NAD(P)H: quinone oxidoreductase (DT-diaphorase), Br. J. Canc. 75 (1) (1997) 69–75.
[29] M.F. Lavin, N. Gueven, The complexity of p53 stabilization and activation, Cell Death Differ. 13 (6) (2006) 941–950.
[30] M. Hollstein, K. Rice, M.S. Greenblatt, T. Soussi, R. Fuchs, T. Sørlie, C.C. Harris, Database of p53 gene somatic mutations in human tumors and cell lines, Nucleic Acids Res. 22 (17) (1994) 3551–3555.
[31] S. Srivastava, Y.A. Tong, K. Devadas, Z. Zou, Y. Chen, K.F. Pirouo, E.H. Chang, The status of the p53 gene in human papilloma virus positive or negative cervical carcinoma cell lines, Oncol. Res. 13 (7) (1992) 1273–1275.
[32] M. Huovinen, J. Loikkanen, P. Myllynen, K.H. Vähäkangas, Characterization of human breast cancer cell lines for the studies on p53 in chemical carcinogenesis, Toxicol. In Vitro 25 (5) (2011) 1007–1017.
[33] E.C. Goodwin, D. DiMaio, Repression of human papillomavirus oncogenes in HeLa cervical carcinoma cells causes the orderly reactivation of dormant tumor suppressor pathways, Proc. Natl. Acad. Sci. 97 (23) (2002) 12513–12518.
[34] D.P. Lane, C.F. Cheok, S. Lain, P53-Based cancer therapy, Cold Spring Harbor Perspect. Biol. 1–24 (2010).
[35] E.T. Oh, H.J. Park, Implications of NQO1 in cancer therapy, BMB Reports 48 (11) (2015) 609–617.
[36] A. Mizumoto, S. Ohashi, M. Kamada, T. Saito, Y. Nakai, K. Baba, M. Muto, Combination treatment with highly bioavailable curcumin and NQO1 inhibitor exhibits potent antitumor effects on esophageal squamous cell carcinoma, J. Gastroenterol. 54 (8) (2019) 687–698.
[37] C. Braicu, A.G. Atanasov, I. Berindan-Neagoe, S.M. Nabavi, B. Vladimirov, N. Mehterov, V. Sarafian, Nutrigenomics in cancer: revisiting the effects of natural compounds, Semin. Cancer Biol. 46 (2017) 84–106.
[38] A.B. Kunnumakkara, D. Bordoloi, G. Padmavathi, J. Monisha, N.K. Roy, S. Prasad, B.B. Aggarwal, Curcumin, the golden nutraceutical: multitargeting for multiple chronic diseases, Br. J. Pharmacol. 174 (11) (2017) 1325–1348.
[39] K. Taguchi, M. Yamamoto, The KEAP1–NRF2 system in cancer, Front. Oncol. 7 (2017) 85.
[40] P. Tsvetkov, G. Asher, V. Reiss, Y. Shaul, L. Sachs, J. Lotem, Inhibition of NAD(P)H:quinone oxidoreductase 1 activity and induction of p53 degradation by the natural phenolic compound curcumin, Proc. Natl. Acad. Sci. 102 (15) (2005) 5535–5540.
[41] P. Zeekpudsa, V. Kukongviriyapan, L. Senggunprai, B. Sripa, Suppression of NAD(P) H-quinone oxidoreductase 1 enhanced the susceptibility of cholangiocarcinoma cells to chemotherapeutic agents, J. Exp. Clin. Cancer Res. 33 (1) (2014) 1–13.
[42] L, F. Navazio, Soluble diaphorase in animal tissues, Acta Chem. Scand. 12 (1958) 595–602.
[43] G. Asher, O. Dym, P. Tsvetkov, J. Adler, Y. Shaul, The crystal structure of NAD(P)H quinone oxidoreductase 1 in complex with its potent inhibitor dicoumarol, Biochemistry 45 (20) (2006) 6372–6378.
[44] A.J. Levine, M. Oren, The first 30 years of p53: growing ever more complex, Nat. Rev. Cancer 9 (10) (2010) 749–758.